January 2016

Quantum Walks: Theory, Application, And Implementation

Albert Thomas Schmitz

Recommended Citation

QUANTUM WALKS: THEORY, APPLICATION, AND IMPLEMENTATION

by

Albert Thomas Schmitz

Bachelor of Science, Bemidji State University, 2011

A thesis

submitted to the Graduate Faculty of the

University of North Dakota

in partial fulfillment of the requirements for the degree of
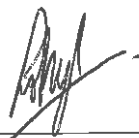
Master of Science

Grand Forks, North Dakota

May
2016
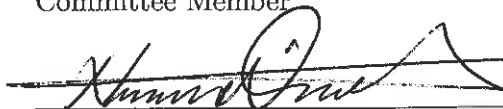
This thesis, submitted by Albert Thomas Schmitz in partial fulfillment of the requirements of the Degree of Master of Science from the University of North Dakota, has been read by the Faculty Advisory Committee under whom the work has been done and is hereby approved.

William A Schwalm

William Schwalm
Chairperson

Yen Lee Loh
Committee Member

Nuri Oncel
Committee Member

This thesis is being submitted by the appointed advisory committee as having met all the requirements of the School of Graduate Studies at the University of North Dakota and is hereby approved.

Wayne Swisher
Dean of the School of Graduate Studies

April 29, 2016

Date

ii

PERMISSION

Title	Quantum Walks: Theory, Application, and Implementation
Department	Department of Physics and Astrophysics
Degree	Master of Science

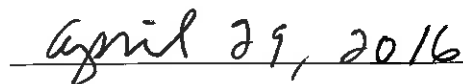In presenting this thesis in partial fulfillment of the requirements for a graduate degree from the University of North Dakota, I agree that the library of this University shall make it freely available for inspection. I further agree that permission for extensive copying for scholarly purposes may be granted by the professor who supervised my thesis work or, in his absence, by the Chairperson of the department or the dean of the School of Graduate Studies. It is understood that any copying or publication or other use of this thesis or part thereof for financial gain shall not be allowed without my written permission. It is also understood that due recognition shall be given to me and to the University of North Dakota in any scholarly use which may be made of any material in my thesis.

Albert Thomas Schmitz
05-05-2016

CONTENTS

LIST OF FIGURES

ACKNOWLEDGMENTS

ABSTRACT

The quantum walk is a method for conceptualizing and designing quantum computing algorithms and it comes in two forms: the continuous-time and discrete-time quantum walk. The thesis is organized into three parts, each of which looks to develop the concept and uses of the quantum walk. The first part is the theory of the quantum walk. This includes definitions and considerations for the various incarnations of the discrete-time quantum walk and a discussion on the general method for connecting the continuous-time and discrete-time versions. As a result, it is shown that most versions of the discrete-time quantum walk can be put into a general form and this can be used to simulate any continuous-time quantum walk. The second part uses these results for a hypothetical application. The application presented is a search algorithm that appears to scale in the time for completion independent of the size of the search space. This behavior is then elaborated upon and shown to have general qualitative agreement with simulations to within the approximations that are made. The third part introduces a method of implementation. Given a universal quantum computer, the method is discussed and shown to simulate an arbitrary discrete-time quantum walk. Some of the benefits of this method are that half the unitary evolution can be achieved without the use of any gates and there may be some possibility for error detection. The three parts combined suggest a possible experiment, given a quantum computing scheme of sufficient robustness.

CHAPTER I

INTRODUCTION

The quantum walk is a concept introduced as a method for designing quantum computing algorithms. It is considered to be an analog of the classical random walk which behaves according to the rules of quantum mechanics. Thus, one should be able to create algorithms for quantum computing analogous to classical algorithms based on the random walk. Though quantum mechanics has some similarities to the random walk, it is clear the concepts of time evolution and probability of the walker's position are dramatically different in the quantum case. Furthermore, the classical random walk does not have any properties analogous to superposition and entanglement. These differences are what motivate computer scientists, mathematicians and physicists to explore the possibility that quantum systems might improve on the current computational efficiency or create behavior that is not possible in the classical case. This as it may, the focus of this thesis is on a different use of the theory and understanding of quantum mechanics. Here, the goal is not to use quantum mechanics to understand the properties or behavior of a preexisting physical system but rather to imagine a hypothetical quantum system which exhibits a desired behavior. This adaptation of quantum theory is termed *quantum engineering* [45]. Ever since it was discussed by Richard Feynman [21, 22] as well as others, the topic has grown to include quantum computing as a sub-discipline of quantum engineering.

Due to its nature, quantum mechanics is less intuitive than classical dynamic behavior, and so it is important to have a robust theoretical apparatus available to find and understand

the desired behavior. As a first step, I state the rules by which a quantum system must behave [35, 45]:

1. The state of any quantum system at any given time is completely characterized by a particular vector of a Hilbert space over the field of complex numbers.

2. For every measurable quantity that characterizes the system, there exists a Hermitian operator such that the eigenvalues of the operator represent the possible outcomes of the measurement. The associated orthonormal basis eigenvectors represent the probability amplitude for measuring the corresponding eigenvalue. By this it is meant that the probability to measure an eigenvalue is given by the expectation value of the projection into the space spanned by eigenvectors associated with the particular eigenvalue.

3. Due to the probability interpretation, the inner product of the state with itself must always be 1, and thus it is normalized. Furthermore, time evolution of a closed system between measurements is represented by a group of operators. Because the total probability of measuring any eigenvalue must remain one, all members of the group are unitary and every member translates time (discrete or continuous) by some amount. For my purposes, the group is always generated by a single operator referred to as the *time-translation operator*. A consequence of this is that time evolution of the system between measurements is deterministic and reversible.

4. Upon measurement of any quantity that characterizes a closed system, the state undergoes an irreversible "collapse" to the eigenvector associated with the measurement outcome. By this it is meant that any subsequent measurement of the same operator yields the same eigenvalue with probability 1 unless the system interacts with an outside system, is measured with respects to another operator or allowed to evolve via the time-translation operator. In the case that the system is allowed to evolve,

the time evolution is given by the time-translation operator acting on the eigenvector associated with the previously measured eigenvalue.

Though standard principles of quantum mechanics, it is import to reiterate these rules here, since these are the constraints for the hypothetical engineered systems.

The most important aspect one might exploit is the property of superposition. The vehicle for classical probability dynamics of the random walk is given by multiplication and addition of positive, real numbers. For example, the probability of taking a certain path is the multiplication of the probabilities for each individual step and the total probability is the sum over all such paths. This behavior is monotonic. Quantum mechanics is dominated by the superposition of paths weighted by complex amplitudes as shown in Feynman's path integral formalism [35]. Thus, paths constructively and destructively interfere, making the behavior no longer monotonic. However, probability is still conserved, which tends to make quantum dynamics ballistic rather than diffusive and results in faster redistribution of probability amplitude. Furthermore, a classical walker must take one definite path for each member of an ensemble, where as a quantum particle exists in a superposition of position states and is only found in one particular position after measurement. A quantum algorithm is designed to take advantage of these properties in order to increase its efficiency. This is most often characterized in four ways. The first is the time needed for completion of the algorithm and how this scales with the size of the problem. The size of the problem is understood as the number of items that are sorted through or searched. Two more ways of characterizing a quantum or random walk based algorithms are the *hitting time* and *mixing rate* [44]. Roughly speaking, the hitting time is the time it takes for the walker to go from one position in the graph to another with non-trivial probability. The mixing rate is the speed at which the probability distribution approaches its limit distribution. Finally,

a metric of physical consequence is the number of hypothetical primitive gates necessary to implement the algorithm. More on this in Ch. V.

One of the two most well-known and successful quantum algorithms is Shor's factorization algorithm. The algorithm purports to finding prime factors of an integer in polynomial time, which classically take sub-exponential time [39]. The second is the Grover search algorithm. This algorithm is an example of the use of a quantum oracle. A classical oracle is any function which marks a given element of a finite set called the *search space* [44]:

Definition I.1. Let a search space of N objects be numbered so that they are related bijectively to the set $S = \{0, 1, 2, \ldots, N - 1\}$. Then the oracle is a function $O : S \to \{0, 1\}$ such that $O(n) = \delta_{nm}$, where m corresponds to the marked element.

Note that this says nothing about how the oracle works internally. A quantum oracle is a linear operator $\hat{O}$ on a Hilbert space, $\mathcal{H}_N \otimes \mathcal{H}_2$, where $\mathcal{H}_N$ and $\mathcal{H}_2$ are Hilbert spaces of dimension N and 2, respectively. Their bases represent the domain and co-domain of the oracle function. The action of the quantum oracle on an arbitrary element of the basis, $|n\rangle |b\rangle$, where $n \in S$ and $b \in \{0, 1\}$, is $\hat{O} |n\rangle |b\rangle = |n\rangle |b \oplus O(n)\rangle$. The symbol $\oplus$ is the binary XOR operation. So if $n = m$ is the marked element, then the co-domain qubit is flipped. Otherwise, it is left alone. Classically, the search problem can be thought of as repeated queries to the oracle until the oracle indicates the marked element. Thus, the number of queries needed to get the correct answer with high probability goes as the number of elements in the domain, N. Using a quantum oracle, Grover's search algorithm [23] manages the analogous result of measuring the marked basis state with high probability and does so with the number of queries to the quantum oracle going as $\sqrt{N}$. Here is a prime example of the goal of theoretical quantum algorithm design: construct a Hilbert space and set of unitary operations so as to achieve a desired measurement outcome with high probability.

Since my experience lies in the understanding and manipulation of quantum systems, my primary focus is on the construction of these hypothetical systems and understanding their behavior. I am not as concerned with characterizing their use and evaluating their efficiency as an algorithm for computation, except for when it becomes relevant to motivation. Furthermore, I focus on algorithms which rely on the concepts and methods of the quantum walk.

I.1   Overview of the Quantum Walk

This section is intended as a cursory overview of the quantum walk (QW). A more thorough discussion is given in Ch. II. Each QW is associated with a graph, where the vertices represent the position of a hypothetical walker and the edges represent paths of advancement from one vertex to another. QWs comes in two broad categories. The first category is the continuous-time quantum walk (CTQW), which was first introduced by Fahri and Gutmann [19]. The walk takes place in a Hilbert space spanned by basis vectors associated with the vertices of the graph, also known as the *vertex space*. Any CTQW is characterized by a *graph Hamiltonian* operator for which the time-translation operator satisfies the Shrödinger equation. This was inspired by the similarity between the Schrödinger equation and the continuous-time limit for a Markov process. So the CTQW is essentially the same as spatially discretized quantum mechanical models such as those given by the tight-binding approximation.

The other version is the discrete-time quantum walk (DTQW), which is generally considered to have been introduced first by Aharonov et al. [1]. However, Meyer essentially was using the concept in his work on quantum cellular automata in Refs. [30, 31]. In these works, Meyer showed that no homogeneous, local, unitary operator in the vertex space of an

arbitrary-dimensional Euclidean lattice could be constructed with non-trivial dynamics. That is to say, any such operator satisfying these properties must be a discrete spatial-translation operator up to global phase. Because a discrete-time version of the paradigm model could not be realized in the vertex space, the Hilbert space of the DTQW was expanded, which led to the idea of the coined quantum walk (CQW). In the CQW, the Hilbert space is spanned by a basis representing both the position of the walker and the direction of advancement. This extra degree of freedom is referred to as the *coin*, which in the case of a regular graph is achieved by the product space of the vertex space with a *coin space* of dimension equal to the degree of the graph. Otherwise, each vertex has its own coin space and the entire space is the union over all coin spaces. The discrete time-translation operator is the product of two operators: the first is a unitary operator called the *coin operator*, which updates the states within each individual coin space, making it block diagonal in those subspaces. The second operator is the *shift operator*, which transfers the probability amplitude from one coin space to adjacent coin spaces in accordance with the basis states of the coin. The total time evolution is given by integer powers of the complete time-translation operator. As a concrete example, consider the one-dimensional lattice or a cycle on N vertices, for which the space of the CQW can be formed as a product of the vertex space and a two-dimensional space. The former is spanned by the basis $\{|i\rangle : i \in \mathbb{Z}_N\}$ and the latter by the basis $\{|\uparrow\rangle, |\downarrow\rangle\}$. The labeling of the second basis is inspired by associating the coin with spin as in Refs. [1, 40, 41]. Note for a spatially-homogeneous walk, a coin operator can be formed by the vertex space identity in direct product with any two-dimensional unitary matrix. One often used example is the Hadamard coin operator represented by

$$\hat{C}_H \doteq \frac{1}{\sqrt{2}} \begin{pmatrix} 1 & 1 \\ 1 & -1 \end{pmatrix}. \tag{I.1}$$

Note that although this coin operator is common in the literature, it is only a particular choice. The coin operator is as arbitrary to the CQW as the graph Hamiltonian is to the CTQW. More on this in Ch. III. The typical shift operator interprets the spin-up state as advancing forward and the spin-down state as advancing backward, so the shift operator, $\tilde{S}_{1D}$, can be written as

$$\tilde{S}_{1D} = \sum_{i \in \mathbb{Z}} \Big(|i-1\rangle\langle i| \otimes |\downarrow\rangle\langle\downarrow| + |i+1\rangle\langle i| \otimes |\uparrow\rangle\langle\uparrow| \Big). \tag{I.2}$$

Further exploration of this model will be demonstrated in Sec. III.5, as well as found in Ref. [44].

Consider that every direction of advance is in one-to-one correspondence with the directed edges of the graph. That being the case, a more general way to think of the expanded space is to assert that the DTQW takes place in the *edge space*, which is spanned by a basis associated with directed edges of the graph. This is the viewpoint of the scattering quantum walk (SQW). For the SQW, the time-translation operator is a set of scattering matrices, one for each vertex, and the time evolution is a series of scattering events between vertices. For more on SQW, see Ref. [20].

To summarize, the CQW views the walker to be at a vertex advancing by way of the edges, whereas the SQW views the walker to be at an edge and advancing by scattering from the vertices. Though these seem to be dual in a sense, they are in fact essentially equivalent. More specifically, their time-translation operators are equivalent up to a unitary transformation as argued by Andrade and da Luz [3]. This is also addressed in Sec. II.4.

There are many examples of using QW in the design of a hypothetical algorithm. A large category involves the search algorithm, which is meant to solve the same problem as the Grover algorithm. An important example is provided by Shenvi et al. [37], who used a CQW

on the hypercube of $N = 2^d$ vertices. This algorithm as well as the hypercube is discussed in Ch. IV. Other examples include Childs and Goldstone [10], who used a CTQW with a local perturbation on the marked element, and Magniez et al. [28], who used a DTQW to search based upon a Markov chain. There are many more examples, far too many to list here. Another related but slightly different problem is to find two or more equal items in a list of N items, termed the element distinctness problem. Ambainis [2] used a QW to find k equal elements in $\mathcal{O}(N^{\frac{k}{k+1}})$ queries. A final example is the triangle problem, which finds a triangle in an undirected graph or outputs a null result if no triangle is found. Magniez with Santha and Szegedy [29] used a QW to solve this problem. As a further demonstration of the power of the QW, it was found that the QW can be used to form a set of quantum computational primitives by Childs [7] for the CTQW case and Lovett et al. [27] for the DTQW case.

Aside from their use in computational theory, there are also many examples of implementing a quantum walk in both optical and material media. For example, Du et.al [18] presented a method using a nuclear-magnetic-resonance (NMR) quantum computer, Karski et al. [26] used neutral atoms in a one-dimensional spin-dependent optical lattice, and Penuzzo et al. [34] managed to obtain the QW of two photons through an array of coupled waveguides in a SiO_xN_y chip. There are many other examples, though none seem to be completely general. However, they do show a proof of concept. For this thesis, I do not address the physical implementation of a quantum walk. My perspective is to assume a universal gate set realized hypothetically in some physical system and how that can be used to simulate a general DTQW. More on this in Ch. V.

I.2 Attempts to Connect the Discrete-time and Continuous-time Quantum Walk

Due to the enlargement of the state space, there is no obvious DTQW that in some limit yields the dynamics of a CTQW. Strauch [40, 41] proposed a limit for the standard DTQW on the one-dimensional lattice, which gave the Dirac equation or, for a different limit of that parameter, two decoupled versions of the CTQW with a Laplacian graph Hamiltonian. This was then generalized to any Euclidean lattice. A similar process was adapted by D'Alessandro and collaborators [12, 13] to any regular graph with a general Hamiltonian. However, D'Alessandro's process is for a continuous-time operator in the expanded space– sometimes called a "coined" continuous-time quantum walk–and it is not clear to me how this is related to a CTQW in the vertex space. Furthermore, the method is somewhat obscure in its practical use. In Ref. [15], Dheeraj and Brun proposed a limit process which applied to a coined CTQW. This method is discussed in Sec. II.6. Childs [8] developed another method which approximated a CTQW with a DTQW by using a specific type of coin operator. This coin operator was generated by an isometry particular to the graph Hamiltonian and was adapted from work done by Szegedy on quantum Markov processes [42]. In a certain limit, the method reduced to the CTQW for the graph Hamiltonian, but it did so by enlarging the state space even further and I am unable to see that the process conserved probability for all times and all values of the limit parameter. Some aspects of this process are discussed in Ch. III. Other attempts to find limits are presented by Debbasch and Di Molfetta [14, 16] involving both temporal and spatial limits of the one- and two-dimensional lattices. Also, it was shown by Chisaki et al. [11] that the limit distributions for a one-dimensional lattice model similar to that used by Strauch showed crossover from DTQW to CTQW by using intermediate position measurements for the set time over which the walk occurred. For more on this, see Ref. [38].

In a paper by myself and Schwalm [36], we discussed a method for connecting any CTQW to a DTQW which within certain limits had approximately the same probability dynamics. Furthermore, the time-translation operator was unitary for all values of the limit parameters and was simple to construct for a given graph Hamiltonian. All of those results are included and elaborated on in Ch. III.

I.3   Thesis Organization

The organization of the thesis is as follows: Ch. II is a rigorous and detailed description of both the CTQW and the DTQW as well as some general results for approximating unitary operators in the edge space by a DTQW. This is followed in Ch. III by a discussion of the general method for connecting a CTQW to a DTQW as well as the analytic solution to the model, given the spectral decomposition and some restrictions on the graph Hamiltonian. This also includes example simulations for the one- and two-dimensional lattices as well as some comments on how this method relates to some of the previously mentioned results for connecting the CTQW to the DTQW. In Ch. IV, these ideas are applied to the design of an algorithm. Specifically, I consider a particular search algorithm for which completion time does not appear to scale with the size of the search space. Implementation is covered in Ch. V, where I discuss quantum gates and how a certain universal gate set can be used to realize a strategy for implementing an arbitrary QW. Finally, Ch. VI makes some summary conclusions and remarks.

CHAPTER II

DESCRIPTION OF THE QUANTUM WALK

II.1   Structure and Spaces

Many of the conventions presented here are adapted from Refs. [3, 7, 12, 19, 20, 44]. Let a graph be given by $\mathcal{G} = (\mathcal{V}, \mathcal{E})$, where $\mathcal{V}$ is the vertex set and $\mathcal{E}$ is the edge set of the graph. $\mathcal{V}$ is the set of all vertices and $\mathcal{E}$ is a subset of $\mathcal{V} \times \mathcal{V}$ such that every member represents a directed edge going from the first vertex of the 2-tuple to the second. Vertices are denoted by lowercase letters i, j, k and so on.

Definition II.1. @ is defined as the relation between members of $\mathcal{V}$ such that for all $i, j \in \mathcal{V}$, $i@j$ if and only if $(i, j) \in \mathcal{E}$. $i@j$ is read "i is adjacent to j."

The first vertex in the 2-tuple is the *tail* of the edge and the second vertex in the 2-tuple is the *head* of the edge. As a convention, sums involving adjacency are written in the form $\sum_{j@i}$, which is understood as the sum over all j such that it is adjacent to the fixed i.

Consider two Hilbert spaces, $\mathcal{H}_\mathcal{V}$ and $\mathcal{H}_\mathcal{E}$, called the vertex space and edge space, respectively. The vertex space is spanned by an orthonormal basis $\{|i\rangle : i \in \mathcal{V}\}$. This basis is interpreted as the eigenbasis of the operator associated with measurement of the walker's vertex position. The edge space is spanned by an orthonormal basis $\{|i, j\rangle : (i, j) \in \mathcal{E}\}$.

This basis is interpreted as the eigenbasis of the operator associated with measurement of the position and direction of advancement (or equivalently, the coin degree of freedom). For example, I interpret the basis state $|i,j\rangle$ as the eigenstate related to the walker being at j and coming from i. To distinguish between operators acting in the different spaces, any operator acting in $\mathcal{H}_\mathcal{V}$ is subscripted with 0, and any operator acting in $\mathcal{H}_\mathcal{E}$ is subscripted with 1. For operators acting between the spaces, no subscript is given to avoid excessive decoration.

From $\mathcal{H}_\mathcal{E}$, define a collection of subspaces:

Definition II.2. For each $i \in \mathcal{V}$,

$$\mathcal{I}_i = \mathrm{span}\{|j,i\rangle \ : j \in \mathcal{V} \text{ and } (j,i) \in \mathcal{E}\}, \text{ and} \qquad \text{(II.1a)}$$

$$\mathcal{O}_i = \mathrm{span}\{|i,j\rangle \ : j \in \mathcal{V} \text{ and } (i,j) \in \mathcal{E}\}, \qquad \text{(II.1b)}$$

where these subspaces are referred to as the *incoming space* and *outgoing space* of i, respectively.

The incoming space of i is the collection of all possible vectors (in $\mathcal{H}_\mathcal{E}$) coming into the vertex i exclusively, and the outgoing space is the collection of all possible vectors going out of the vertex i exclusively. These are similar to definitions given by Feldman and Hillary [20]. I interpret the incoming spaces as the coin spaces as discussed in Ch. I. This interpretation is made clear in Sec. II.3. Note the collection of all incoming spaces forms a partitioning of $\mathcal{H}_\mathcal{E}$. Likewise, the collection of all outgoing spaces forms a different partitioning of $\mathcal{H}_\mathcal{E}$. Another important relationship is for all $i,j \in \mathcal{V}$, $\mathcal{O}_i$ and $\mathcal{I}_j$ have a non-empty intersection if and only if i is adjacent to j. This is stated without proof as it is obvious. For the purposes of this thesis, the formalism is general enough to include self-loops ($(i,i) \in \mathcal{E}$, for some $i \in \mathcal{V}$), but I exclude the possibility of vertices connected by multiple edges. Also, the

Hermitian-ness of the graph Hamiltonian in the CTQW requires the graph be a bigraph, which is to say the @ relation is symmetric. Because of this, I restrict to bigraphs in all cases. As a consequence, $dim(\mathcal{I}_i) = dim(\mathcal{O}_i)$, for all $i \in \mathcal{V}$.

II.2 Description of the Continuous-time Quantum Walk

Any CTQW takes place in $\mathcal{H}_\mathcal{V}$ for some graph $\mathcal{G}$. The time evolution of the state is characterized by a normalized initial state, $|\phi, t = 0\rangle$, and the time-translation operator, $\hat{U}_0(t)$, which satisfies the Schrödinger equation:

$$i \frac{\partial \hat{U}_0(t)}{\partial t} = \hat{H}_0 \, \hat{U}_0(t); \tag{II.2a}$$

$$U_0(t = 0) = \hat{I}_0, \tag{II.2b}$$

where t is the continuous time parameter, $\hat{I}_0$ is the $\mathcal{H}_\mathcal{V}$ identity, and $\hat{H}_0$ is the graph Hamiltonian for the QW. From quantum mechanics, $\hat{H}_0$ is the operator associated with energy measurement. For a time-independent graph Hamiltonian, the solution to Eq. (II.2a) is given by

$$\hat{U}_0(t) = \exp\left(-it \, \hat{H}_0\right). \tag{II.3}$$

From this equation, one sees that $\hat{U}_0$ is unitary if and only if $\hat{H}_0$ is Hermitian. Based upon intuition from quantum mechanics, I also require that $\hat{H}_0$ be *local*:

Definition II.3. An operator $\hat{O}_0$ in $\mathcal{H}_\mathcal{V}$ has the property of being local if and only if for all $i, j \in \mathcal{V}$, $i \neq j$ and $(i, j) \notin \mathcal{E}$ implies $\langle i|\hat{O}_0|j\rangle = 0$.

The reason for this requirement in quantum mechanics is causality and the Hamiltonian's relation to the time derivative in the Schrödinger equation. In the case of the CTQW, this requirement is artificial since a designer can always add edges to the graph to make a graph Hamiltonian local. Still, I maintain this requirement to allow for the connectedness of the graph to correlate to the dynamics of the system. Expanding the graph Hamiltonian in the position basis,

$$\hat{H}_0 = \sum_{i,j \in V} \tau_{ij} \, |i\rangle\langle j| \,, \tag{II.4}$$

where τ_{ij} is an arbitrary weight related to the amount of probability amplitude transferred from state $|j\rangle$ to state $|i\rangle$ in an infinitesimal amount of time. In accordance with the vocabulary of tight binding, I refer to these coefficients as *hopping amplitudes*. From the given constraints on the graph Hamiltonian, $i \neq j$ and $(i,j) \notin \mathcal{E}$ implies $\tau_{ij} = 0$ to insure the local property, and $\tau_{ij}^* = \tau_{ji}$ to insure $\hat{H}_0$ is Hermitian. Even though the hopping amplitudes are arbitrary up to the above constraints, two of the most common choices are the adjacency Hamiltonian and the Laplacian Hamiltonian (or just Laplacian). The adjacency Hamiltonian is given by the hopping amplitudes $\tau_{ij} = 1$ for $i@j$ and $\tau_{ij} = 0$ otherwise. Typically such a model does not include self-loops. The Laplacian has the negative hopping amplitudes of the adjacency Hamiltonian for non-diagonal elements, and diagonal elements given by $\tau_{ii} = deg(i)$, where $deg(i)$ is the degree or coordination number of the vertex i. Note for a regular graph, the difference in the dynamics generated by these two is trivial, since when used in Eq. (II.3), the Laplacian only contributes a global phase over the adjacency Hamiltonian. This has no effect on the probability interpretation.

The state of the system at any time is given by

$$|\phi, t\rangle = \hat{U}_0(t) \, |\phi, 0\rangle \,, \tag{II.5}$$

14

and according to my interpretation of the position basis, the probability to measure the walker's position as i at time t is given by

$$P_i^0(t) = \langle \phi, t | i \rangle \langle i | \phi, t \rangle = |\langle i | \phi, t \rangle|^2. \tag{II.6}$$

So as claimed, the CTQW is the same formalism as standard quantum mechanics for models with discrete space and continuous time.

II.3   Description of the Discrete-time Quantum Walk

Unlike the CTQW, the conventions used here are not universal in the literature. Where there is a large departure, I discuss how this formalism compares to other conventions but this does not cover all of the possible definitions and extensions. The means to extend the ideas presented here are obvious in some cases, but I do not include them. One example is the possibility of time-dependent coin operators. After the discussion, it should be clear how to extend the formalism to include this possibility. However, I consider the topic beyond the intended scope of this thesis.

Any DTQW takes place in $\mathcal{H}_{\mathcal{E}}$ for some graph $\mathcal{G}$. Discrete-time evolution is characterized by a normalized initial state, $|\psi, t = 0\rangle$, and the time-translation operator. Like the graph Hamiltonian in $\mathcal{H}_{\mathcal{V}}$, the need for some intuition about the dynamic behavior generated by the time-translation operator leads me to require it satisfy a locality property with an analogous definition in $\mathcal{H}_{\mathcal{E}}$:

Definition II.4. An operator $\hat{O}_1$ acting in $\mathcal{H}_{\mathcal{E}}$ is local if and only if for all $(i, j), (k, l) \in \mathcal{E}$, $i \neq k$ and $i \neq l$ and $j \neq k$ and $j \neq l$ implies $\langle i, j | \hat{O}_1 | k, l \rangle = 0$.

This definition of local requires the operator have matrix elements between basis states that share at least one vertex. As a local operator in $\mathcal{H}_\mathcal{V}$ connects vertices through an edge, a local operator in $\mathcal{H}_\mathcal{E}$ connects edges through a vertex. The four conditions in Def. II.4 can be interpreted as saying a local operator only contains incoming-to-incoming, incoming-to-outgoing, outgoing-to-incoming or outgoing-to-outgoing matrix elements.

To construct a local unitary operator, the DTQW time-translation operator is the product of two operators. The first operator is the coin operator, $\hat{C}_1$, which has the form

$$\hat{C}_1 = \bigoplus_{i \in \mathcal{V}} \hat{C}^{(i)}, \tag{II.7}$$

where $\hat{C}^{(i)}$ acts only in the incoming space of i, is unitary in that subspace, but is otherwise arbitrary. As a result, $\hat{C}_1$ is also unitary. For this thesis, the shift operator as discussed in Ch. I is always the *swap operator*, $\hat{S}_1$. It is defined as a linear operator which for every basis vector, $|i, j\rangle$,

$$\hat{S}_1 |i, j\rangle = |j, i\rangle. \tag{II.8}$$

Note that $\hat{S}_1$ is its own inverse, Hermitian, and thus unitary.

The time-translation operator is given by $\hat{U}_1 = \hat{S}_1 \hat{C}_1$ and the state of the system after t integer steps is given by

$$|\psi, t\rangle = \left(\hat{U}_1\right)^t |\psi, 0\rangle = \left(\hat{S}_1 \hat{C}_1\right)^t |\psi, 0\rangle. \tag{II.9}$$

To understand the behavior of the time-translation operator, consider Figs. II.1a-II.1c. At any given time and for some vertex, probability amplitude comes in from adjacent vertices. The coin operator mixes these incoming states in some prescribed, unitary way. The swap

16

operator then takes these updated incoming states to outgoing state, which are incoming on the adjacent vertices. When put together, one sees that this can be interpreted as a scattering event as depicted in Fig. II.1d. $\hat{C}^{(i)}$ is the scattering matrix for vertex i with the diagonal elements being the reflection coefficients and the off-diagonal elements transmission coefficients. Furthermore, it is clear that $\hat{U}_1$ is local as it only has incoming-to-outgoing and possibly outgoing-to-incoming matrix elements.

| (a) incoming states | (b) action of the coin operator | (c) action of the swap operator | (d) scattering viewpoint |
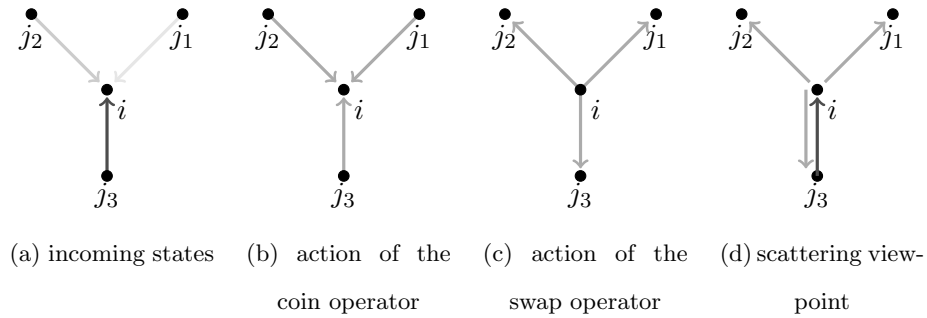
FIGURE II.1: Intuitive interpretation for the action of the DTQW time-translation operator on a single vertex.

Probability can be interpreted many ways in the edge space. The SQW interpretation places the walker on the edges and so the probability to be on that edge is the sum of the two probabilities associated with the edge. I take the perspective of the CQW which still puts the walker on the vertices. Typically, this means one is not concerned with the direction in which the walker enters the vertex and so one sums over the extra degree of freedom. According to my interpretation of the basis states, this means the probability for the walker to be at vertex i is the expectation value of the projection onto the incoming space of i, $\mathscr{P}_1^{(i)}$, which is the same as summing the probabilities over all incoming basis states of i.

Written out explicitly,

$$P_i^{(in)} = \langle \psi, t | \hat{\mathscr{P}}_i^{(i)} | \psi, t \rangle = \sum_{j@i} |\langle j, i | \psi, t \rangle|^2. \tag{II.10}$$

II.4 Alternative Considerations for the Discrete-time Quantum Walk

There are other ways to define the time-homogeneous version of the DTQW, but I argue that they are mostly if not entirely equivalent to some DTQW as described above. I assert that any two time-translation operators in $\mathcal{H}_\mathcal{E}$ are equivalent if they satisfy the following definition:

Definition II.5. For all unitary operators $\hat{V}_1$ and $\hat{W}_1$ acting in $\mathcal{H}_\mathcal{E}$, $\hat{V}_1$ and $\hat{W}_1$ are equivalent if and only if there exists a unitary operator $\hat{T}_1$ such that $\hat{V}_1 = \hat{T}_1^\dagger \hat{W}_1 \hat{T}_1$.

Two equivalent time-translation operators are essentially the same model. The leading factor of $\hat{T}_1$ amounts to a different choice of initial state, $|\psi, 0\rangle \to \hat{T}_1^\dagger |\psi, 0\rangle$. The factor of $\hat{T}_1^\dagger$ amounts to a different probability interpretation given by the unitary transform of the projection operators. For example, the probability interpretation above would be mapped $\hat{\mathscr{P}}_1^{(i)} \to \hat{T}_1^\dagger \hat{\mathscr{P}}_1^{(i)} \hat{T}_1$. Since this is invertible, the two models are isomorphic to each other.

One possible alternative form of the DTQW is to interpret the coin spaces as the outgoing spaces. Then the coin operator must be block diagonal in the outgoing spaces. This can be achieved by taking a coin operator as defined above and performing a similarity transform with $\hat{S}_1$. Thus, this new time-translation operator–call it $\tilde{U}_1$–is given by

$$\tilde{U}_1 = \hat{S}_1 (\hat{S}_1 \hat{C}_1 \hat{S}_1) = \hat{S}_1 \hat{U}_1 \hat{S}_1. \tag{II.11}$$

Not surprisingly, the equivalence transformation is given by the swap operator. An interesting note is that it is also equivalent to switching the order of the swap and coin operators. The only reason for choosing the incoming space perspective is that aesthetically speaking, the time-translation operator has an appearance that resembles forward-moving scattering events.

The more common difference that one might find in the literature is a difference in the shift operator or the second operation in the decomposition of the time-translation operator. As an example, consider the one-dimensional lattice model mentioned in Ch. I. If I interpret $|i\rangle |\uparrow\rangle = |i+1, i\rangle$ and $|i\rangle |\downarrow\rangle = |i-1, i\rangle$, then the 1D swap operator, $\hat{S}_{1D}$, can be written as

$$
\begin{aligned}
\hat{S}_{1D} &= \sum_{i \in \mathbb{Z}_N} \Big(|i, i-1\rangle\langle i-1, i| + |i, i+1\rangle\langle i+1, i| \Big) \\
&= \sum_{i \in \mathbb{Z}_N} \Big(|i-1\rangle |\uparrow\rangle\langle i| \langle\downarrow| + |i+1\rangle |\downarrow\rangle\langle i| \langle\uparrow| \Big) \\
&= \sum_{i \in \mathbb{Z}_N} \Big(|i-1\rangle\langle i| \otimes |\uparrow\rangle\langle\downarrow| + |i+1\rangle\langle i| \otimes |\downarrow\rangle\langle\uparrow| \Big) \\
&= (\hat{I}_0 \otimes \hat{\sigma}_x)\tilde{S}_{1D}, \quad\quad\quad\quad\quad\quad\quad\quad\quad\quad (\text{II.12})
\end{aligned}
$$

where $\hat{\sigma}_x$ is the x-direction Pauli spin operator and $\tilde{S}_{1D}$ is the shift operator of Eq. (I.2). So for a forward-moving spin-up state, the shift operator takes it to a spin-up state on the forward adjacent vertex, whereas the swap operator takes that same state to a spin-down state on the forward adjacent vertex. Thus, the $\hat{\sigma}_x$ is needed to permute the spin-down to a spin-up for the two operators to have the same action. The same is true of spin-down states but in the opposite direction.

To generalize this and show equivalence, the result of Eq. (II.12) is used as insight. An alternative shift operator must take any basis state in one incoming space to an incoming basis state for an adjacent vertex, and it must do so in a bijective fashion. That is, it cannot

take two different basis states into the same basis state, and every basis state must be mapped onto by the shift operator. I assert that any shift operator, $\tilde{S}_1$, can be decomposed into a direct sum of permutation operators acting amongst incoming basis states, followed by the swap operator, followed by another sum of permutation operators not necessarily the same as the first. This is depicted in Fig. II.2. Note that in Fig. II.2, the shift operator demonstrated there is not local as given by Def. II.4. To accommodate such a shift operator, the definition of local would have to be extended to allow matrix elements between basis states which share at least one adjacent vertex. I show there is no need for this according to the following argument.
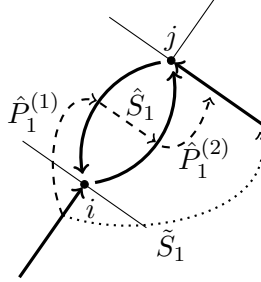
FIGURE II.2: Depiction of an arbitrary shift operator decomposed into a permutation operator, the swap operator and another permutation operator. The bold arrows represent basis states, the dashed arrows represent the action of each operator in the decomposition of $\tilde{S}_1$ and the dotted arrow represents the resultant action of $\tilde{S}_1$.

Let the first and third operators in the decomposition of $\tilde{S}_1$ be written as

$$\hat{P}_1^{(a)} = \bigoplus_{i \in \mathcal{V}} \hat{P}^{(a,i)}, \tag{II.13}$$

where $\hat{P}^{(a,i)}$ only permutes the basis states within the incoming space on vertex i and a can take on the values 1 or 2, 1 corresponding the first permutation in the subspace and 2 corresponding to the second. Thus $\tilde{S}_1 = \hat{P}_1^{(2)} \hat{S}_1 \hat{P}_1^{(1)}$. Now suppose one is given an

alternative time-translation operator using $\tilde{S}_1$, such that

$$
\begin{aligned}
\tilde{U}_1 = \tilde{S}_1 \tilde{C}_1 &= (\hat{P}_1^{(2)} \hat{S}_1 \hat{P}_1^{(1)}) \tilde{C}_1 \\
&= \hat{P}_1^{(2)} \left[\hat{S}_1 (\hat{P}_1^{(1)} \tilde{C}_1 \hat{P}_1^{(2)}) \right] (\hat{P}_1^{(2)})^{-1}.
\end{aligned}
\tag{II.14}
$$

Note that $\hat{P}_1^{(1)}$ and $\hat{P}_1^{(2)}$ are both unitary and block diagonal in the incoming spaces. Thus by Eq. (II.14), $\tilde{U}_1$ is equivalent to a DTQW as described in the last section with a coin operator

$$
\hat{C}_1 = \hat{P}_1^{(1)} \tilde{C}_1 \hat{P}_1^{(2)},
\tag{II.15}
$$

which satisfies all the required properties.

Interpreting the description given in Sec. II.3 for the DTQW as a SQW and any generalized alternative of the form given in Eq. (II.14) as a CQW, the results say that for any CQW, there exists an equivalent SQW with a coin operator (scattering matrices) given by Eq. (II.15) and vice versa. Because of this, I henceforth drop any distinction between the CQW and SQW, referring to any such model as simply a DTQW. This idea of unitary equivalence between the two versions of the DTQW is similar to that given by Andrade and da Luz [3], though the presentation of the results is a bit more obscure.

II.5   Continuous-time Dynamics in the Edge Space

In Ch. I, I referenced a model that comes up in the literature which is sometimes called a coined continuous-time quantum walk. It is also a part of the strategy in Ch. III to relate a CTQW in $\mathcal{H}_\mathcal{V}$ to continuous-time dynamics in $\mathcal{H}_\mathcal{E}$ and approximate that with a DTQW model. However, the method of approximation is more general and so I discuss it here.

Continuous-time dynamics in $\mathcal{H}_\mathcal{E}$ is analogous to continuous-time dynamics in $\mathcal{H}_\mathcal{V}$, where the time-translation operator satisfies the Schrödinger equation for some edge space Hamiltonian, $\hat{\mathscr{H}}_1$. This operator is referred to as an *edge Hamiltonian*. Thus the time-translation operator is

$$\hat{U}_1(t) = \exp\left(-it\,\hat{\mathscr{H}}_1\right). \tag{II.16}$$

Like the CTQW, I require that the edge Hamiltonian be local as in Def. II.4. Defining $(\hat{\mathscr{H}}_1)_{ij,kl} = \langle i,j|\hat{\mathscr{H}}_1|k,l\rangle\,(1-\frac{1}{2}\delta_{ij})(1-\frac{1}{2}\delta_{kl})$, locality is enforced with Kronecker deltas:

$$(\hat{\mathscr{H}}_1)_{ij,kl} = (\hat{\mathscr{H}}_1)_{ij,kl}(\delta_{ik} + \delta_{il} + \delta_{jk} + \delta_{jl} - \delta_{jk}\delta_{il} - \delta_{ik}\delta_{il}). \tag{II.17}$$

Using this to expand the edge Hamiltonian,

$$\begin{aligned}
\hat{\mathscr{H}}_1 = \sum_i \sum_{j@i} \sum_{k@i} (1 - \frac{1}{2}\delta_{jk}) &\left((\hat{\mathscr{H}}_1)_{ji,ki}\,|j,i\rangle\langle k,i| + (\hat{\mathscr{H}}_1)_{ji,ik}\,|j,i\rangle\langle i,k| \right. \\
&\left. + (\hat{\mathscr{H}}_1)_{ij,ki}\,|i,j\rangle\langle k,i| + (\hat{\mathscr{H}}_1)_{ij,ik}\,|i,j\rangle\langle i,k| \right).
\end{aligned} \tag{II.18}$$

The four terms inside the brackets represent the four conditions in the definition of local. I can then break up the edge Hamiltonian into four pieces:

$$(\hat{\mathscr{H}}_1)_{in,in} = \sum_i \sum_{j@i} \sum_{k@i} (1 - \frac{1}{2}\delta_{jk})(\hat{\mathscr{H}}_1)_{ji,ki}\,|j,i\rangle\langle k,i|\,; \tag{II.19a}$$

$$(\hat{\mathscr{H}}_1)_{in,out} = \sum_i \sum_{j@i} \sum_{k@i} (1 - \frac{1}{2}\delta_{jk})(\hat{\mathscr{H}}_1)_{ji,ik}\,|j,i\rangle\langle i,k|\,; \tag{II.19b}$$

$$(\hat{\mathscr{H}}_1)_{out,in} = \sum_i \sum_{j@i} \sum_{k@i} (1 - \frac{1}{2}\delta_{jk})(\hat{\mathscr{H}}_1)_{ij,ki}\,|i,j\rangle\langle k,i|\,; \tag{II.19c}$$

$$(\hat{\mathscr{H}}_1)_{out,out} = \sum_i \sum_{j@i} \sum_{k@i} (1 - \frac{1}{2}\delta_{jk})(\hat{\mathscr{H}}_1)_{ij,ik}\,|i,j\rangle\langle i,k|\,, \tag{II.19d}$$

where $(1 - \frac{1}{2}\delta_{jk})$ splits the matrix element evenly in the case of ambiguous character (*in-out*, *out-in*, and so on) for that term, and the definition of $(\hat{\mathscr{H}_1})_{ij,kl}$ keeps self-loop states from being double counted. Note that $(\hat{\mathscr{H}_1})_{in,in}$ and $(\hat{\mathscr{H}_1})_{out,out}$ are both block diagonal, though in different block forms. A Hermitian edge Hamiltonian means these two must themselves be Hermitian. Moreover, the Hermitian constraint requires $(\hat{\mathscr{H}_1})_{in,out} = (\hat{\mathscr{H}_1})^\dagger_{out,in}$. Another assumption one can make is that the edge Hamiltonian and swap operator commute. This is a reasonable symmetry since if they did not commute, that would imply the edge Hamiltonian treats some of the edge basis states differently than their swapped counterparts. In that case, $\hat{S}_1\hat{\mathscr{H}_1}\hat{S}_1 = \hat{\mathscr{H}_1}$, or by matching operator characters, I have that $(\hat{\mathscr{H}_1})_{in,in} = \hat{S}_1(\hat{\mathscr{H}_1})_{out,out}\hat{S}_1$, and $(\hat{\mathscr{H}_1})_{in,out}\hat{S}_1 = \hat{S}_1(\hat{\mathscr{H}_1})_{out,in} = \left(\hat{S}_1(\hat{\mathscr{H}_1})_{out,in}\right)^\dagger$, where the last equality is given by the Hermitian condition. Note that both equalities are of the *in-in* character, or operators that are block diagonal in the incoming spaces. Thus, I come to the conclusion that for any edge Hamiltonian which respects swap symmetry, there exists two operators, $\hat{K}_1$ and $\hat{L}_1$, which are both block diagonal in the incoming spaces and Hermitian. With these operators, the edge Hamiltonian is written as

$$\hat{\mathscr{H}_1} = \hat{L}_1 + \hat{S}_1\hat{L}_1\hat{S}_1 + \hat{S}_1\hat{K}_1 + \hat{K}_1\hat{S}_1. \tag{II.20}$$

Note the exponentiation of either $\hat{K}_1$ or $\hat{L}_1$ could be a choice of coin operator. To relate this to a DTQW, one realizes a local edge Hamiltonian only yields an approximate local unitary operator if the edge Hamiltonian is modified by a small parameter ϵ. Before doing this for the arbitrary edge Hamiltonian (with appropriate constraints), I need the concept of a *lazy discrete-time quantum walk*.

II.6   The Lazy Discrete-time Quantum Walk

For a Markov process or classical random walk, the walker must transition on each time step, and this is analogous to the fact that the second step of the DTQW always swaps. In the classical case, this can be modified to allow some probability for the walker to loiter on the vertex. This is called the lazy (classical) random walk. The limit which approaches near perfect laziness and a small time step leads to the continuous-time Markov process which solves an equation similar to the Schrödinger equation [19]. Just as the classical random walk can be lazied, so too can the DTQW by extending the definition of the time-translation operator. Consider the unitary operator

$$\hat{U}_1(\epsilon) = \exp\left(-i\alpha\epsilon\,\hat{S}_1\right)\exp\left(-i\epsilon\,\hat{K}_1\right), \tag{II.21}$$

where ϵ and α are positive definite parameters. ϵ is used to approach a continuous-time limit, and α is used to control the laziness of the DTQW independent of a finite ϵ. $\hat{K}_1$ is a Hermitian, block diagonal operator as discussed in Sec II.5. To see that this is analogous to the lazy random walk, note that the exponentiation of $\hat{S}_1$ can be expanded, and since the swap operator is its own inverse, the terms separate into even and odd powers. From this, one can see

$$\exp\left(-i\alpha\epsilon\,\hat{S}_1\right) = \cos\left(\alpha\epsilon\right)\hat{I}_1 - i\sin\left(\alpha\epsilon\right)\hat{S}_1. \tag{II.22}$$

When $\alpha\epsilon = \frac{\pi}{2}$, Eq. (II.21) gives the standard DTQW with the coin operator $\hat{C}_1 = -i\exp\left(-i\epsilon\,\hat{K}_1\right)$. This is referred to as the *QW choice*. When $0 < \alpha\epsilon < \frac{\pi}{2}$, there is some amount of the state vector that is not swapped on each time step, and this has an effect analogous to the walker loitering on the vertex. This is referred to as the *lazy QW*

choice. So Eq. (II.21) is the natural extension to the DTQW time-translation operator and is similar to the limit presented by Dheeraj and Brun [15].

II.7   Approximating the Edge Space Hamiltonian Dynamics

If one wants to approximate Eq. (II.16) with an edge Hamiltonian in the form of Eq. (II.20), I propose that it can be done with a generalized DTQW method. Let continuous time $t \to \epsilon t$, where t is now an integer and ϵ is the time step. Eq. (II.16) is given by integer powers of the operator

$$
\begin{aligned}
\hat{U}_1(\epsilon) &= \exp\left(-i\epsilon\,\hat{\mathscr{H}}_1\right) \\
&= \exp\left(-i\epsilon(\hat{S}_1\hat{L}_1\hat{S}_1 + \hat{L}_1)\right)\exp\left(-i\epsilon(\hat{S}_1\hat{K}_1 + \hat{K}_1\hat{S}_1)\right) + \mathcal{O}(\epsilon^2).
\end{aligned}
\tag{II.23}
$$

Considering the first factor, one can split the sum in the exponent again into factors as an approximation:

$$
\begin{aligned}
\exp\left(-i\epsilon(\hat{S}_1\hat{L}_1\hat{S}_1 + \hat{L}_1)\right) &= \exp\left(-i\epsilon\hat{S}_1\hat{L}_1\hat{S}_1\right)\exp\left(-i\epsilon\hat{L}_1\right) + \mathcal{O}(\epsilon^2) \\
&= \hat{S}_1\exp\left(-i\epsilon\hat{L}_1\right)\hat{S}_1\exp\left(-i\epsilon\hat{L}_1\right) + \mathcal{O}(\epsilon^2),
\end{aligned}
\tag{II.24}
$$

where the fact that first factor is the similarity transform of the second is used. This is two steps of a DTQW with coin operator $\hat{C}_1 = \exp\left(-i\epsilon\hat{L}_1\right)$. As for the second factor in Eq. (II.23), consider the lazy DTQW time-translation operator in Eq. (II.21),

$$
\begin{aligned}
&\exp\left(-i\alpha\epsilon\,\hat{S}_1\right)\exp\left(-i\epsilon\,\hat{K}_1\right) \\
&= \exp\left(-i\epsilon(\alpha\hat{S}_1 + \hat{K}_1)\right) + \mathcal{O}(\epsilon^2).
\end{aligned}
\tag{II.25}
$$

If I make the walk lazy such that $\epsilon \ll \alpha\epsilon \ll 1$, α is relatively large. Consider when α is much larger than $\|\hat{K}\|_2$, where $\|\cdot\|_2$ is the operator norm induced by the ℓ_2 norm or the Hilbert space vector norm of $\mathcal{H}_\mathcal{E}$. In this case, the lazy DTQW approximates the unitary operator generated by the edge Hamiltonian $\alpha\hat{S}_1 + \hat{K}_1$. Using the properties of the swap operator, this edge Hamiltonian can be factored and rewritten as

$$
\begin{aligned}
\alpha\hat{S}_1 + \hat{K}_1 &= \left(\alpha + \hat{K}_1\hat{S}_1\right)\hat{S}_1 = \hat{S}_1\left(\alpha + \hat{S}_1\hat{K}_1\right) \\
&= \left[\left(\alpha + \hat{K}_1\hat{S}_1\right)\left(\alpha + \hat{S}_1\hat{K}_1\right)\right]^{\frac{1}{2}} \\
&= \alpha\left[\hat{I}_1 + \left(\frac{1}{\alpha}\right)\left(\hat{S}_1\hat{K}_1 + \hat{K}_1\hat{S}_1\right) + \left(\frac{\hat{K}_1}{\alpha}\right)^2\right]^{\frac{1}{2}}.
\end{aligned}
\tag{II.26}
$$

Approximating the root to first order in $\frac{1}{\alpha}$, one sees that the edge Hamiltonian dynamics approximated by Eq. (II.25) is $\alpha\hat{I}_1 + \frac{1}{2}(\hat{S}_1\hat{K}_1 + \hat{K}_1\hat{S}_1)$, which is the other half of the general edge Hamiltonian up to the constant α. This amounts to a global phase.

Putting all these results together, I can approximate the general edge Hamiltonian dynamics as

$$
\begin{aligned}
\exp&\left(-i\epsilon\,\hat{\mathscr{H}}_1\right) \\
&\approx e^{(i2\epsilon\alpha)}\left(\hat{S}_1\exp\left(-i\epsilon\hat{L}_1\right)\right)^2\left(\exp\left(-i\alpha\epsilon\,\hat{S}_1\right)\exp\left(-i\epsilon\,\hat{K}_1\right)\right)^2,
\end{aligned}
\tag{II.27}
$$

which fits into a slightly more general form of the DTQW. As a final consideration, one could choose $\frac{\pi}{2} < \alpha\epsilon < \pi$, which would also have the effect of lazying the DTQW. In most cases, this might create problems with the terms of order $(\alpha\epsilon)^2$ becoming relatively large. However, if I define the independent parameter,

$$
a = \pi - \alpha\epsilon,
\tag{II.28}
$$

then the small a limit competes with the ϵ limit. For Eq. (II.27), this is a problem, but for $\hat{L}_1 = 0$, this limit is useful as shown in Ch. III. There, the edge Hamiltonian is more specific and so a condition is found for a such that this becomes relevant.

CHAPTER III

CONNECTING THE CONTINUOUS-TIME TO THE DISCRETE-TIME QUANTUM WALK

CTQW dynamics are characterized by the graph Hamiltonian, while the DTQW dynamics are characterized by the coin operator. To connect the two, I present a coin operator which generates approximately the same probability dynamics as those generated by a given graph Hamiltonian. The method is to obtain an appropriate edge Hamiltonian and use the results of Sec II.7 to approximate it. Linking the two models in this way is possible, but going from a general DTQW to some CTQW might not be. That is, given a coin operator, there is not always a related graph Hamiltonian. More on this later in the chapter.

III.1 Relating the Graph Hamiltonian to Operators in the Edge Space

Connecting the CTQW to the DTQW requires operators that act between $\mathcal{H}_\mathcal{V}$ and $\mathcal{H}_\mathcal{E}$. Consider two such operators,

$$\hat{A} = \sum_{(i,j)} T_{ij} |i\rangle\langle j, i| ; \qquad \text{(III.1)}$$

$$\hat{B} = \sum_{(i,j)} T_{ij} |i\rangle\langle i, j| , \qquad \text{(III.2)}$$

where T_{ij} is some arbitrary complex weight. $\hat{A}$ and $\hat{B}$ act much like projection maps, and so I refer to them as *projectors*. The A-projector maps an edge basis state onto the head of the edge and the B-projector maps that same state onto the tail, both with the weights T_{ij}. The adjoints of these operators promote a vertex basis state to a superposition of the incoming and outgoing basis states, respectively, with the same weights. Clearly the two are related by $\hat{A} = \hat{B}\hat{S}_1$, but also,

$$\begin{aligned}
\hat{A}\hat{B}^\dagger &= \hat{A}\hat{S}_1\hat{S}_1\hat{B}^\dagger = \hat{B}\hat{A}^\dagger \\
&= \sum_{(i,j)}\sum_{(k,l)} T_{ij}T_{kl}^* |i\rangle\langle j, i|k, l\rangle\langle k| \\
&= \sum_{(i,j)} T_{ij}T_{ji}^* |i\rangle\langle j| = \hat{H}_0, \qquad \text{(III.3)}
\end{aligned}$$

if I chose the weights such that

$$T_{ij}T_{ji}^* = \tau_{ij}. \qquad \text{(III.4)}$$

Thus, it is sufficient (but not necessary) to have $T_{ij} = \sqrt{\tau_{ij}}$. $\hat{A}$ and $\hat{B}$ are then closely related to the procedure proposed by Szegedy [42] and extended by Childs, where $\hat{B}^\dagger$ is

similar to the isometry in Ref. [8]. Another useful relation is

$$
\begin{aligned}
\hat{\Omega}_0 = \hat{A}\hat{A}^\dagger &= \hat{A}\hat{S}_1\hat{S}_1\hat{A}^\dagger = \hat{B}\hat{B}^\dagger \\
&= \sum_{(i,j)}\sum_{(k,l)} \sqrt{\tau_{ij}}\sqrt{\tau_{kl}^*}\,|i\rangle\langle j, i|l, k\rangle\langle k| \\
&= \sum_{(i,j)} |\tau_{ij}|\,|i\rangle\langle i| = \sum_i \omega_i\,|i\rangle\langle i|\,,
\end{aligned}
\tag{III.5}
$$

where $\omega_i = \sum_{j @ i} |\tau_{ij}|$, which is the sum over the modulus of the entries in the ith column of the matrix representing the graph Hamiltonian. A special case is defined as such:

Definition III.1. A graph Hamiltonian has the property of being *regular* if and only if $\omega_i = \omega$, for all $i \in \mathcal{V}$ and some positive, real ω.

The term regular comes from the fact that a regular adjacency Hamiltonian implies the graph is regular with degree ω. Furthermore, such an operator could be interpreted as representing a Markov process with a transition rate of ω [19, 42]. Thus the condition represents a large number of useful models.

With the projectors, one can promote a normalized initial state in the vertex space to a normalized state in the edge space:

$$
|\psi, 0\rangle = \hat{A}^\dagger\,\hat{\Omega}_0^{-\frac{1}{2}}\,|\phi, 0\rangle\,,
\tag{III.6a}
$$

or,

$$
|\psi, 0\rangle = \hat{B}^\dagger\,\hat{\Omega}_0^{-\frac{1}{2}}\,|\phi, 0\rangle\,,
\tag{III.6b}
$$

both of which are normalized according to Eq. (III.5). Also using Eqs. (III.3) and (III.5), $\hat{U}_0(t)$ can be rewritten in terms of dynamics in $\mathcal{H}_\mathcal{E}$ as

$$\begin{aligned}
\hat{U}_0(t) &= \hat{A} \, \exp\left(-it\,\hat{B}^\dagger\hat{A}\right) \hat{A}^\dagger \hat{\Omega}_0^{-1} \\
&= \hat{\Omega}_0^{-1} \hat{A} \, \exp\left(-it\,\hat{A}^\dagger\hat{B}\right) \hat{A}^\dagger.
\end{aligned} \tag{III.7}$$

Naively, one might be tempted to use either $\hat{B}^\dagger\hat{A}$ or $\hat{A}^\dagger\hat{B}$ as an edge Hamiltonian for analogous continuous-time dynamics in $\mathcal{H}_\mathcal{E}$, but neither are Hermitian, even though they are local. This is not surprising, however, since different spaces have different meanings for the conservation of probability. To understand this, assume a regular adjacency Hamiltonian for simplicity and consider the inner product related to position measurement,

$$\langle i|\phi, t\rangle = \langle i|\exp\left(-it\hat{H}_0\right)|\phi, 0\rangle = \frac{1}{\omega}\,\langle i|\hat{A}\exp\left(-it\,\hat{B}^\dagger\hat{A}\right)\hat{A}^\dagger|\phi, 0\rangle. \tag{III.8}$$

For the sake of argument, consider the state of the system in the edge space to be $|\psi, t\rangle = \exp\left(-it\,\hat{B}^\dagger\hat{A}\right)\frac{1}{\sqrt{\omega}}\hat{A}^\dagger|\phi, 0\rangle$, so that the inner product becomes

$$\langle i|\phi, t\rangle = \frac{1}{\sqrt{\omega}}\,\langle i|\hat{A}|\psi, t\rangle = \sqrt{\frac{1}{\omega}}\sum_{j@i}\langle j, i|\psi, t\rangle. \tag{III.9}$$

Aside from the factor of $\sqrt{\frac{1}{\omega}}$, the probability given by taking the modulus squared of this inner product has cross terms not present in the incoming probability given by Eq. (II.10). This is not to say Eq. (III.9) represents a state for which probability is not conserved. Probability must be conserved since I started with a unitary operator. What it does say is that probability-conserving dynamics which projects up, evolves the state and then projects back down requires non-unitary evolution in $\mathcal{H}_\mathcal{E}$. This is what was meant in Ch. I when I claimed that the method described in Ref. [8] does not appear to conserve probability for all values of the parameters.

Still, the expansion in Eq.(III.7) does suggest a possible edge Hamiltonian since both candidates have the same Hermitian part, namely,

$$\hat{H}_1 = \frac{1}{2}\left(\hat{B}^\dagger\hat{A} + \hat{A}^\dagger\hat{B}\right).$$

(III.10)

This operator respects $\hat{S}_1$ symmetry.

III.2   The Dynamic Space Generated by the Projectors

Before looking at the dynamics generated by $\hat{H}_1$, I must prove a more general and useful result. First define a specific subspace:

Definition III.2. For a given graph Hamiltonian, let the dynamic space, $\mathcal{H}_{dyn} \subseteq \mathcal{H}_\mathcal{E}$, be defined as $\mathcal{H}_{dyn} = \mathrm{span}\{\hat{A}^\dagger\left|i\right\rangle, \hat{B}^\dagger\left|i\right\rangle : i \in \mathcal{V}\}$.

The dynamic space is the collect of all states promoted by the projectors. It is important to recognize the set $\{\hat{A}^\dagger\left|i\right\rangle, \hat{B}^\dagger\left|i\right\rangle : i \in \mathcal{V}\}$ is not necessarily a basis for the dynamic space, and by virtue of Eq. (III.3), it is not orthogonal. As a counter example to prove the first claim, consider any regular adjacency Hamiltonian. For each vertex i, $\hat{A}^\dagger\left|i\right\rangle = \sum_{j@i}\left|j,i\right\rangle$ which is an equal superposition over all incoming basis states of i. Now summing over all such i, $\sum_i \hat{A}^\dagger\left|i\right\rangle = \sum_{(i,j)}\left|j,i\right\rangle = \sum_{(i,j)}\left|i,j\right\rangle = \sum_i \hat{B}^\dagger\left|i\right\rangle$, where I use the fact that both the union of incoming basis states and the union of outgoing basis states form the entire edge basis and adjacency is symmetric. Therefore in this case, there is at least some linear dependence in that set and so it cannot form a basis. However, I can form an orthonormal basis by first noting that the identity and swap operators form the reflection group, $\mathbb{Z}_2$, which is represented by symmetric and anti-symmetric combinations. So, define

the symmetric projector (S-projector) as $\frac{1}{\sqrt{2}}(\hat{I}_1 + \hat{S}_1)\hat{A}^\dagger = \frac{1}{\sqrt{2}}(\hat{A}^\dagger + \hat{B}^\dagger)$ and the anti-symmetric projector(AS-projector) as $\frac{1}{\sqrt{2}}(\hat{I}_1 - \hat{S}_1)\hat{A}^\dagger = \frac{1}{\sqrt{2}}(\hat{A}^\dagger - \hat{B}^\dagger)$. These projectors effectively split the dynamic space into two orthogonal subspaces. Furthermore, consider a vector in $\mathcal{H}_\mathcal{V}$, $|\phi_k^\pm\rangle$, which is an eigenvector of the operator $\hat{\Omega}_0 \pm \hat{H}_0$ with eigenvalue $\lambda_k^\pm$. Then one has inner products of the form

$$\left(\langle\phi_l^\pm|\frac{1}{\sqrt{2}}(\hat{A} \pm \hat{B})\right)\left(\frac{1}{\sqrt{2}}(\hat{A}^\dagger \pm \hat{B}^\dagger)|\phi_k^\pm\rangle\right)$$
$$= \frac{1}{2}\langle\phi_l^\pm|(2\hat{\Omega}_0 \pm 2\hat{H}_0)|\phi_k^\pm\rangle = \lambda_k^\pm\delta_{kl}. \tag{III.11}$$

So a good orthonormal basis for the dynamic space might be all vectors of the form

$$|\psi_k^\pm\rangle = \begin{cases} \frac{1}{\sqrt{2\lambda_k^\pm}}(\hat{A}^\dagger \pm \hat{B}^\dagger)|\phi_k^\pm\rangle & \text{, if } \lambda_k^\pm \neq 0 \\ 0 & \text{, otherwise} \end{cases}. \tag{III.12}$$

Applying $\hat{H}_1$ to $|\psi_k^\pm\rangle$, one sees that it is an eigenvector of $\hat{H}_1$ with eigenvalue $\pm\frac{\lambda_k^\pm}{2}$.

It may seem that such a basis would have the same number of elements as $\{\hat{A}^\dagger|i\rangle, \hat{B}^\dagger|i\rangle : i \in \mathcal{V}\}$, but that assumes neither the S-projector nor the AS-projector annihilates the eigenvectors, and $\lambda_k^\pm \neq 0$. For the regular adjacency Hamiltonian, the coincidence of these two conditions is why the dynamic space loses a basis vector, since any regular graph has an eigenvector, $|\phi_0^-\rangle$, composed of an equal superposition over all basis states with eigenvalue equal to the degree of the graph. This coincides with $\lambda_0^- = 0$. The connection between the two conditions can be generalized.

Proposition III.3. $(\hat{A}^\dagger \pm \hat{B}^\dagger)|\phi_k^\pm\rangle = 0$ *if and only* $|\phi_k^\pm\rangle$ *is an eigenvector of* $\hat{\Omega}_0 \pm \hat{H}_0$ *with eigenvalue* $\lambda_k^\pm = 0$.

Proof. Start by assuming that $(\hat{A}^\dagger \pm \hat{B}^\dagger) |\phi_k^\pm\rangle = 0$. Then $0 = \hat{A}0 = \hat{A}(\hat{A}^\dagger \pm \hat{B}^\dagger) |\phi_k^\pm\rangle = (\hat{\Omega}_0 \pm \hat{H}_0) |\phi_k^\pm\rangle$, which implies $|\phi_k^\pm\rangle$ is an eigenvector of $\hat{\Omega}_0 \pm \hat{H}_0$ with eigenvalue $\lambda_k^\pm = 0$. Now assume that $|\phi_k^\pm\rangle$ is an eigenvector of $\hat{\Omega}_0 \pm \hat{H}_0$ with eigenvalue $\lambda_k^\pm = 0$. Using Eq. (III.11), one has that

$$\langle\phi_k^\pm| \left(\hat{A} \pm \hat{B}\right) \left(\hat{A}^\dagger \pm \hat{B}^\dagger\right) |\phi_k^\pm\rangle = 2\lambda_k^\pm = 0.$$

This is true if and only if $(\hat{A}^\dagger \pm \hat{B}^\dagger) |\phi_k^\pm\rangle = 0$. □

A corollary to Prop. III.3 is that the only linear dependence in the set $\{\hat{A}^\dagger |i\rangle, \hat{B}^\dagger |i\rangle : i \in \mathcal{V}\}$ is characterized by eigenvectors $|\phi_k^\pm\rangle$ for which $\lambda_k^\pm = 0$. This is important for two reasons. First, it allows me to safely write the dynamic space projection operator since the $|\psi_k^\pm\rangle$'s are properly defined and span the dynamic space. Furthermore, it gives me a method for finding the dimension of the dynamic space.

What I ultimately want to prove is that edge space operators made up of the identity, the swap operator and the projectors maintain support of any dynamic space vector in that space. Any appropriate combinations of these operators "collapse" into operators that can be described as projecting down into the vertex space, performing some operation and then projecting back up to the edge space. In that case, I state the proposition this way:

Proposition III.4. *Let* $\hat{\mathscr{P}}_{dyn}$ *be the projection operator onto the dynamic space. For any edge space operator,* $\hat{W}_1$*, if their exists vertex space operators,* $\hat{V}_0^{(1)}, \hat{V}_0^{(2)}, \hat{V}_0^{(3)}$*, and* $\hat{V}_0^{(4)}$ *such that* $\hat{W}_1 = \hat{A}^\dagger \hat{V}_0^{(1)} \hat{A} + \hat{A}^\dagger \hat{V}_0^{(2)} \hat{B} + \hat{B}^\dagger \hat{V}_0^{(3)} \hat{A} + \hat{B}^\dagger \hat{V}_0^{(4)} \hat{B}$*, then* $\hat{W}_1 = \hat{\mathscr{P}}_{dyn} \hat{W}_1 \hat{\mathscr{P}}_{dyn}$*.*

Proof. Note that $\{|\phi_k^+\rangle\}_{k \in \mathcal{V}}$ and $\{|\phi_k^-\rangle\}_{k \in \mathcal{V}}$ both form orthonormal bases for $\mathcal{H}_\mathcal{V}$ and can be used to expand the identity in $\mathcal{H}_\mathcal{V}$. Furthermore, if I use $\{|\psi_k^\pm\rangle\}_{k \in \mathcal{V}; \pm}$ to write $\hat{\mathscr{P}}_{dyn}$,

then consider the combination

$$
\begin{aligned}
\hat{A}\hat{\mathscr{P}}_{dyn} =& \hat{A}\sideset{}{'}\sum_{k,\pm} \frac{1}{2\lambda_k^{\pm}}(\hat{A}^{\dagger} \pm \hat{B}^{\dagger})\,|\phi_k^{\pm}\rangle\langle\phi_k^{\pm}|\,(\hat{A} \pm \hat{B}) \\
=& \sideset{}{'}\sum_{k,\pm} \frac{1}{2\lambda_k^{\pm}}(\hat{\Omega}_0 \pm \hat{H}_0)\,|\phi_k^{\pm}\rangle\langle\phi_k^{\pm}|\,(\hat{A} \pm \hat{B}) \\
=& \frac{1}{2}\sum_{k,\pm}|\phi_k^{\pm}\rangle\langle\phi_k^{\pm}|\,(\hat{A} \pm \hat{B}) = \frac{1}{2}(\hat{A} + \hat{B} + \hat{A} - \hat{B}) \\
=& \hat{A},
\end{aligned}
$$

where the prime sum omits the cases when $\lambda_k^{\pm} = 0$ and the last sum adds in the appropriate zero terms to complete the identity in $\mathcal{H}_{\mathcal{V}}$. This also implies $\hat{B}\hat{\mathscr{P}}_{dyn} = \hat{B}$. Therefore,

$$
\begin{aligned}
\hat{\mathscr{P}}_{dyn}\hat{W}_1\hat{\mathscr{P}}_{dyn} =& \hat{\mathscr{P}}_{dyn}\left(\hat{A}^{\dagger}\hat{V}_0^{(1)}\hat{A} + \hat{A}^{\dagger}\hat{V}_0^{(2)}\hat{B} + \hat{B}^{\dagger}\hat{V}_0^{(3)}\hat{A} + \hat{B}^{\dagger}\hat{V}_0^{(4)}\hat{B}\right)\hat{\mathscr{P}}_{dyn} \\
=& \hat{A}^{\dagger}\hat{V}_0^{(1)}\hat{A} + \hat{A}^{\dagger}\hat{V}_0^{(2)}\hat{B} + \hat{B}^{\dagger}\hat{V}_0^{(3)}\hat{A} + \hat{B}^{\dagger}\hat{V}_0^{(4)}\hat{B} = \hat{W}_1.
\end{aligned}
$$

$\square$

This becomes useful because a corollary to Prop. III.4 is that if $\hat{W}_1$ has the form as given above and α and β are any complex numbers, then there exists a $\hat{f}_0$ and $\hat{g}_0$ such that $\hat{W}_1(\alpha\hat{A}^{\dagger} + \beta\hat{B}^{\dagger}) = \hat{A}^{\dagger}\hat{f}_0 + \hat{B}^{\dagger}\hat{g}_0$. Unfortunately, $\hat{f}_0$ and $\hat{g}_0$ are only unique up to an operator in the union of the null spaces of $\hat{\Omega}_0 + \hat{H}_0$ and $\hat{\Omega}_0 - \hat{H}_0$. When using this corollary, I assume such operators can be taken as zero. Note, the identity does not satisfy the condition of the proposition. However, $\hat{\mathscr{P}}_{dyn}$ does.

I can also use this result to understand the probability dynamics. If $\hat{W}_1$ is unitary and I use it to evolve the initial state (III.6a), then by the corollary, the probability of measuring

35

the walker at position i as given by Eq. (II.10) is

$$
\begin{aligned}
P_i^{(in)} &= \sum_{j@i} |\langle j,i|\hat{W}_1\hat{A}^\dagger\hat{\Omega}_0^{-\frac{1}{2}}|\phi,0\rangle|^2 \\
&= \sum_{j@i} |\langle j,i|\hat{A}^\dagger\hat{f}_0\hat{\Omega}_0^{-\frac{1}{2}}|\phi,0\rangle + \langle j,i|\hat{B}^\dagger\hat{g}_0\hat{\Omega}_0^{-\frac{1}{2}}|\phi,0\rangle|^2 \\
&= \sum_{j@i} |\sqrt{\tau_{ji}}\,\langle i|\hat{f}_0\hat{\Omega}_0^{-\frac{1}{2}}|\phi,0\rangle + \sqrt{\tau_{ij}}\,\langle j|\hat{g}_0\hat{\Omega}_0^{-\frac{1}{2}}|\phi,0\rangle|^2 \\
&= \omega_i|\langle i|\hat{f}_0\hat{\Omega}_0^{-\frac{1}{2}}|\phi,0\rangle|^2 + \sum_{j@i}|\tau_{ij}|\,|\langle j|\hat{g}_0\hat{\Omega}_0^{-\frac{1}{2}}|\phi,0\rangle|^2 \\
&\quad + 2\,\mathrm{Re}\sum_{j@i}\tau_{ij}\,\langle\phi,0|\hat{\Omega}_0^{-\frac{1}{2}}\hat{f}_0^\dagger|i\rangle\langle j|\hat{g}_0\hat{\Omega}_0^{-\frac{1}{2}}|\phi,0\rangle\,. \qquad\text{(III.13)}
\end{aligned}
$$

Specifically, if the Hamiltonian is regular,

$$
\begin{aligned}
P_i^{(in)} &= |\langle i|\hat{f}_0|\phi,0\rangle|^2 + \frac{1}{\omega}\sum_{j@i}|\tau_{ij}|\,|\langle j|\hat{g}_0|\phi,0\rangle|^2 \\
&\quad + \frac{2}{\omega}\,\mathrm{Re}\sum_{j@i}\tau_{ij}\,\langle\phi,0|\hat{f}_0^\dagger|i\rangle\langle j|\hat{g}_0|\phi,0\rangle\,. \qquad\text{(III.14)}
\end{aligned}
$$

In the last equation, I interpret the first term as probability propagated directly to i through $\hat{f}_0$. The second term is the weighted average of the probabilities propagated to the neighbors through $\hat{g}_0$ and attributed to i. The last term is an unavoidable cross term, but in important cases later in this thesis, it is zero or negligible. Also note that when $\hat{g}_0 = 0$, the probability becomes exactly the probability given by the action of a vertex operator, $\hat{f}_0$.

III.3   Continuous-time Dynamics in the Dynamic Space

I can apply the results of the last section to the exponentiation of $\hat{H}_1$, and since I am going to initialize the state in $\mathcal{H}_{dyn}$, I am concerned with $\exp{(-it\hat{H}_1)}\hat{A}^\dagger$ and $\exp{(-it\hat{H}_1)}\hat{B}^\dagger$. The

difficult part of expanding these operators is the various powers of $\hat{H}_1$, but each power satisfies the conditions of Prop. III.4, so I can use the corollary to write for each positive integer n,

$$\left(\hat{H}_1\right)^n \hat{A}^\dagger = \hat{A}^\dagger \, \hat{f}_0^{(n)} + \hat{B}^\dagger \, \hat{g}_0^{(n)}. \tag{III.15}$$

Multiplying by $\hat{H}_1$ on the left,

$$\begin{aligned}
\left(\hat{H}_1\right)^{n+1} \hat{A}^\dagger &= \frac{1}{2}\left(\hat{B}^\dagger\hat{A} + \hat{A}^\dagger\hat{B}\right)\left(\hat{A}^\dagger \, \hat{f}_0^{(n)} + \hat{B}^\dagger \, \hat{g}_0^{(n)}\right) \\
&= \frac{1}{2}\left(\hat{A}^\dagger\left(\hat{H}_0\hat{f}_0^{(n)} + \hat{\Omega}_0\hat{g}_0^{(n)}\right) + \hat{B}^\dagger\left(\hat{H}_0\hat{g}_0^{(n)} + \hat{\Omega}_0\hat{f}_0^{(n)}\right)\right) \\
&= \hat{A}^\dagger \, \hat{f}_0^{(n+1)} + \hat{B}^\dagger \, \hat{g}_0^{(n+1)}.
\end{aligned} \tag{III.16}$$

Equating like operators on both sides, the resulting recursions can be interpreted as a matrix equation and written along with the initial condition as

$$\begin{pmatrix} \hat{f}_0^{(n+1)} \\ \hat{g}_0^{(n+1)} \end{pmatrix} = \frac{1}{2}\begin{pmatrix} \hat{H}_0 & \hat{\Omega}_0 \\ \hat{\Omega}_0 & \hat{H}_0 \end{pmatrix}\begin{pmatrix} \hat{f}_0^{(n)} \\ \hat{g}_0^{(n)} \end{pmatrix}; \tag{III.17a}$$

$$\begin{pmatrix} \hat{f}_0^{(0)} \\ \hat{g}_0^{(0)} \end{pmatrix} = \begin{pmatrix} 1 \\ 0 \end{pmatrix}, \tag{III.17b}$$

where scalar values are understood as being multiplied by the identity. The solution is the nth power of the matrix which can be expanded in spectral representation. This is a simple matrix and by inspection, one finds the eigenvalue operators are $\frac{1}{2}\left(\hat{H}_0 \pm \hat{\Omega}_0\right)$ with eigenvector operators $\hat{x} \pm \hat{y}$, where $\hat{x}$ and $\hat{y}$ are the two-dimensional unit vectors. Thus the

solution is given by

$$
\begin{aligned}
\begin{pmatrix} \hat{f}_0^{(n)} \\ \hat{g}_0^{(n)} \end{pmatrix} &= \left(\frac{1}{2} \right)^n \begin{pmatrix} \hat{H}_0 & \hat{\Omega}_0 \\ \hat{\Omega}_0 & \hat{H}_0 \end{pmatrix}^n \begin{pmatrix} 1 \\ 0 \end{pmatrix} \\
&= \left(\frac{1}{2} \right)^{n+1} \begin{pmatrix} 1 & 1 \\ 1 & -1 \end{pmatrix} \begin{pmatrix} \left(\hat{H}_0 + \hat{\Omega}_0 \right)^n & 0 \\ 0 & \left(\hat{H}_0 - \hat{\Omega}_0 \right)^n \end{pmatrix} \begin{pmatrix} 1 & 1 \\ 1 & -1 \end{pmatrix} \begin{pmatrix} 1 \\ 0 \end{pmatrix} \\
&= \left(\frac{1}{2} \right)^{n+1} \begin{pmatrix} \left(\hat{H}_0 + \hat{\Omega}_0 \right)^n + \left(\hat{H}_0 - \hat{\Omega}_0 \right)^n \\ \left(\hat{H}_0 + \hat{\Omega}_0 \right)^n - \left(\hat{H}_0 - \hat{\Omega}_0 \right)^n \end{pmatrix}.
\end{aligned} \tag{III.18}
$$

Using this to expand the exponentiation of $\hat{H}_1$,

$$
\begin{aligned}
\exp\left(-it\hat{H}_1 \right) \hat{A}^\dagger &= \begin{pmatrix} \hat{A}^\dagger & \hat{B}^\dagger \end{pmatrix} \sum_n^\infty \frac{(-it)^n}{n!} \begin{pmatrix} \hat{f}_0^{(n)} \\ \hat{g}_0^{(n)} \end{pmatrix} \\
&= \begin{pmatrix} \hat{A}^\dagger & \hat{B}^\dagger \end{pmatrix} \frac{1}{2} \begin{pmatrix} \exp\left(-\frac{it}{2} \left(\hat{H}_0 + \hat{\Omega}_0 \right) \right) + \exp\left(-\frac{it}{2} \left(\hat{H}_0 - \hat{\Omega}_0 \right) \right) \\ \exp\left(-\frac{it}{2} \left(\hat{H}_0 + \hat{\Omega}_0 \right) \right) - \exp\left(-\frac{it}{2} \left(\hat{H}_0 - \hat{\Omega}_0 \right) \right) \end{pmatrix}.
\end{aligned} \tag{III.19}
$$

A similar expression is found for $\exp\left(-it\hat{H}_1 \right) \hat{B}^\dagger$ by noting that $\hat{S}_1$ and $\hat{H}_1$ commute and so multiplication by $\hat{S}_1$ on both sides of Eq. (III.19) gives the result. Although this is exact and general, it is a bit cumbersome, but consider when the graph Hamiltonian is regular. In that case, $\hat{\Omega}_0 = \omega \hat{I}_0$, which allows $\exp\left(-\frac{it}{2} \hat{H}_0 \right)$ to be factored out, and the remainder can be written in terms of trigonometric functions. The final result is

$$
\exp\left(-it\, \hat{H}_1 \right) \begin{pmatrix} \hat{A}^\dagger & \hat{B}^\dagger \end{pmatrix} \tag{III.20}
$$

$$
= \begin{pmatrix} \hat{A}^\dagger & \hat{B}^\dagger \end{pmatrix} \begin{pmatrix} \cos\left(\frac{\omega}{2}t \right) & -i\sin\left(\frac{\omega}{2}t \right) \\ -i\sin\left(\frac{\omega}{2}t \right) & \cos\left(\frac{\omega}{2}t \right) \end{pmatrix} \exp\left(-\frac{it}{2}\, \hat{H}_0 \right).
$$

What this says is that continuous time evolution given by $\hat{H}_1$ in the dynamic space is equivalent to evolving a state with the dynamics generated by $\hat{H}_0$, projecting up and "rotating" between the A-projector and B-projector. This shows that the dynamics generated by $\hat{H}_1$ are inherited from dynamics generated by $\hat{H}_0$. To understand the result more clearly, consider measuring the probability given by Eq. (III.14) for the time evolution given by $\hat{H}_1$. This makes $\hat{f}_0 = \cos\left(\frac{\omega t}{2}\right)\exp\left(\frac{-it}{2}\hat{H}_0\right)$ and $\hat{g}_0 = -i\sin\left(\frac{\omega}{2}t\right)\exp\left(\frac{-it}{2}\hat{H}_0\right)$. When the continuous-time t satisfies $\frac{\omega t}{2} = n\pi$ for any interger n, then $P_i^0(t) = P_i^{(in)}(\frac{t}{2})$. So $\hat{H}_1$ is the edge Hamiltonian that approximates the CTQW. This suggests the DTQW described in Eq. (II.27) with $\hat{K}_1 = \hat{A}^\dagger\hat{A}$ and $\hat{L}_1 = 0$, written here as

$$\hat{U}_1(\epsilon) = \exp\left(-i\alpha\epsilon\,\hat{S}_1\right)\exp\left(-i\epsilon\,\hat{A}^\dagger\hat{A}\right). \tag{III.21}$$

As a final point in this section, it is worth considering $\hat{L}_1 = \hat{A}^\dagger\hat{A}$ and $\hat{K}_1 = 0$, which gives an edge Hamiltonian of

$$\hat{J}_1 = \frac{1}{2}\left(\hat{A}^\dagger\hat{A} + \hat{B}^\dagger\hat{B}\right). \tag{III.22}$$

Since $\hat{J}_1$ commutes with $\hat{H}_1$, they share eigenvectors, but for $|\psi_k^\pm\rangle$, the eigenvalue is $\frac{\lambda_k^\pm}{2}$. By Prop. III.4, the rest of the eigenvectors form the null space of this operator, $\mathcal{H}_\mathcal{E}\backslash\mathcal{H}_{dyn}$. For the same reasons as above, one can expand $\exp\left(-it\hat{J}_1\right)\hat{A}^\dagger$ using the same method as used for the dynamics generated by $\hat{H}_1$. It is easy to see that the only difference is $\hat{H}_0$ and $\hat{\Omega}_0$ switch places in the calculation, from which I can immediately infer

$$\exp\left(-it\hat{J}_1\right)\hat{A}^\dagger$$
$$= \begin{pmatrix}\hat{A}^\dagger & \hat{B}^\dagger\end{pmatrix}\frac{1}{2}\begin{pmatrix}\exp\left(-\frac{it}{2}\left(\hat{\Omega}_0 + \hat{H}_0\right)\right) + \exp\left(-\frac{it}{2}\left(\hat{\Omega}_0 - \hat{H}_0\right)\right) \\ \exp\left(-\frac{it}{2}\left(\hat{\Omega}_0 + \hat{H}_0\right)\right) - \exp\left(-\frac{it}{2}\left(\hat{\Omega}_0 - \hat{H}_0\right)\right)\end{pmatrix}, \tag{III.23}$$

and in the case of a regular Hamiltonian,

$$\exp\left(-it\,\hat{J}_1\right)\begin{pmatrix}\hat{A}^\dagger & \hat{B}^\dagger\end{pmatrix} \tag{III.24}$$

$$=\begin{pmatrix}\hat{A}^\dagger & \hat{B}^\dagger\end{pmatrix}\begin{pmatrix}\cos\left(\frac{\hat{H}_0}{2}t\right) & -i\sin\left(\frac{\hat{H}_0}{2}t\right) \\ -i\sin\left(\frac{\hat{H}_0}{2}t\right) & \cos\left(\frac{\hat{H}_0}{2}t\right)\end{pmatrix}\exp\left(-\frac{i\omega t}{2}\right).$$

The QW that would approximate the edge space dynamics generated by $\hat{J}_1$ is given by

$$\hat{U}_1(\epsilon) = \hat{S}_1\,\exp\left(-i\epsilon\,\hat{A}^\dagger\hat{A}\right), \tag{III.25}$$

for even time steps. This amounts to the QW choice up to a phase. By Eq. (III.24), the probability dynamics of this QW should result in $\hat{f}_0 \approx \exp\left(-\frac{i\omega\epsilon t}{2}\right)\cos\left(\frac{\hat{H}_0}{2}\epsilon t\right)$, and $\hat{g}_0 \approx -i\exp\left(-\frac{i\omega\epsilon t}{2}\right)\sin\left(\frac{\hat{H}_0}{2}\epsilon t\right)$. Consider how this compares to the CTQW dynamics. Note $\hat{f}_0$ has all the even powers of the Hamiltonian in $\hat{U}_0(t)$ and $\hat{g}_0$ has all the odd powers. No matter the hopping amplitudes, the nth power of the graph Hamiltonian has only matrix elements which connect vertices n classical steps away in the graph. Then consider when t is even, the initial state is $|i\rangle$ and one wants to measure whether or not the walker is at vertex j. $\hat{f}_0$ is responsible for the probability amplitude propagated directly to j as given by Eq. (III.14). So its contribution to the probability is non-zero if j is an even number of steps away from i. $\hat{g}_0$ is responsible for the probability amplitude contributing to j but propagated to its neighbors, again, as understood by Eq. (III.14). Since the neighbors of j are always one additional step from i, $\hat{g}_0$'s contribution to the probability is non-zero under the same conditions. The cross term in Eq. (III.14) is zero for real hopping amplitudes due to the factor of i in $\hat{g}_0$. So for any j that is an odd number of steps from i, the probability amplitude that would have been assigned to its basis vector in the CTQW is distributed to its neighbors in accordance with the weighted average given in Eq. (III.14).Thus for a

bipartite graph, probability amplitude initialize on one sub-lattice will stay on that sub-lattice. This is analogous to behavior for the classical random walk if only even steps are considered and comes from the fact that at each time step, the state of the system must swap with no amplitude allowed to loiter. This behavior is also observed later in the chapter where odd time steps are considered.

III.4   The Coin Operator Generated by $\hat{A}^\dagger \hat{A}$

Much of what follows parallels and expands on the properties of the isometry used in Ref. [8]. $\hat{A}^\dagger \hat{A}$ has some important properties. Expanded in the edge basis,

$$\hat{A}^\dagger \hat{A} = \sum_i \hat{A}^\dagger \, |i\rangle\langle i| \, \hat{A} = \sum_i \sum_{j@i} \sum_{k@i} \sqrt{\tau_{ji}} \sqrt{\tau_{ik}} \, |j,i\rangle\langle k,i| \,. \tag{III.26}$$

The matrix elements of this operator can be found using diagrams of the graph. For a given vertex, i, imagine the vertices in the immediate neighborhood of i with the attached directed edges, each weighted by its hopping amplitude. Then the matrix element, say $\langle j,i|\hat{A}^\dagger \hat{A}|k,i\rangle$, is the square root of the two hopping amplitudes picked up by going from k to j through i, as can be seen from Eq. (III.26). This process is depicted in Fig. III.1. However, some care should be taken with the square roots. In general, the square roots are split and handled in accordance with the choice of branch cut. It seems the natural choice is along the negative real axis. In that case, negative real values of τ_{ij} are modified with an infinitesimal phase factor which is taken to be zero once the matrix element is found. If this convention is followed, $\hat{A}^\dagger \hat{A}$ is Hermitian and has the correct signs.
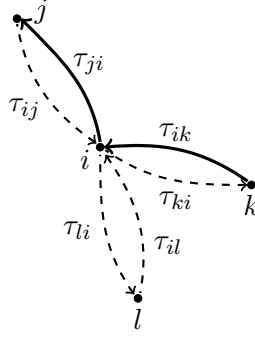
FIGURE III.1: Depiction of the process of determining matrix elements of $\hat{A}^\dagger \hat{A}$ from the graph. Here specifically, the bold arrows show $\langle j, i | \hat{A}^\dagger \hat{A} | k, i \rangle = \sqrt{\tau_{ji}} \sqrt{\tau_{ik}}$.

Note $\left(\hat{A}^\dagger \hat{A} \right)^2 = \hat{A}^\dagger \hat{\Omega}_0 \hat{A} = \hat{\Omega}_1 \hat{A}^\dagger \hat{A}$, where $\hat{\Omega}_1$ is a diagonal edge space operator with diagonal elements $\langle j, i | \hat{\Omega}_1 | j, i \rangle = \omega_i$ for all $j@i$. Also, $\hat{\Omega}_1$ commutes with $\hat{A}^\dagger \hat{A}$. By inspection, this near idempotence is due to the first equality in Eq. (III.26), which shows $\hat{A}^\dagger \hat{A}$ is almost a projection operator onto a subspace of the dynamic space, except any basis vectors in that space such as $\hat{A}^\dagger | i \rangle$ is not normalized. This property can be used to expand the coin part of Eq. (III.21) and (III.25):

$$
\begin{aligned}
\exp \left(-i\epsilon \hat{A}^\dagger \hat{A} \right) &= \sum_{n=0}^{\infty} \frac{(-i\epsilon)^n}{n!} \left(\hat{A}^\dagger \hat{A} \right)^n \\
&= \hat{I}_1 + \sum_{n=1}^{\infty} \frac{(-i\epsilon)^n}{n!} \hat{\Omega}_1^{n-1} \hat{A}^\dagger \hat{A} \\
&= \hat{I}_1 - i\hat{\mathscr{E}}_1 \hat{A}^\dagger \hat{A},
\end{aligned}
\tag{III.27}
$$

where

$$
\hat{\mathscr{E}}_1 = i\hat{\Omega}_1^{-1} \left(\exp \left(-i\epsilon \hat{\Omega}_1 \right) - \hat{I}_1 \right) = \hat{I}_1 \epsilon + \mathcal{O}(\epsilon^2).
\tag{III.28}
$$

Note that $\hat{\mathscr{E}}_1$ is diagonal with matrix elements $\langle j, i | \hat{\mathscr{E}}_1 | j, i \rangle = \frac{i}{\omega_i} (\exp \left(-i\omega_i \epsilon \right) - 1)$ for all $j@i$. Thus Eq. (III.27) along with the discussion of obtaining the elements of $\hat{A}^\dagger \hat{A}$ is a simple

42
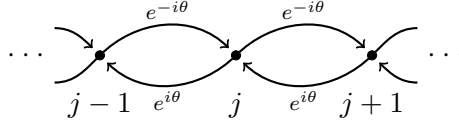
FIGURE III.2: Graphical depiction of a spatially symmetric one-dimensional lattice with arbitrary phase angle, θ, associated with each edge. Note the splitting of the directed edges with opposite phase is necessary for the Hamiltonian to be Hermitian.

way to find the matrix elements of the coin operator. A special case is for a regular graph Hamiltonian when $\omega\epsilon = \pi$:

$$\exp\left(-i\frac{\pi}{\omega}\hat{A}^{\dagger}\hat{A}\right) = \hat{I}_1 - \frac{2}{\omega}\hat{A}^{\dagger}\hat{A}. \tag{III.29}$$

The fact that $\frac{1}{\omega}\hat{A}^{\dagger}\hat{A}$ is exactly a projection operator makes Eq. (III.29) a reflection operator up to a sign, which is a common way to construct coin operators. For example, $\omega = 1$ corresponds to the coin operator suggested by Szegedy in the context of a quantum Markov processes [8, 42], and for the adjacency Hamiltonian, this is the Grover coin [37].

In the case of the one-dimensional lattice, the most general CTQW which maintains translation symmetry has an arbitrary phase associated with all edges. This graph is depicted in Fig. III.2. From this, I can write

$$\left[\hat{A}^{\dagger}\hat{A}\right]_j \doteq \begin{pmatrix} 1 & e^{-i\theta} \\ e^{i\theta} & 1 \end{pmatrix} = \hat{I}_2 + e^{-i\theta}\hat{\sigma}_+ + e^{i\theta}\hat{\sigma}_-, \tag{III.30}$$

where $[\,\cdot\,]_j$ denotes the block part for the incoming space of j, $\hat{I}_2$ is the 2×2 identity, and $\hat{\sigma}_+$, $\hat{\sigma}_-$ are the spin raising and lowering operators. Using Eq. (III.27), I can write the coin

operator generated by this as

$$
\begin{aligned}
\left[\exp\left(-i\epsilon\hat{A}^\dagger\hat{A}\right)\right]_j &\doteq \hat{I}_2 + \frac{1}{2}(\exp\left(-i2\epsilon\right)-1)(\hat{I}_2 + e^{-i\theta}\hat{\sigma}_+ + e^{+i\theta}\hat{\sigma}_-) \\
&= \frac{1}{2}(\exp\left(-i2\epsilon\right)+1)\hat{I}_2 + \frac{1}{2}(\exp\left(-i2\epsilon\right)-1)(e^{-i\theta}\hat{\sigma}_+ + e^{i\theta}\hat{\sigma}_-) \\
&\doteq e^{-i\epsilon}\begin{pmatrix} \cos\left(\epsilon\right) & -ie^{-i\theta}\sin\left(\epsilon\right) \\ -ie^{i\theta}\sin\left(\epsilon\right) & \cos\left(\epsilon\right) \end{pmatrix}.
\end{aligned}
\tag{III.31}
$$

This is similar to the types of coins used by Strauch in Refs. [40, 41] and Debbasch and Di Molfetta in Refs. [14, 16] with one caveat. Those papers used the shift operator given by Eq. (I.2), which means the coin must be modified by $\hat{\sigma}_x$. Still, a similar limit is obtained with a shift in ϵ. In particular, consider when $\theta = -\frac{\pi}{2}$ and $\epsilon = \frac{\pi}{4}$:

$$
\begin{aligned}
\left[\exp\left(-i\frac{\pi}{4}\hat{A}^\dagger\hat{A}\right)\right]_j &\doteq \frac{\exp\left(-i\frac{\pi}{4}\right)}{\sqrt{2}}\begin{pmatrix} 1 & 1 \\ -1 & 1 \end{pmatrix} \\
&\doteq \exp\left(-i\frac{\pi}{4}\right)\hat{C}_H\,\hat{\sigma}_x.
\end{aligned}
\tag{III.32}
$$

Thus the Hadamard walk can be linked directly to a graph Hamiltonian with pure imaginary hopping amplitudes, which might be described as the one-dimensional lattice in the presence of a constant magnetic vector potential of a specific strength [33], i.e. a cycle encircling the outside of a solenoid.

Finally, I can put a constraint on the size of ϵ. In Ch. II, I assumed that $\|\hat{K}_1\|_2$ was much less than α. The induced ℓ_2-norm is the largest eigenvalue in absolute value [25], and it is clear from the first equality of Eq. (III.26) that $\|\hat{A}^\dagger\hat{A}\|_2 = \max_i \omega_i$, which is actually the induced ℓ_1-norm of $\hat{H}_0$. So for the lazy QW choice (and likewise for the QW choice), one

needs to fix α such that $\alpha\epsilon \ll 1 < \frac{\pi}{2}$, which gives the constraint

$$\max_i \omega_i\, \epsilon \ll \frac{\pi}{2}. \tag{III.33}$$

III.5 Examples of the Correspondence: Motivating the Very-lazy Quantum Walk

The simplest possible model is the one depicted in Fig. III.2 with $\theta = 0$. By standard methods, the CTQW propagator can found to be

$$\langle n| \exp\left(-it\hat{H}_0^{(1D)}\right)|0\rangle = (i)^n \mathcal{J}_n(2t), \tag{III.34}$$

where $\mathcal{J}_n(x)$ is the nth Bessel function. The details of this derivation are provided in Appendix A. This is compared against the DTQW method described above in Figs. III.3. As suspected, the QW choice in Fig. III.3a results in a checkerboard pattern. The pattern is shown more clearly in Fig. III.4. As mentioned at the end of Ch. II, one can lazy the swap half of the time-translation operator for $\frac{\pi}{2} < \alpha\epsilon < \pi$. In that case, the internal patterns change until at a relatively lazy condition ($a = \epsilon$, for a defined in Eq. (II.28)) the pattern become smooth in Fig III.3d. The surprising result is Fig. III.3e. When $a = \frac{\epsilon}{10} \ll \frac{\epsilon\omega}{2}$, the pattern is virtually the same as the CTQW solution in Fig. III.3f, but at the cost of ten times the number of steps. The lazy QW choice is only supposed to give the exact probability of the CTQW at periodic times, but not for all times. As mentioned in Sec. II.7, one expects as a becomes very small compared to ϵ, the smallness of a overtakes that of ϵ. I conjecture the condition is $a \ll \frac{\epsilon\omega}{2}$, which I refer to as the *very-lazy QW choice*. It is argued in the next three sections that all these observations hold for any DTQW connected to a regular CTQW.

(a) $\alpha\epsilon = \frac{\pi}{2}$

(b) $\alpha\epsilon = \frac{11\pi}{20}$

(c) $\alpha\epsilon = \frac{3\pi}{4}$

(d) $\alpha\epsilon = \frac{39\pi}{40}$

(e) $\alpha\epsilon = \frac{39.9\pi}{40}$

(f) CTQW
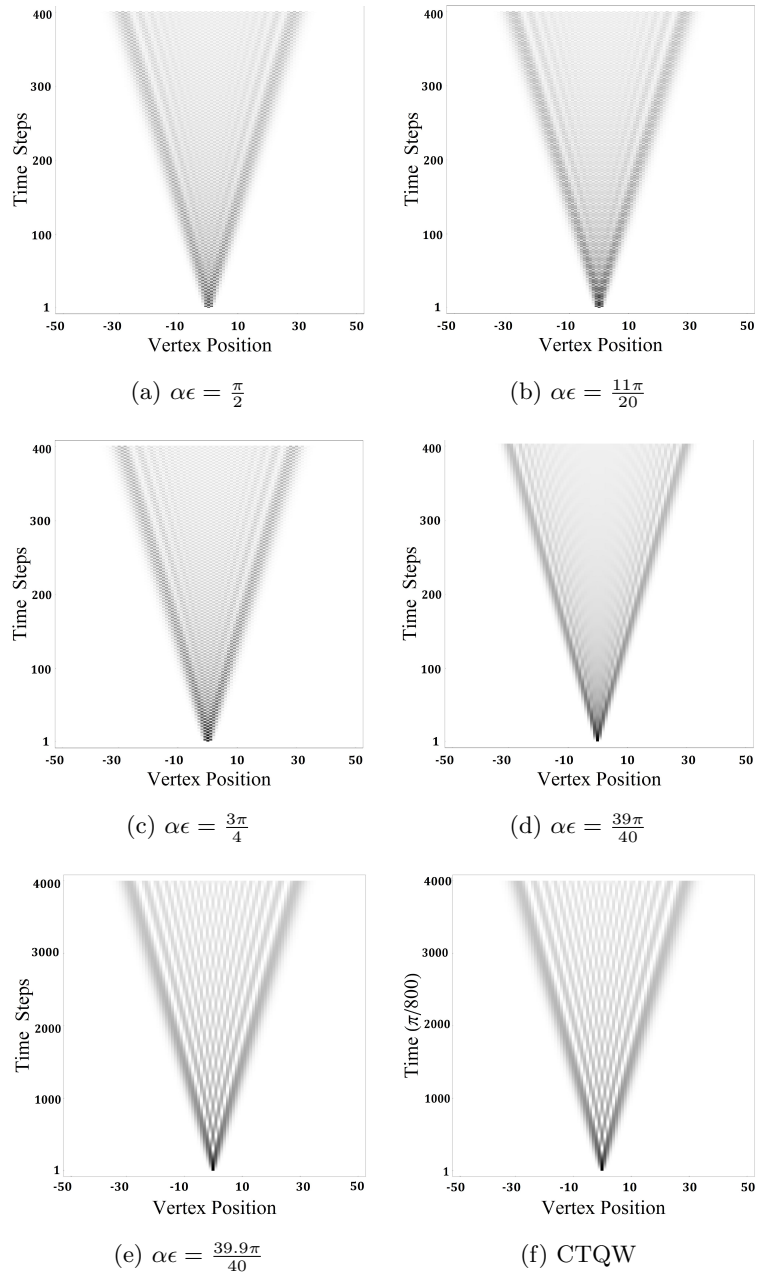
FIGURE III.3: Simulations on a cycle of 100 vertices with hopping amplitudes of 1 and the center vertex basis state as the initial state. (a)-(e) are DTQW with $\epsilon = \frac{\pi}{40}$ and $\alpha\epsilon$ as labeled. Note the increase in time steps for (e). (f) is a CTQW based upon the modulus squared of Eq. (III.34).

46
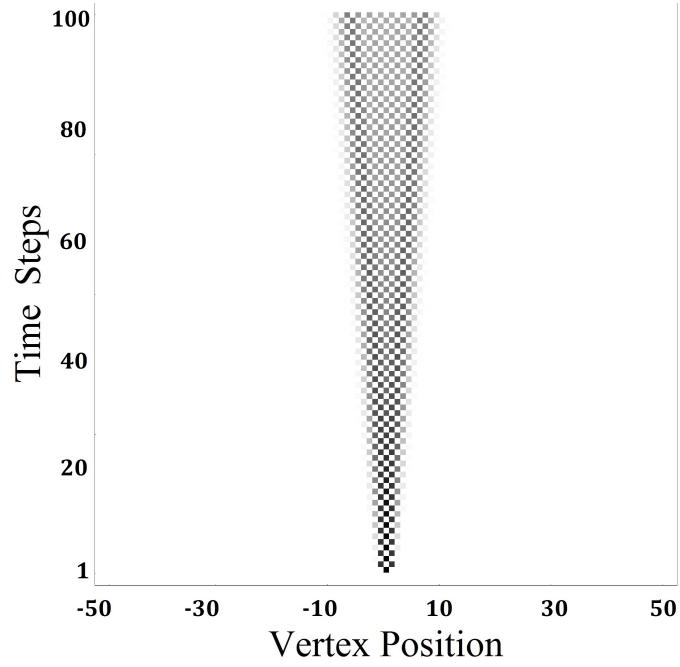
FIGURE III.4: The same simulation as Fig. III.3a but with fewer time steps to show the checkerboard pattern given by the QW choice.

The one-dimensional lattice naturally extends to the two-dimensional lattice with the adjacency Hamiltonian. For the CTQW, the graph Hamiltonian is separable, and so the propagator is given by the product of two one-dimensional propagators:

$$\langle (n,m)| \exp\left(-it\hat{H}_0^{(2D)}\right)|(0,0)\rangle = (i)^{n+m}\mathcal{J}_n(2t)\mathcal{J}_m(2t). \qquad (III.35)$$

The result is also derived in Appendix A. This model is compared against the DTQW simulation for the QW choice and the very-lazy QW choice in Figs. III.5. Both choices show the same relationship to the CTQW as found in the one-dimensional model. However, the very-lazy QW choice still does not render some of the detail of the CTQW, especially where the probability is nearly zero. The error is shown in Fig. III.5d.

(a) CTQW

(b) QW choice

(c) very-lazy QW

(d) Error in (c)
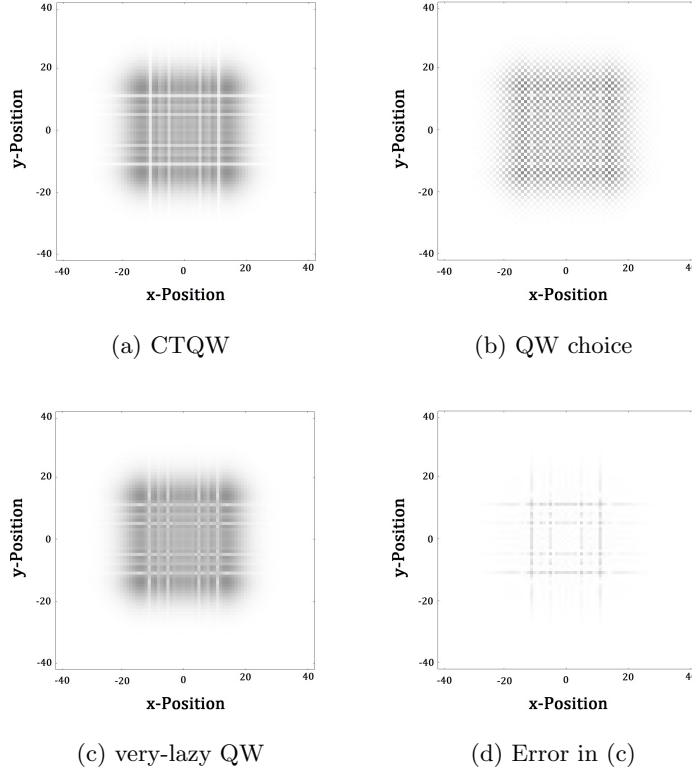
FIGURE III.5: Simulations on an 80 by 80 square lattice with periodic boundary conditions and hopping amplitudes of 1. The center vertex basis state is the initial state and $\epsilon = \frac{\pi}{80}$. (a) is the CTQW solution given by the modulus squared of Eq. (III.35) at time 100ϵ. (b) is the QW choice after 200 steps. (c) is the very-lazy QW choice after 8000 steps with $a = \frac{\epsilon}{10}$. (d) is the absolute difference between (a) and (c).

III.6 Exact Expansion of the Discrete-time Quantum Walk

To understand the behavior exhibited in the last section and to show that it is general for a large number of graph Hamiltonians, I expand the general DTQW time-translation operator given in Eq. (III.21) using a method similar to that used to expand $\hat{H}_1$ and $\hat{J}_1$ earlier in this chapter. I assume again that the initial state is contained in $\mathcal{H}_{dyn}$ and for simplicity, I also assume the graph Hamiltonian is regular. Since $\hat{U}_1(\epsilon)$ satisfies the properties of the

conditional in Prop. III.4, I can use the corollary to assume that for any integer power t,

$$\left(\hat{U}_1(\epsilon)\right)^t \hat{A}^\dagger = \hat{A}^\dagger \hat{f}_0^{(t)} + \hat{B}^\dagger \hat{g}_0^{(t)}. \tag{III.36}$$

To simplify the notation, let $\not{c} = \cos(\alpha\epsilon)$ and $\not{s} = \sin(\alpha\epsilon)$ and let multiplication by the identity be understood for scalar terms. Also note $\hat{\mathscr{E}}_1 = \mathscr{E}\hat{I}_1$, where $\mathscr{E} = \frac{1}{\omega}(\exp(-i\epsilon\omega) - 1)$. Multiplying on the left of Eq. (III.36) by $\hat{U}_1(\epsilon)$, I have

$$
\begin{aligned}
\left(\hat{U}_1(\epsilon)\right)^{t+1} \hat{A}^\dagger &= \left(\not{c} - i\not{s}\hat{S}_1\right)\left(1 - i\mathscr{E}\hat{A}^\dagger\hat{A}\right)\left(\hat{A}^\dagger \hat{f}_0^{(t)} + \hat{B}^\dagger \hat{g}_0^{(t)}\right) \\
&= \hat{A}^\dagger\left(\not{c}\hat{f}_0^{(t)}(1 - i\mathscr{E}\omega) - i\hat{g}_0^{(t)}\left(\not{c}\mathscr{E}\hat{H}_0 + \not{s}\right)\right) \tag{III.37} \\
&\quad + \hat{B}^\dagger\left(\hat{g}_0^{(t)}\left(\not{c} - \not{s}\mathscr{E}\hat{H}_0\right) - i\not{s}\hat{f}_0^{(t)}(1 - i\mathscr{E}\omega)\right) \\
&= \hat{A}^\dagger \hat{f}_0^{(t+1)} + \hat{B}^\dagger \hat{g}_0^{(t+1)}. \tag{III.38}
\end{aligned}
$$

I can use the exact relation, $1 - i\mathscr{E}\omega = \exp(-i\epsilon\omega)$ to simplify the expression, and by equating like operators on both sides, I get the matrix recursion

$$\begin{pmatrix} \hat{f}_0^{(t+1)} \\ \hat{g}_0^{(t+1)} \end{pmatrix} = \begin{pmatrix} \not{c} & -i\not{s} \\ -i\not{s} & \not{c} \end{pmatrix}\begin{pmatrix} \exp(-i\epsilon\omega) & -i\mathscr{E}\hat{H}_0 \\ 0 & 1 \end{pmatrix}\begin{pmatrix} \hat{f}_0^{(t)} \\ \hat{g}_0^{(t)} \end{pmatrix}, \tag{III.39a}$$

with the un-normalized initial condition

$$\begin{pmatrix} \hat{f}_0^{(0)} \\ \hat{g}_0^{(0)} \end{pmatrix} = \begin{pmatrix} 1 \\ 0 \end{pmatrix}. \tag{III.39b}$$

49

If I denote the multiplication of the two matrices in Eq. (III.39a) by $\underline{U}$, then the solution to Eq. (III.39) is

$$
\begin{pmatrix} \hat{f}_0^{(t)} \\ \hat{g}_0^{(t)} \end{pmatrix} = \underline{U}^t \begin{pmatrix} 1 \\ 0 \end{pmatrix}.
\tag{III.40}
$$

To simplify this, I need to find the eigenvalue operators and eigenvector operators of $\underline{U}$. The determinant of $\underline{U}$ is equal to the product of the determinants of its constituents, implying $\det(\underline{U}) = \exp(-i\epsilon\omega)$. Also by performing the multiplication, one finds the trace to be $\mathrm{Tr}(\underline{U}) = \cancel{c}\exp(-i\epsilon\omega) - \cancel{s}\mathscr{E}\hat{H}_0 + \cancel{c}$. For a 2×2 matrix, this immediately leads to the eigenvalue operators

$$
\begin{aligned}
\hat{\lambda}_0^\pm &= \frac{1}{2}\left(\mathrm{Tr}(\underline{U}) \pm \sqrt{\mathrm{Tr}(\underline{U})^2 - 4\exp(-i\epsilon\omega)}\right) \\
&= \exp(-\frac{i\epsilon\omega}{2})\left(\hat{\gamma}_0 \pm i\sqrt{1-\hat{\gamma}_0^2}\right) = \exp\left(-\frac{i\epsilon\omega}{2}\right)\exp(\pm i\arccos(\hat{\gamma}_0)),
\end{aligned}
\tag{III.41a}
$$

where

$$
\begin{aligned}
\hat{\gamma}_0 &= \frac{\exp\left(\frac{i\epsilon\omega}{2}\right)}{2}\,\mathrm{Tr}(\underline{U}) \\
&= \frac{\exp\left(\frac{i\epsilon\omega}{2}\right)}{2}\left(\cancel{c}(\exp(-i\epsilon\omega)+1) - i\cancel{s}(\exp(-i\epsilon\omega)-1)\frac{\hat{H}_0}{\omega}\right) \\
&= \cos(\alpha\epsilon)\cos\left(\frac{\epsilon\omega}{2}\right) - \sin(\alpha\epsilon)\sin\left(\frac{\epsilon\omega}{2}\right)\frac{\hat{H}_0}{\omega}.
\end{aligned}
\tag{III.41b}
$$

From here, it is a tedious exercise to find the eigenvector operators and expand the powers of $\underline{U}$, but the result is

$$
\begin{pmatrix} \hat{f}_0^{(t)} \\ \hat{g}_0^{(t)} \end{pmatrix} = \exp\left(-\frac{i\omega\epsilon(t+1)}{2}\right)\begin{pmatrix} \cancel{c}\,p_{t-1}(\hat{\gamma}_0) - \exp\left(i\frac{\epsilon\omega}{2}\right)p_{t-2}(\hat{\gamma}_0) \\ -i\cancel{s}\,p_{t-1}(\hat{\gamma}_0) \end{pmatrix},
\tag{III.42}
$$

where p_n is the nth Chebyshev polynomial of the second kind. For the properties of the Chebyshev polynomials, see Refs. [17, 32]. A rigorous proof that Eq. (III.42) is equivalent to Eq. (III.40) is given in Appendix B. As claimed, if the spectral decomposition of the graph Hamiltonian is known, Eq. (III.42) can be expanded and probability given by Eq. (III.13). As a final point, it is important to show that $\gamma_0(E) \in [-1, 1]$, where E is an eigenvalue of $\hat{H}_0$. This is the traditional domain of the Chebyshev polynomials. By inspection, it should be sufficient to show that

Proposition III.5. *For any eigenvalue of $\hat{H}_0$, E, $\frac{|E|}{\omega} \leq 1$.*

Proof. From matrix analysis, the spectrum of any matrix is bounded by any norm [25]. Since $\omega = \|\hat{H}_0\|_1$, this implies $|E| \leq \omega$. $\qquad\square$

III.7 Understanding the Various Choices for the Discrete-time Quantum Walk

I can show that Eq. (III.42) agrees with the result that the QW choice approximates the exponentiation of $\exp\left(-it\hat{J}_1\right)$ given in Eq. (III.24) for even time steps. In this case, $\cos(\alpha\epsilon) = 0$ and $\sin(\alpha\epsilon) = 1$, leaving

$$\begin{pmatrix} \hat{f}_0^{(t)} \\ \hat{g}_0^{(t)} \end{pmatrix} = \exp\left(-\frac{i\omega\epsilon t}{2}\right) \begin{pmatrix} -p_{t-2}(\hat{\gamma}_0) \\ -i\exp\left(-i\frac{\omega\epsilon}{2}\right)p_{t-1}(\hat{\gamma}_0) \end{pmatrix}; \tag{III.43}$$

$$\hat{\gamma}_0 = -\sin\left(\frac{\epsilon\omega}{2}\right)\frac{\hat{H}_0}{\omega} = \cos\left(\frac{\pi}{2} - \frac{\epsilon}{2}\hat{H}_0\right) + \mathcal{O}(\epsilon^3), \tag{III.44}$$

where a shift in the sine function was used in the last equality. Using this expression for $\hat{\gamma}_0$ and the properties of the Chebyshev polynomials,

$$p_{n-1}(\hat{\gamma}_0) = \frac{\sin\left(\frac{n\pi}{2} - \frac{n\epsilon}{2}\hat{H}_0\right)}{\cos\left(\frac{\epsilon}{2}\hat{H}_0\right)} + \mathcal{O}(\epsilon^3). \tag{III.45}$$

Thus, $\hat{f}_0^{(t)}$ and $\hat{g}_0^{(t)}$ are given to first order in ϵ (ϵt treated as non-negligible)

$$\begin{pmatrix} \hat{f}_0^{(t)} \\ \hat{g}_0^{(t)} \end{pmatrix} \approx \exp\left(-\frac{i\omega\epsilon t}{2}\right) \begin{cases} (-1)^{\frac{t}{2}}\begin{pmatrix} \cos\left(\frac{\epsilon(t-1)}{2}\hat{H}_0\right) \\ i\exp\left(-\frac{i\omega\epsilon}{2}\right)\sin\left(\frac{\epsilon t}{2}\hat{H}_0\right) \end{pmatrix}, & t \text{ even} \\[2em] (-1)^{\frac{(t-1)}{2}}\begin{pmatrix} \sin\left(\frac{\epsilon(t-1)}{2}\hat{H}_0\right) \\ -i\exp\left(-\frac{i\omega\epsilon}{2}\right)\cos\left(\frac{\epsilon t}{2}\hat{H}_0\right) \end{pmatrix}, & t \text{ odd} \end{cases}. \tag{III.46}$$

Note that as expected, this compares to a CTQW time interval of $\Delta t = \frac{\epsilon}{2}$. Also, the even time steps agree with Eq. (III.24), but one can also see that for an initial state on one sub-lattice of a bipartite graph, odd time steps only have support on the other sub-lattice. The behavior is similar to the classical random walk, where the walker is only found on even vertices for even time steps and odd vertices for odd time steps. So the state initialized on one sub-lattice of a bipartite graph flip-flops between the two sub-lattices according to the even-oddness of the time steps. In fact, this even-odd dependence is true for the QW choice regardless of the size of ϵ, since $\hat{\gamma}_0 \propto \hat{H}_0$ and $p_n(\hat{\gamma}_0)$ only has $n - 2k$ powers of $\hat{\gamma}_0$ for integer k such that $0 \leq k \leq \lfloor\frac{n}{2}\rfloor$. Such behavior is broken to some extent by all other choice of $\alpha\epsilon$ modulo π.

Due to the competing limits, understanding the very-lazy QW choice is more complicated. To start, I assume that both a and ϵ are small compared to 1 and note that

$$\hat{\gamma}_0 = \not{c}' - \hat{\gamma}_0', \tag{III.47}$$

where $\hat{\gamma}_0' = \sin(\alpha\epsilon)\sin\left(\frac{\epsilon\omega}{2}\right)\left(I_0 + \frac{\hat{H}_0}{\omega}\right)$ and $\not{c}' = \cos\left(\alpha\epsilon - \frac{\epsilon\omega}{2}\right)$. Since $\hat{\gamma}_0'$ is small under the assumptions, one can expand the inverse cosine about $\not{c}'$ as

$$\arccos(\hat{\gamma}_0) = \alpha\epsilon - \frac{\epsilon\omega}{2} + \frac{\sin(\alpha\epsilon)\sin\left(\frac{\epsilon\omega}{2}\right)}{|\sin\left(\alpha\epsilon - \frac{\epsilon\omega}{2}\right)|}\left(I_0 + \frac{\hat{H}_0}{\omega}\right) + \mathcal{O}\left((\hat{\gamma}_0')^2\right). \tag{III.48}$$

Care has to be taken since the derivatives of the inverse cosine are singular at π. Thus the powers of sine in the denominator of such derivatives are the most important, i.e. $\left(\frac{d}{dx}\right)^n \arccos(x)|_{x=\not{c}'} \sim \left(\cos\left(\alpha\epsilon - \frac{\epsilon\omega}{2}\right)\right)^{n-1}\left|\sin\left(\alpha\epsilon - \frac{\epsilon\omega}{2}\right)\right|^{1-2n}$. The factors of cosine are not so important since they are nearly 1, and so the nth term in the expansion including the relevant facts from $\hat{\gamma}_0'$ go as

$$\left(\sin(a)\sin\left(\frac{\epsilon\omega}{2}\right)\right)^n \left|\sin\left(a + \frac{\epsilon\omega}{2}\right)\right|^{1-2n}, \tag{III.49}$$

where $\alpha\epsilon = \pi - a$ is used. Thus it is clear that the higher order terms in Eq. (III.48) are negligible. Using only the first order terms in ϵ and a, Eq. (III.48) can be written as

$$\arccos(\hat{\gamma}_0) = \pi - a - \frac{\epsilon\omega}{2} + \frac{a\epsilon\omega}{|2a - \epsilon\omega|}\left(I_0 + \frac{\hat{H}_0}{\omega}\right) + \mathcal{O}(\epsilon^2, a^2). \tag{III.50}$$

This is where one must know the relative sizes of the parameters so that the denominator of the fourth term in Eq. (III.50) can be expanded. If $\frac{2a}{\epsilon\omega} < 1$, then

$$\arccos(\hat{\gamma}_0) = \pi - \frac{\epsilon\omega}{2} + \frac{a}{\omega}\hat{H}_0 + \mathcal{O}\left(\epsilon^2, a^2, \left(\frac{2a}{\epsilon\omega}\right)\right). \tag{III.51}$$

Note the assumption here is the same as the hypothesis for the very-lazy QW choice as mentioned in Sec. III.5. In that case, $\hat{f}_0^{(t)}$ and $\hat{g}_0^{(t)}$ are given by

$$
\begin{pmatrix} \hat{f}_0^{(t)} \\ \hat{g}_0^{(t)} \end{pmatrix} = \frac{\exp\left(-i\frac{\omega\epsilon(t+1)}{2}\right)}{\sqrt{1-\hat{\gamma}_0^2}} \begin{pmatrix} \not{c} \; \sin\left(t \arccos\left(\hat{\gamma}_0\right)\right) - \exp\left(i\frac{\epsilon\omega}{2}\right) \; \sin\left((t-1)(\arccos\left(\hat{\gamma}_0\right))\right) \\ -i\not{s} \; \sin\left(t \arccos\left(\hat{\gamma}_0\right)\right) \end{pmatrix}
$$

$$
\approx (-1)^t \frac{\exp\left(-i\frac{\omega\epsilon(t+1)}{2}\right)}{\sqrt{1-\hat{\gamma}_0^2}} \begin{pmatrix} \sin\left(t(\frac{a}{\omega}\hat{H}_0 - \frac{\epsilon\omega}{2})\right) - \exp\left(i\frac{\epsilon\omega}{2}\right) \; \sin\left((t-1)(\frac{a}{\omega}\hat{H}_0 - \frac{\epsilon\omega}{2})\right) \\ -ia \; \sin\left(t(\frac{a}{\omega}\hat{H}_0 - \frac{\epsilon\omega}{2})\right) \end{pmatrix}
$$

$$\text{(III.52)}$$

Already one sees that $\hat{g}_0^{(t)}$ goes as a. Considering $\hat{f}_0^{(t)}$, the sine functions can be expanded as exponentials and after a lot of tedious work, one finds

$$
\begin{pmatrix} \hat{f}_0^{(t)} \\ \hat{g}_0^{(t)} \end{pmatrix} = (-1)^{t-1} \exp\left(-i\omega\epsilon(t+\frac{1}{2})\right) \begin{pmatrix} \exp\left(i\frac{a}{\omega}t\hat{H}_0\right) \\ 0 \end{pmatrix} + \mathcal{O}\left(\epsilon, a, \frac{2a}{\epsilon\omega}\right) \qquad \text{(III.53)}
$$

As mentioned earlier in the chapter, Eq. (III.13) says as $\hat{g}_0^{(t)}$ approaches zero, $\hat{f}_0^{(t)}$ becomes the only contribution to the probability, here $\exp\left(i\frac{a}{\omega}t\hat{H}_0\right)$ up to the global phase. This is actually the adjoint of the CTQW time-translation operator, but such a distinction should not affect the probability. Also the interval goes from $\frac{\epsilon}{2}$ for the QW choice to $\frac{a}{\omega}$ in the very-lazy QW choice as observed in Sec. III.5.

III.8   Consequences of Connecting the Continuous-time to the Discrete-time Quantum Walk

As a consequence of the connection, I claim that for a quantum system capable of performing any arbitrary DTQW of the form discussed here, that system could simulate any CTQW.

Furthermore, such a system could be used to simulate spatially discretized quantum models, ideally ones that are more complicated such as models that lack spatial and temporal symmetry. Furthermore, not every DTQW has a corresponding CTQW, which is to say the DTQW has more freedom over the CTQW. This is by virtue of the fact that $\mathcal{H}_{dyn} \subseteq \mathcal{H}_{\mathcal{E}}$, where the subset is strict in all cases except for the one-dimensional cycle and perhaps a few other trivial graphs. This is not surprising given the enlarged space, but it is an argument for using the DTQW over the CTQW, if that freedom can be exploited. With that in mind, it is worth making a distinction between DTQWs that do and do not satisfy the following:

Definition III.6. A DTQW is *connected* to a CTQW if and only if

1. $i\ln(\hat{C}_1)$ can be written as $\beta \hat{A}^{\dagger} \hat{A} + \phi$, for some β, $\phi \in \mathbb{R}$ and $\hat{A}$ in the form of Eq. (III.1) for an arbitrary set of complex numbers $\{T_{ij} : (i,j) \in \mathcal{E}\}$, and

2. the initial state is a member of $\mathcal{H}_{dyn}$.

The CTQW connected to such a DTQW is characterized by a graph Hamiltonian with hopping amplitudes given by Eq. (III.4) and initial state dependent on the initial state in the edge space.

CHAPTER IV

APPLICATION: SEARCH ON THE HYPERCUBE

Search algorithms are one of the quintessential categories of quantum algorithms and there are several examples, some of which were mentioned in Ch. I. The setup is as follows: a quantum system is prepared in such a way that one measurement outcome representing the marked element is preferred but the exact outcome and structure of the system is unknown to the user. The user has control over a limited set of inputs such as the initial state, time of measurement and so on, and the goal is that the user measures the preferred outcome with a high probability, typically 50% or better. It is important for a quantum search algorithm that the exact time to measure is known since the measurement de-coheres the state, and if the measurement is performed too late, the state of the system evolves past the intended state. Typically, this reduces the probability of measuring the mark element by a significant margin. This is a considerable difference from the classical oracle search. The probability in the classical case monotonically increases with queries to the oracle.

A noteworthy DTQW search algorithm example is discussed by Shenvi et al. [37], and a CTQW version is described by Childs and Goldstone [10]. These quantum search algorithms represent the search space as vertices and must somehow distinguish the marked element in the time-translation operator. The CTQW method involves using the adjacency Hamiltonian modified with the *oracle Hamiltonian*. If m is the marked element, the oracle Hamiltonian is given as $-|m\rangle\langle m|$. For the DTQW, Shenvi uses the *hypercube* graph (to be

discussed in the next section). The coin operator is a modified version of the Grover coin operator as described in Sec. III.4, where the block part for the marked element is replaced by negative one times the identity in that subspace. A quantum oracle (discussed in Ch. I) is used to "choose" the appropriate block part of the coin operator for the marked element.

It has been proven that any search algorithm based on a quantum oracle can achieve the desired result in no fewer than $\mathcal{O}(\sqrt{N})$ queries to the oracle [5, 6, 46]. If I equate the number of queries to the oracle with the number of time steps in the DTQW, then the search algorithm I propose on the hypercube appears to reach a probability greater than 50% for measuring the marked element in a number of steps that does not scale with N. Because of the proofs presented in Refs.[5, 6, 46], this is a controversial claim, and at this time, there is only numerical results to support it. Thus, it is not clear that the behavior persists for any dimension of the hypercube. Furthermore, there is a free parameter which must be determined to optimize the probability. Still, I present the algorithm, the numerical results and the current understanding of the anomalous behavior.

IV.1   Basics of the Hypercube

The graph of the hypercube is defined as follows:

Definition   IV.1. The d-dimensional   hypercube   is   the   graph   such   that $\mathcal{V} = \{n : n \in \mathbb{Z} \cap [0, 2^d)\}$ and $(n, m) \in \mathcal{E}$ if and only if the binary expansion of n is different from that of m by a single digit (bit).

Fig. IV.1 is a visual representation of the hypercube for $d = 3$. I am going to suppress any notation on operators, states and spaces which signifies the dimension of the hypercube since it is understood that I am working in an arbitrary dimension d. In general, the size
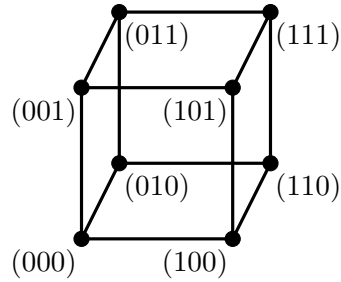
FIGURE IV.1: Visual representation of the $d = 3$ hypercube. The vertices are labeled based upon their binary expansion.

of the search space is $N = 2^d$ and the degree or coordination number of every vertex is d. Some useful concepts for the hypercube are the *Hamming weight, Hamming distance* and the *binary dot product*.

Definition IV.2. For any positive integer n, let $n_i \in \{0, 1\}$ be the ith digit in the binary expansion of n. Then one can define the following:

1. the Hamming weight of a positive integer n, denoted $\|n\|$, is given by $\|n\| = \sum_i n_i$,

2. the Hamming distance between two positive integers n and m is given by $\|n \oplus m\|$, where $\oplus$ is the bitwise XOR operation, and

3. the binary dot product between two positive integers n and m, denoted by $n \circ m$, is given by $n \circ m = \sum_i n_i m_i$.

The Hamming weight is the number of ones in the binary expansion, the Hamming distance is the number of binary digits which are unequal between the two values, and the binary dot product is the number of digits in which the two values have an overlapping 1. The Hamming distance also gives the graph distance. This means I can restate the connectivity condition of the hypercube by saying that $n@m$ if and only $\|n \oplus m\| = 1$, which implies

there exists an integer p, such that $0 \leq p < d$ and $n = m \oplus 2^p$. Also for dimension d, the number of vertices with Hamming weight p is given by the binomial coefficient $\binom{d}{p}$.

Eigenvectors and values of the adjacency Hamiltonian for the hypercube can be found using representation theory. The details of the method are given by Tinkham [43]. There are a number of symmetry groups of the hypercube, but the simplest is given by $\{\hat{\bigoplus}_n : n \in \mathbb{Z} \cap [0, N)\}$, where for any basis state, $|n\rangle$, $\hat{\bigoplus}_m |n\rangle = |m \oplus n\rangle$. Because XOR is associative, commutative and its own inverse, this group preserves the connectedness of the hypercube, is Abelian and every element is its own inverse. Thus all the representations consist of 1's and -1's from which the eigenvectors can be formed. A convenient way to represent this is given in the following proposition:

Proposition IV.3. *Let $\hat{H}_0 = \sum_{n=0}^{N-1} \sum_{p=0}^{d-1} |n\rangle\langle n \oplus 2^p|$ be the graph Hamiltonian for the hypercube. Then for all $k \in \mathbb{Z} \cap [0, N)$, $|\phi_k\rangle = \frac{1}{\sqrt{N}} \sum_{n=0}^{N-1} (-1)^{n \circ k} |n\rangle$ is an eigenvector of $\hat{H}_0$ with eigenvalue $E_k = d - 2\|k\|$.*

Proof. Consider

$$
\begin{aligned}
\hat{H}_0 |\phi_k\rangle =& \frac{1}{\sqrt{N}} \sum_{m=0}^{N-1} \sum_{n=0}^{N-1} \sum_{p=0}^{d-1} (-1)^{m \circ k} |n\rangle\langle n \oplus 2^p|m\rangle \\
=& \frac{1}{\sqrt{N}} \sum_{n=0}^{N-1} (-1)^{n \circ k} \left(\sum_{p=0}^{d-1} (-1)^{n \circ k} (-1)^{(n \oplus 2^p) \circ k} \right) |n\rangle .
\end{aligned}
\tag{IV.1}
$$

Looking at the exponent of any term in the bracketed sum, one has

$$
n \circ k + (n \oplus 2^p) \circ k = \sum_{i \neq p} 2n_i k_i + (n_p + n_p \oplus 1)k_p = 2 \sum_{i \neq p} n_i k_i + k_p.
\tag{IV.2}
$$

The first term in Eq. (IV.2) is even and results in a factor of 1 for the pth term in the bracketed sum of Eq. (IV.1). The remaining term in Eq. (IV.2) is independent of n which

implies the bracketed sum can be factored out of the sum on n. Therefore, I have

$$\hat{H}_0 \left| \phi_k \right\rangle = E_k \left| \phi_k \right\rangle; \tag{IV.3}$$

$$E_k = \sum_{p=0}^{d-1} (-1)^{k_p} = d - 2\|k\|. \tag{IV.4}$$

$\square$

The spectrum of the hypercube takes on integer values, is bounded as $|E_k| \leq d$, skips every other integer and has the degeneracy $\binom{d}{\|k\|}$. Since $\hat{H}_0$ is Hermitian, a corollary to this is that for any k, $l \in \mathbb{Z} \cap [0, N)$,

$$\sum_{n=0}^{N-1} (-1)^{k \circ n} (-1)^{l \circ n} = N \delta_{kl}, \tag{IV.5}$$

but really this is a consequence of the orthogonality theorem of representation theory [43].

IV.2   Proposed Algorithm and Numerical Results

The algorithm I propose takes place on a modified hypercube in dimension d, where one element is considered marked. Let that element be m. Also, let any object associated with this modified hypercube be denoted with a prime. In $\mathcal{H}'_\mathcal{V} = \mathcal{H}_\mathcal{V}$, the hypercube is modified with self-loops on each vertex, and the graph Hamiltonian is the adjacency Hamiltonian without self-loops plus a diagonal perturbation such that $\hat{H}'_0 = \hat{H}_0 + \hat{W}_0$, which is given by

$$\hat{W}_0 = \sum_{n=0}^{N-1} w_n \left| n \right\rangle\!\left\langle n \right|, \tag{IV.6a}$$

and

$$w_n = (1-x)^{\|n \oplus m\|}(1+x)^{d-\|n \oplus m\|}. \tag{IV.6b}$$

$x \in [0,1]$ is an optimization parameter. The new graph is depicted in Fig. IV.2. The self-loop weights, $\{w_n : n \in \mathbb{Z} \cap [0,N)\}$, may seem arbitrary, but they have some interesting properties. First, they satisfy a sum rule independent of x:

$$\sum_{n=0}^{N-1} w_n = \sum_{p=0}^{d} \binom{d}{p}(1-x)^p(1+x)^{d-p} = (1-x+1+x)^p = N. \tag{IV.7}$$

They also preserve some of the symmetry of the hypercube. The perturbation fixes the marked corner and the vertex furthest away, but any transformation which preserves both the connectivity and Hamming distance from m is a symmetry of the graph Hamiltonian. Also for all values of x except 0 and 1, the marked element has the largest weight and the furthest corner from the marked element has the smallest. Furthermore, $\hat{W}_0$ expanded in the eigenbasis of the unperturbed hypercube is particularly useful. All of this is more thoroughly discussed later in this chapter.
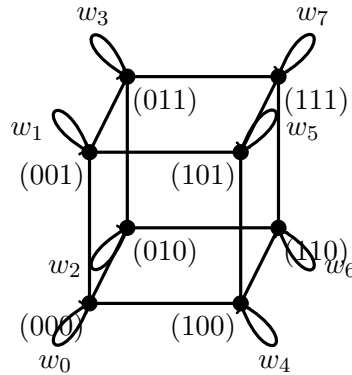

FIGURE IV.2: Visual representation of the modification made to the $d = 3$ hypercube for the proposed search algorithm.

Given the perturbed graph Hamiltonian, the algorithm uses a DTQW in the form of Eq. (III.25) (which is the QW choice). To keep $\mathcal{H}'_{\mathcal{E}} = \mathcal{H}_{\mathcal{E}}$, it is understood that for the unperturbed system, there are basis states, $|n, n\rangle \in \mathcal{H}_{\mathcal{E}}$, but they are connected to the rest of the hypercube only by the perturbation. Since the marked element is unknown, the initial state must reflect this:

$$|\psi, 0\rangle = \frac{1}{\sqrt{dN}} \sum_{n=0}^{N-1} \sum_{p=0}^{d-1} |n \oplus 2^p, n\rangle = \frac{1}{2\sqrt{dN}} \left(\hat{A}^{\dagger} + \hat{B}^{\dagger} \right) |\phi_0\rangle, \quad (\text{IV.8})$$

which is an equal superposition over all edges internal to the hypercube but with no support on the self-loop basis states. Note that although the coin operator is connected to the perturbed CTQW as per Def. III.6, the initial state is not connected to the perturbed CTQW but rather to the unperturbed CTQW. I claim that for a specific value of x and at a certain number of time steps, the probability to measure m as given by Eq. (II.10) is greater than 50%. The extreme possibilities for the self-loop weights occurs when $x = 0$, which gives $w_n = 1$ for all n and $x = 1$, which gives $w_n = N\delta_{nm}$. Based upon the typical CTQW search, one would suspect that the optimal case is when $x = 1$, but that turns out to be not true. Furthermore the numerical simulations presented in Figs. IV.3 show that the apparent best case found by trial and error is dependent on d. There is a condition I can use to get close to this result which is for $m = 0$, $w_0 - w_1 \approx \frac{3}{2}$. This was found empirically and seems to get worse as the dimension increases. Also Figs. IV.3 support my claim that the number of steps needed to achieve the desired result does not appear to scale with N.
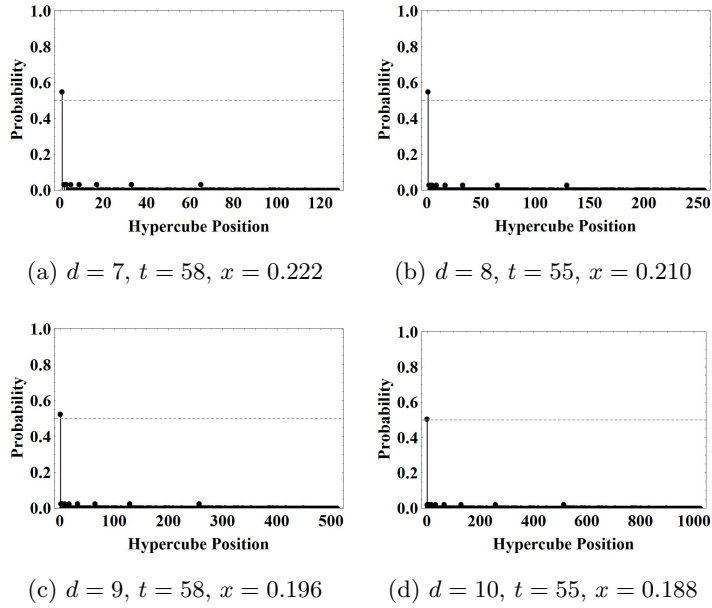
(a) $d = 7$, $t = 58$, $x = 0.222$

(b) $d = 8$, $t = 55$, $x = 0.210$

(c) $d = 9$, $t = 58$, $x = 0.196$

(d) $d = 10$, $t = 55$, $x = 0.188$

FIGURE IV.3: Simulations of the probability for the proposed search algorithm at particular values of x and t and for various dimensions. The values shown here are found to have the greatest probability on the marked element. In all cases, $m = 0$ and $\epsilon = \frac{\pi}{60}$.

Some observations from the simulations give hints to the reasons for this behavior. One observation is that $\epsilon t \approx \pi$. This suggests eigenvalues of the perturbed time-translation operator are still nearly integers. Furthermore, when the number of time steps is doubled, the probability on vertex 0 is nearly zero, and at three times the number of steps, that probability goes back to a similar value as shown in Figs. IV.3. This suggests there is constructive interference when ϵt is nearly an odd integer and destructive interference when ϵt is nearly an even integer. This is further supported by the observation that changing x away from optimum changes not only the height of the maximum probability but also when it occurs. Another observation is that the probability on vertex 0 is correlated to probability on vertices within Hamming distance 1. This is because the states move as $\left(\left(\hat{A}' \right)^{\dagger} \pm \left(\hat{B}' \right)^{\dagger} \right) |n\rangle$, and for reasons shown later in the chapter, this is always the plus sign. Another subtle observation is that the exact time of maximum might be slightly

dependent on the even-oddness of the dimension. However, in discrete-time, this small difference may be an artifact.

The method of analysis is to find the eigenvectors and values of the edge Hamiltonian, $\hat{J}_1' = \frac{1}{2}\left(\left(\hat{A}^\dagger\hat{A}\right)' + \left(\hat{B}^\dagger\hat{B}\right)'\right) = \hat{J}_1 + \hat{W}_1$, where $\hat{J}_1$ is given by Eq. (III.22) for the unperturbed hypercube and $\hat{W}_1$ can be written as

$$\hat{W}_1 = \frac{1}{2}\left(\sum_{n=0}^{N-1}\sum_{p=0}^{d-1}\sqrt{w_n}\Big(|n\oplus 2^p, n\rangle\langle n, n| + |n, n\rangle\langle n\oplus 2^p, n|\Big) + \sum_{n=0}^{N-1} w_n\,|n, n\rangle\langle n, n|\right)$$
$$+ \Big(\text{unitary transform by } \hat{S}_1\Big). \tag{IV.9}$$

Since the DTQW is approximated by the exponentiation of this operator, the edge space dynamics generated by $\hat{J}_1'$ with initial state (IV.8) should give the same behavior.

IV.3 Characterizing Edge Space Dynamics for the Unperturbed Hypercube

Based upon the results of Sec. IV.1 and Eq. (III.12), I already know all the eigenvectors in the dynamic space of the unperturbed hypercube. Since $\hat{\Omega}_0 = d\hat{I}_1$, the eigenvectors of $\hat{J}_1$ are

$$|\psi_k^\pm\rangle = \frac{1}{2\sqrt{\lambda_k^\pm}}\left(\hat{A}^\dagger \pm \hat{B}^\dagger\right)|\phi_k\rangle, \tag{IV.10}$$

with eigenvalues

$$\lambda_k^\pm = \begin{cases} d - \|k\| & ,+ \\ \|k\| & ,- \end{cases}, \tag{IV.11}$$

except for $|\psi_{N-1}^+\rangle = |\psi_0^-\rangle = 0$. Note $|\psi_0^+\rangle = |\psi, 0\rangle$, which shows that the initial state is a stationary state of the unperturbed hypercube. So the dynamic space has dimension $2N-2$, which leaves a $(d-2)N+2$ dimensional null space for $\hat{J}_1$ plus the N self-loop vectors which are also null. It is worth characterizing what kind of vectors are in the null space since it is possible they are not null for $\hat{J}_1'$. To do this, it is best to expand in a symmetrized basis, $\{|s_k^p\rangle : k \in \mathbb{Z} \cap [0, N) \text{ and } p \in \mathbb{Z} \cap [0, d)\}$, where the basis vectors are given by

$$|s_k^p\rangle = \frac{1}{\sqrt{N}} \sum_{n=0}^{N-1} (-1)^{k \circ n} |n \oplus 2^p, n\rangle . \tag{IV.12}$$

By Eq. (IV.5), these vectors are mutually orthogonal, normalized and there are exactly enough to span the space of internal edges of the hypercube. Thus, these symmetrized states in union with the self-loop states form an orthonormal basis. By inspection, one can see that

$$\hat{A} |s_k^p\rangle = |\phi_k\rangle , \tag{IV.13}$$

which implies

$$\hat{A}^\dagger |\phi_k\rangle = \sum_{l=0}^{N-1} \sum_{p=0}^{d-1} |s_l^p\rangle\langle s_l^p| \hat{A}^\dagger |\phi_k\rangle = \sum_{p=0}^{d-1} |s_k^p\rangle . \tag{IV.14}$$

Also,

$$\hat{S}_1 |s_k^p\rangle = \frac{1}{\sqrt{N}} \sum_{n=0}^{N-1} (-1)^{k \circ n} |n, n \oplus 2^p\rangle = \frac{1}{\sqrt{N}} \sum_{n=0}^{N-1} (-1)^{k \circ (n \oplus 2^p)} |n \oplus 2^p, n\rangle$$

$$= \frac{1}{\sqrt{N}} \sum_{n=0}^{N-1} (-1)^{k \circ n} (-1)^{k_p} |n \oplus 2^p, n\rangle = (-1)^{k_p} |s_k^p\rangle . \tag{IV.15}$$

So define $|\psi_k^{(ij)}\rangle = \frac{1}{\sqrt{2}}(|s_k^i\rangle - |s_k^j\rangle)$. $\hat{A}^\dagger \hat{A} |\psi_k^{(ij)}\rangle = 0$ since the two terms give the same superposition over the k symmetrized states by Eqs. (IV.13) and (IV.14) and if I restrict to the cases where $k_i = k_j$, then $\hat{S}_1 |\psi_k^{(ij)}\rangle = 0$ by Eq. (IV.15). Therefore,

$$\hat{J}_1 |\psi_k^{(ij)}\rangle = \frac{1}{2}\left(\hat{A}^\dagger\hat{A} + \hat{S}_1\hat{A}^\dagger\hat{A}\hat{S}_1\right)|\psi_k^{(ij)}\rangle = 0. \tag{IV.16}$$

For $k = 0$, and $N - 1$, there are $d - 1$ distinct cases of $k_i = k_j$, and for all other values of k, $0 < k < N - 1$, there are $d - 2$ distinct cases where $k_i = k_j$, making $(d - 2)N + 2$ linearly independent states of the form $|\psi_k^{(ij)}\rangle$. Thus I have a complete characterization of the null space of $\hat{J}_1$.

Finally, I can write the eigenvectors in the symmetrized basis:

$$\begin{aligned}
|\psi_k^\pm\rangle &= \frac{1}{2\sqrt{\lambda_k^\pm}} \sum_{l=0}^{N-1}\sum_{p=0}^{d-1} |s_l^p\rangle\langle s_l^p|\left(\hat{A}^\dagger \pm \hat{B}^\dagger\right)|\phi_k\rangle \\
&= \frac{1}{2\sqrt{\lambda_k^\pm}} \sum_{p=0}^{d-1}\left(1 \pm (-1)^{k_p}\right)|s_k^p\rangle \\
&= \frac{1}{\sqrt{\lambda_k^\pm}}\begin{cases} \sum_{p=0}^{d-1}(k_p \oplus 1)\,|s_k^p\rangle & ,+ \\ \sum_{p=0}^{d-1} k_p\,|s_k^p\rangle & ,- \end{cases}.
\end{aligned} \tag{IV.17}$$

IV.4 Characterizing Edge Space Dynamics for the Perturbed Hypercube

For the perturbed hypercube, $\hat{\Omega}_0' = d\hat{I}_0 + \hat{W}_0$. Note this means $\hat{\Omega}_0' - \hat{H}_0' = d\hat{I}_0 + \hat{W}_0 - \hat{H}_0 - \hat{W}_0 = \hat{\Omega}_0 - \hat{H}_0$. By Eq. (III.12), $|\psi_k^-\rangle$ is an eigenvector of $\hat{J}_1'$ as well as $\hat{J}_1$. Since the initial state, $|\psi, 0\rangle$, is an eigenvector of $\hat{J}_1$, it is orthogonal to $|\psi_k^-\rangle$, which reduces the number of relevant eigenvectors for the algorithm by $N - 1$. Also,

I can characterize the null space of $\hat{J}_1'$ to see how the addition of $\hat{W}_1$ changes the null space from that found for $\hat{J}_1$. Consider that $\hat{W}_1$ connects self-loop states to self-loop states and self-loop states to hypercube states, but it does not connect hypercube states to hypercube states, so it is always the case that $\langle s_k^p|\hat{W}_1|s_l^q\rangle = 0$. The only relevant matrix elements of $\hat{W}_1$ in the symmetrized basis are of the form

$$\langle n, n|\hat{W}_1|s_k^p\rangle = \frac{1}{2}\sum_{q=0}^{d-1}\sqrt{w_n}\,\langle n\oplus 2^q, n|\left(\hat{I}_1 + \hat{S}_1\right)|s_k^p\rangle = \frac{\sqrt{w_n}(-1)^{k\circ n}(k_p\oplus 1)}{\sqrt{N}}. \tag{IV.18}$$

Since $k_i = k_j$ for $|\psi_k^{(i,j)}\rangle$, one sees that $\hat{W}_1|\psi_k^{(i,j)}\rangle = 0$, which means that part of the null space stays in the null space. However, it must be that the self-loop states which were null in the unperturbed system are a part of the perturbed dynamic space. Assuming that no eigenvalues of $\hat{\Omega}_0' + \hat{H}_0'$ are zero, the perturbed dynamic space must be of dimension $2N - 1$, and $N - 1$ are already accounted for. So the remaining space of interest is given by $\mathrm{span}\{|\psi_k^+\rangle, |n, n\rangle : k, n \in \mathbb{Z}\cap[0, N),\ \text{except}\ k = N - 1\}$, which intersects the dynamic space with dimension N and the null space with dimension $N - 1$. I already know what the dynamic space eigenvectors are. If $|\phi_k'\rangle$ is an eigenvector of $\hat{\Omega}_0' + \hat{H}_0' = d\hat{I}_0 + \hat{H}_0 + 2\hat{W}_0$ with eigenvalue λ_k', then the dynamic space eigenvectors of $\hat{J}_1'$ are

$$|\psi_k'\rangle = \frac{1}{\sqrt{2\lambda_k'}}\left(\left(\hat{A}'\right)^\dagger + \left(\hat{B}'\right)^\dagger\right)|\phi_k'\rangle, \tag{IV.19}$$

with eigenvalues $\frac{\lambda_k'}{2}$. As for the null space eigenvectors, I need to expand $\hat{W}_1$ in this subspace. Clearly,

$$\langle n, n|\hat{W}_1|m, m\rangle = w_n\delta_{nm}. \tag{IV.20}$$

For the only other non-zero matrix elements, I use the symmetrized basis to find

$$
\begin{aligned}
W_{k,n} = \langle \psi_k^+ | \hat{W}_1 | n, n \rangle &= \frac{1}{\sqrt{d - \|k\|}} \sum_{p=0}^{d-1} (k_p \oplus 1) \langle s_k^p | \hat{W}_1 | n, n \rangle \\
&= \frac{\sqrt{w_n}(-1)^{k \circ n}}{\sqrt{N(d - \|k\|)}} \sum_{p=0}^{d-1} (k_p \oplus 1)^2 = \frac{\sqrt{w_n(d - \|k\|)}(-1)^{k \circ n}}{\sqrt{N}} \\
&= \frac{\sqrt{w_n \lambda_k^+}(-1)^{k \circ n}}{\sqrt{N}}.
\end{aligned}
\tag{IV.21}
$$

If I write a null vector as $|\psi^{null}\rangle = \sum_{k=0}^{N-2} \beta_k |\psi_k^+\rangle + \sum_{n=0}^{N-1} \alpha_n |n, n\rangle$, then my eigenvector equation is

$$
\begin{aligned}
\hat{J}_1' |\psi^{null}\rangle &= \sum_{k=0}^{N-2} \beta_k \left(\hat{J}_1 + \hat{W}_1 \right) |\psi_k^+\rangle + \sum_{n=0}^{N-1} \alpha_n \left(\hat{J}_1 + \hat{W}_1 \right) |n, n\rangle \\
&= \sum_{k=0}^{N-2} \left(\lambda_k^+ \beta_k + \sum_{n=0}^{N-1} \alpha_n W_{k,n} \right) |\psi_k^+\rangle \\
&\quad + \sum_{n=0}^{N-1} \left(w_n \alpha_n + \sum_{k=0}^{N-2} \beta_k W_{k,n} \right) |n, n\rangle = 0.
\end{aligned}
\tag{IV.22}
$$

This implies that the terms in the brackets are zero for all n and k. Assuming no $w_n \neq 0$, I solve for α_n in the second condition and plug it into the sum of the first:

$$
\begin{aligned}
\sum_{n=0}^{N-1} \alpha_n W_{k,n} &= -\sum_{n=0}^{N-1} \sum_{l=0}^{N-2} \frac{\beta_l}{w_n} W_{l,n} W_{k,n} \\
&= -\sum_{l=0}^{N-2} \beta_l \sqrt{\lambda_k^+ \lambda_l^+} \sum_{n=0}^{N-1} \frac{(-1)^{k \circ n}(-1)^{l \circ n}}{N} = -\beta_k \lambda_k^+,
\end{aligned}
\tag{IV.23}
$$

where Eq. (IV.5) is used. Thus any set of β_k's satisfy the null eigenvector condition so long as $\alpha_n = \frac{1}{w_n} \sum_{k=0}^{N-2} W_{n,k} \beta_k$. The projection of $|\psi_0^+\rangle$ into the null space of $\hat{J}_1'$ must align with

the null vector for which $\beta_k = \delta_{k0}$. This implies

$$\hat{\mathscr{P}}_1^{null} |\psi_0^+\rangle = C^2 \left(|\psi_0^+\rangle - \sum_{n=0}^{N-1} \sqrt{\frac{d}{Nw_n}} |n,n\rangle \right), \tag{IV.24}$$

where C is the normalization constant found to be

$$C = \left(1 + \frac{d}{N} \sum_{n=0}^{N-1} \frac{1}{w_n} \right)^{-\frac{1}{2}} = \left(1 + \frac{d}{N} \sum_{p=0}^{d} \binom{d}{p} \left(\frac{1}{(1-x)} \right)^p \left(\frac{1}{(1+x)} \right)^{d-p} \right)^{-\frac{1}{2}}$$

$$= \left(1 + \frac{d}{(1-x^2)^d} \right)^{-\frac{1}{2}}. \tag{IV.25}$$

Aside from the last equation, the analysis has made no assumptions about the w_n's (other than $w_n \neq 0$). Thus how the choice of self-loop weights results in the behavior of Figs. IV.3 comes down to finding the eigenvectors and values of $d\hat{I}_0 + \hat{H}_0 + 2\hat{W}_0$.

IV.5   Eigenvectors and Values of the Perturbed Hypercube

For simplicity and without loss of generality, I only analyze the case when the marked element $m = 0$. Then the Hamming distances become Hamming weights in Eq. (IV.6b). It is not effective to use perturbation theory in this case to find the eigenvector and values. The purpose of the self-loops is to perturb the system strongly enough so that a once stationary state now changes in time. As mentioned before, the perturbation does not completely remove the symmetry of the hypercube and so one might consider symmetry reduction using the VanVleck projection operators [43]. Since the self-loop hopping amplitudes are only dependent on Hamming weight, one finds that for any permutation on the binary digits of the vertices, g, $w_n = w_{g(n)}$. Furthermore, performing g on all vertices preserves the connectedness of the graph, which is to say $n@q$ if and only if $g(n)@g(q)$. Therefore, the

remaining symmetry group is isomorphic to the group of permutations on d items, $\mathcal{S}_d$. Still, this is a rather cumbersome group to work with for arbitrary dimension and at best it would block diagonalize the problem. However, this does suggest that not all eigenvectors are of importance in this case. I claim the symmetry requires only some of the eigenvectors have support on $|0\rangle$. The argument is as follows: consider finding the irreducible representations of the group and thus the VanVleck projection operators. For the exact form of these projection operators, see Tinkham [43]. The group of operators on $\mathcal{H}_\mathcal{V}$ which represent $\mathcal{S}_d$ must connect basis states to basis states with the same Hamming weight. So each term in the sum of the VanVleck projection operator must take $|0\rangle$ into $|0\rangle$. If the irreducible representation is not the identity, then any vector given after the projection has support on $|0\rangle$ as the sum over the group elements of the matrix entries for that row, column and representation used to form the projection operator. Since it is not the identity by hypothesis, the sum must be zero by the orthogonality theorem of representation theory. Thus the only projection operator that maintains support on $|0\rangle$ is the one corresponding to the identity representation. Numerical calculations on relatively small matrices representing $d\hat{I}_0 + \hat{H}_0 + 2\hat{W}_0$ suggest there are only $d+1$ such eigenvectors and this is supported by the calculation later in this chapter. If this holds, then only $d+1$ of the N eigenvectors are of importance to this problem. Furthermore, this suggests that these eigenvectors have a useful property. The identity representation is the representation of 1 for every member of the group, which means the VanVleck projection operator responsible for these states treats any basis state with the same Hamming weight equally. Thus I conjecture that any eigenvector, $|\phi'\rangle$, with support on the marked element has the property, $\|n\| = \|q\|$ implies $\langle n|\phi'\rangle = \langle q|\phi'\rangle$. Again, this is supported by numerical work and the calculation to follow.

As mentioned earlier, $\hat{W}_0$ in the eigenbasis of the unperturbed hypercube has a form more appealing for approximation. However, I need to ensure that the eigenvectors of interest

have the same property in that basis. To show this, the following identity is useful:

$$\sum_{k}^{\|k\|=const.} (-1)^{k \circ n} = \sum_{m=0}^{d} \binom{\|n\|}{m} \binom{d - \|n\|}{\|k\| - m} (-1)^m = P_{\|k\|}^{\|n\|}. \qquad \text{(IV.26)}$$

If one expands $w_n(x)$ as a polynomial in x, it can be shown that $w_n(x)$ is the generating function for the $P_{\|k\|}^{\|n\|}$ coefficients on $\|k\|$. This as well as the proof of Eq. (IV.26) is given in Appendix C. If I assume $|\phi'\rangle$ has the above property in the position basis and define $\phi'_{\|n\|} = \langle n|\phi' \rangle$, then the inner product of the new eigenvector with a member of the old eigenbasis gives

$$\langle \phi_k|\phi' \rangle = \frac{1}{\sqrt{N}} \sum_{n=0}^{N-1} (-1)^{k \circ n} \langle n|\phi' \rangle = \frac{1}{\sqrt{N}} \sum_{p=0}^{d} \phi'_p \sum_{n}^{\|n\|=p} (-1)^{k \circ n}$$

$$= \frac{1}{\sqrt{N}} \sum_{p=0}^{d} P_p^{\|k\|} \phi'_p. \qquad \text{(IV.27)}$$

Since $P_p^{\|k\|}$ depends only on the Hamming weight of k, I have shown that $\|k\| = \|l\|$ implies $\langle \phi_k|\phi' \rangle = \langle \phi_l|\phi' \rangle$.

So to expand, the matrix elements of $\hat{W}_0$ in the eigenbasis of the unperturbed hypercube are

$$\langle \phi_k|\hat{W}_0|\phi_l \rangle = \frac{1}{N} \sum_{n=0}^{N-1} \sum_{q=0}^{N-1} (-1)^{k \circ n} (-1)^{l \circ q} w_n \delta_{nq} = \frac{1}{N} \sum_{n=0}^{N-1} (-1)^{k \circ n + l \circ n} w_n. \qquad \text{(IV.28)}$$

Consider the exponent $k \circ n + l \circ n = \sum_i (k_i + l_i) n_i$. Breaking the terms down by cases, one can see that if $k_i = l_i$, then $(-1)^{(k_i + l_i) n_i} = 1$, and if $k_i \neq l_i$ then $(-1)^{(k_i + l_i) n_i} = (-1)^{n_i}$. This implies that $(-1)^{k \circ n + l \circ n} = (-1)^{n \circ (k \oplus l)}$. Also let $w_n = \tilde{w}_{\|n\|}$ so that I can factor the

self-loop weights out of the $\|n\| = const.$ sum. Using this for the matrix element, I have

$$
\begin{aligned}
\langle \phi_k | \hat{W}_0 | \phi_l \rangle = & \frac{1}{N} \sum_{n=0}^{N-1} (-1)^{n \circ (k \oplus l)} w_n = \frac{1}{N} \sum_{p=0}^{d} \tilde{w}_p \sum_{n}^{\|n\|=p} (-1)^{n \circ (k \oplus l)} \\
= & \frac{1}{N} \sum_{p=0}^{d} \tilde{w}_p P_p^{\|k \oplus l\|}.
\end{aligned} \tag{IV.29}
$$

Now I use the fact that $\tilde{w}_p = (1+x)^d \left(\frac{1-x}{1+x} \right)^p$ and $\tilde{w}_{\|k \oplus l\|}(x)$ is the generating function for $P_p^{\|k \oplus l\|}$. This implies that

$$
\begin{aligned}
\langle \phi_k | \hat{W}_0 | \phi_l \rangle = & \frac{(1+x)^d}{N} \tilde{w}_{\|k \oplus l\|} \left(\frac{1-x}{1+x} \right) \\
= & \frac{(1+x)^d}{N} \left(1 - \frac{1-x}{1+x} \right)^{\|k \oplus l\|} \left(1 + \frac{1-x}{1+x} \right)^{d - \|k \oplus l\|} \\
= & \frac{1}{N} \left(1 + x - 1 + x \right)^{\|k \oplus l\|} \left(1 + x + 1 - x \right)^{d - \|k \oplus l\|} \\
= & x^{\|k \oplus l\|}.
\end{aligned} \tag{IV.30}
$$

Just as real-space has the dual k-space in condensed matter, here I have the k-cube for which $\hat{W}_0$ connects vertices of the k-cube (eigenstates of the original hypercube) based upon the Hamming distance between them. So to expand $\hat{W}_0$ in powers of x, define $\hat{D}_0^{(p)}$ to be the matrix which connects all states of the k-cube with Hamming distance p, so that

$$
\hat{W}_0 = \hat{I}_0 + x \hat{D}_0^{(1)} + x^2 \hat{D}_0^{(2)} + \cdots + x^d \hat{D}_0^{(d)}. \tag{IV.31}
$$

Note $\hat{D}_0^{(1)}$ is the adjacency operator for the k-cube and that all $\hat{D}_0^{(p)}$ are Hermitian. For the sake of this thesis, I only take the first order approximation in x since $x^2 < 0.04$ for the values of interest based upon the simulations of higher dimension. This may appear sufficient but there is a tendency for powers of x to be multiplied by the dimension in the calculations, and this may not be negligible since the optimal x depends on d. More work

must be done to obtain a better approximation.

For any eigenvector of interest, I can write $|\phi'\rangle = \sum_{k=0}^{N-1} \phi'_{\|k\|} |\phi_k\rangle$. The action of $\hat{D}_0^{(1)}$ on such a vector is

$$\hat{D}_0^{(1)} |\phi'\rangle = \sum_{k=0}^{N-1} \left(\sum_{l}^{\|l\|=\|k\|+1} \phi'_{\|l\|-1} |\phi_l\rangle + \sum_{l}^{\|l\|=\|k\|-1} \phi'_{\|l\|+1} |\phi_l\rangle \right). \tag{IV.32}$$

The first sum in the brackets is over the states that move forward by one Hamming weight and the second is over the states that move backward by one under the action of $\hat{D}_0^{(1)}$. If I reorder the sum, a single state $|\phi_k\rangle$ has $\|k\|$ terms coming from states with $\phi'_{\|k\|-1}$ amplitude and $d - \|k\|$ terms coming from states with $\phi'_{\|k\|+1}$ amplitude. Using this and the fact that $\hat{H}_0$ is diagonal in this basis, the action of $d\hat{I}_0 + \hat{H}_0 + 2\left(\hat{I}_0 + x\hat{D}_0^{(1)}\right)$ on $|\phi'\rangle$ with eigenvalue λ' can be written as a recursion equation:

$$d\phi'_k + (d - 2k)\phi'_k + 2\phi'_k + 2x\left(k\phi'_{k-1} + (d-k)\phi'_{k+1}\right) = \lambda'\phi'_k, \tag{IV.33}$$

where the index $\|k\| \to k$. Defining $\mu = \frac{1}{2}\lambda' - d - 1$, the recursion becomes

$$x\left(k\phi'_{k-1} + (d-k)\phi'_{k+1}\right) - k\phi'_k = \mu\phi'_k. \tag{IV.34}$$

Solving Eq. (IV.34) requires a generating function, but notice that the equation itself does not enforce the fact that $0 \leq k \leq d$. So I define the generating function f as

$$f(y; x) = \sum_{k=0}^{N-1} \binom{d}{k} \phi'_k y^k, \tag{IV.35}$$

where the binomial coefficients enforce the domain of k. Note that $\binom{d}{k} = \frac{d-(k-1)}{k}\binom{d}{k-1} = \frac{k+1}{d-k}\binom{d}{k+1}$. Multiplying Eq. (IV.34) by $\binom{d}{k}y^k$ and summing over all k, one finds the recursion

equations become

$$x\left(dyf - y^2 f' + f'\right) - yf' = \mu f, \tag{IV.36a}$$

or

$$\left(y^2 + \frac{y}{x} - 1\right) f' = \left(dy - \frac{\mu}{x}\right) f, \tag{IV.36b}$$

where prime in this case denotes the derivative with respects to y. This is a separable, first-order differential equation which can be integrated by partial fractions. With that in mind, I factor the polynomial $y^2 + \frac{y}{x} - 1 = (y - y_+)(y - y_-)$, where

$$y_\pm = \frac{1}{2x}(-1 \pm \sqrt{1 + 4x^2}). \tag{IV.37}$$

If the partial fraction equation is given as

$$\frac{dy - \frac{\mu}{x}}{(y - y_+)(y - y_-)} = \frac{p}{(y - y_+)} + \frac{q}{(y - y_-)}, \tag{IV.38}$$

then the solution to Eq. (IV.36) is

$$f(y; x) = (y - y_+)^p (y - y_-)^q, \tag{IV.39}$$

where the free constant is taken to be 1 since this is fixed eventually by normalization. The first requirement given by Eq. (IV.38) is $p + q = d$, but to make sure the expansion of f is a finite-order polynomial of order d, I also require that p be an integer such that $0 \leq p \leq d$. This quantization gives $\mu_p = \mu(p)$ from the second condition of Eq. (IV.38),

$\frac{\mu_p}{x} = py_+ + (d - p)y_-$, which yields

$$\mu_p = -\frac{d}{2} + (p - \frac{1}{2})\sqrt{1 + 4x^2}. \qquad \text{(IV.40)}$$

It is interesting but perhaps not surprising this is reminiscent of the energy spectrum of a harmonic oscillator. As anticipated, this part of the spectrum is evenly spaced and nearly integer up to $\mathcal{O}(x^2)$. Finally, I can extract the coefficients of the eigenvector by expanding Eq. (IV.39). Using $y_+ y_- = -1$, the expansion is

$$
\begin{aligned}
f(y; x) =(y - y_+)^p (y + \frac{1}{y_+})^{d-p} &= \sum_{n=0}^{d} \sum_{l=0}^{d} \binom{p}{l} \binom{d-p}{n} (-1)^{p-l} (y_+)^{2p+n-l-d} y^{n+l} \\
&= \sum_{k=0}^{d} \left((-1)^p (y_+)^{2p+k-d} \sum_{l=0}^{d} \binom{p}{l} \binom{d-p}{k-l} (-y_+^2)^{-l} \right) y^k.
\end{aligned} \qquad \text{(IV.41)}
$$

The part in the bracket is almost $\phi'_k(p)$ except that any factors that do not depend on k can be absorbed into a normalization constant, so that

$$\phi'_k(p) = C_p \frac{1}{\binom{d}{k}} \sum_{l=0}^{d} \binom{p}{l} \binom{d-p}{k-l} (y_-)^l (y_+)^{k-l}, \qquad \text{(IV.42)}$$

where C_p is the normalization constant and y_- is reintroduced.

IV.6 Maximizing Probability on the Marked Element

At this point, describing the behavior of the algorithm is a matter of putting the pieces together. Instead of trying to find the probability directly, which to some extent is not possible since all the eigenvectors are not known, I obtain the time-dependent factor multiplying $\left((\hat{A}')^{\dagger} + (\hat{B}')^{\dagger} \right) |0\rangle$ to within the approximation. This is the primary contribution to the probability on vertex 0 and should be fully accounted for based upon the symmetry

argument. Other parts contributing to the probability of measuring vertex 0 come from the projection of the initial state into the null space–which is static–and contributions from the B-projector acting on the neighbor basis states (in the real hypercube) which would require the remaining eigenvectors to be fully accounted for.

Consider the approximate dynamics of the algorithm given by $\hat{J}_1'$:

$$\exp\left(-it\hat{J}_1'\right)|\psi_0^+\rangle = \hat{\mathscr{P}}_1^{null}|\psi_0^+\rangle + \sum_{p=0}^{d}\exp\left(\frac{-it\lambda_p'}{2}\right)|\psi_p'\rangle\langle\psi_p'|\psi_0^+\rangle$$

$$+ \ \ other\ eigenvector\ terms. \tag{IV.43}$$

The inner product in each term of the sum is found to be

$$\langle\psi_p'|\psi_0^+\rangle = \frac{1}{2\sqrt{2\lambda_p'd}}\langle\phi_p'|\left(\hat{A}'+\hat{B}'\right)\left(\hat{A}^\dagger+\hat{B}^\dagger\right)|\phi_0\rangle$$

$$= \frac{1}{\sqrt{2\lambda_p'd}}\langle\phi_p'|\left(d\hat{I}+\hat{H}_0\right)|\phi_0\rangle = \sqrt{\frac{2d}{\lambda_p'}}\langle\phi_p'|\phi_0\rangle$$

$$= \sqrt{\frac{2d}{\lambda_p'}}C_p, \tag{IV.44}$$

where Eq. (IV.19) is used for $|\psi_p'\rangle$. Also $|\phi_p'\rangle$ can be expanded in the position basis:

$$\langle n|\phi_p'\rangle = \sum_{k=0}^{N-1}\phi_{\|k\|}'(p)\langle n|\phi_k\rangle = \frac{1}{\sqrt{N}}\sum_{k=0}^{d}P_k^{\|n\|}\phi_k'(p). \tag{IV.45}$$

This gives the state of the algorithm as

$$\exp\left(-it\hat{J}_1'\right)|\psi_0^+\rangle = \hat{\mathscr{P}}_1^{null}|\psi_0^+\rangle$$

$$+ \sqrt{\frac{d}{N}}\sum_{n=0}^{N-1}\sum_{k,p=0}^{d}\exp\left(\frac{-it\lambda_p'}{2}\right)\frac{C_p}{\lambda_p'}P_k^{\|n\|}\phi_k'(p)\left(\left(\hat{A}'\right)^\dagger+\left(\hat{B}'\right)^\dagger\right)|n\rangle$$

$$+ \ \ other\ eigenvector\ terms. \tag{IV.46}$$

In particular, I want the $n = 0$ term, for which $P_k^0 = \binom{d}{k}$. Using this, the k sum is evaluated as

$$
\begin{aligned}
\sum_{k=0}^{d} P_k^0 \phi_k'(p) &= C_p \sum_{k,l=0}^{d} \binom{p}{l}\binom{d-p}{k-l}(y_+)^{k-l}(y_-)^l \\
&= C_p(1+y_-)^p(1+y_+)^{d-p}.
\end{aligned}
\tag{IV.47}
$$

For the exponentials, $\frac{\lambda_p'}{2} = 1 + \frac{d}{2} - \frac{\sqrt{1+4x^2}}{2} + p\sqrt{1+4x^2}$. All but the $p\sqrt{1+4x^2}$ term amounts to a common phase. So if I take the value of time $t = \frac{\pi}{\sqrt{1+4x^2}} = t_{max}$, then $\exp\left(\frac{-it\lambda_p'}{2}\right) \propto (-1)^p$. This means the function I wish to maximize is

$$
g_0(x) = \sqrt{\frac{d}{N}} \sum_{p=0}^{d}(-1)^p \frac{C_p^2}{\lambda_p'}(1+y_-)^p(1+y_+)^{d-p}.
\tag{IV.48}
$$

By inspection, one can see that $1 + y_- < 0 < 1 + y_+$ for all values of x, which shows that the condition on the time is as I conjectured. This is the case for constructive superposition of all the marked element components of the eigenvectors. Furthermore, for $x = .210$ as in Fig. IV.3b, $t_{max} \approx .93\pi$ which is in good agreement with the numerical value of $\frac{55}{60}\pi$ for maximum probability. However, this agreement is contrasted with the lack of agreement for the maximizing value of x found in Figs. IV.4. There, $x \approx .485$ is the maximizing value in all cases. Still, the fact that there is a maximum suggests that similar results exist for a better approximation of $\hat{W}_0$. Actually if I replace $\hat{W}_0$ with $\hat{I}_0 + x\hat{D}_0^{(1)}$, this result is exact, and the maximum suggests that the behavior would be similar to what is presented in Figs. IV.3. Such a model might even have a distinct advantage in that the maximizing x value appears to not depend on d and furthermore, the diagonal weights in the position basis are simpler.

(a) $d = 7$ (b) $d = 8$ (c) $d = 9$

(d) $d = 10$ (e) $d = 11$ (f) $d = 12$

(g) $d = 13$ (h) $d = 14$ (i) $d = 15$
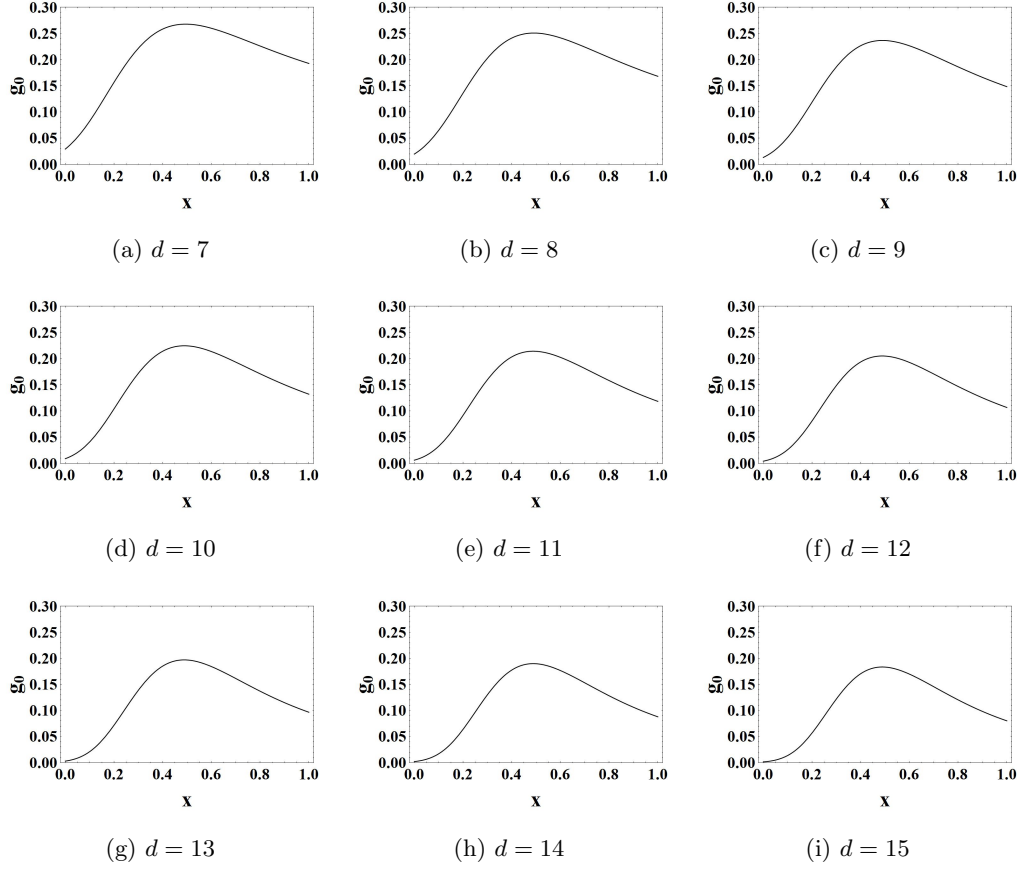
FIGURE IV.4: Plot of $g_0(x)$ versus x for various dimensions. The maximum appears to be $x \approx 0.485$ in all cases.

The error from using $\hat{I}_0 + x\hat{D}_0^{(1)}$ rather than $\hat{W}_0$ can be quantified. Note that every "column" of $\hat{D}_0^{(p)}$ has $\binom{d}{p}$ non-zero entries, which means that $\|\hat{D}_0^{(p)}\|_2 = \binom{d}{p}$. Thus, distance between the two operators can be bounded as

$$\|\hat{W}_0 - (\hat{I}_0 + x\hat{D}_0^{(1)})\|_2 = \|\sum_{p=2}^{d} x^d \hat{D}_0^{(p)}\|_2 \leq (1+x)^p - (1+xp). \qquad \text{(IV.49)}$$

I suspect this limit is tight, so it is not surprising that the agreement in Figs. IV.4 is poor.

IV.7   Unfinished Analysis

There are many unanswered questions. I still do not have a formula for the maximizing x value as a function of d. However, this would be unnecessary with the suggestion of a different perturbation, namely $\hat{W}_0 \to \hat{I}_0 + x\hat{D}_0^{(1)}$. I also do not have a full characterization of the performance at the maximum probability. This can be approximated, but it is not worth doing for this model until a better set of eigenvectors are found. Finally, gate-level implementation is needed to characterize the algorithm in terms of the number of gates required.

IV.8   Final Comments on the Search Algorithm

As mentioned earlier in this chapter, if the results I have presented are to be believed, then it appears there exists a unitary evolution which meets the criteria of the search algorithm and does so without the time scaling with the size of the search space. This is in contradiction with the proof that the best that can be done is $\mathcal{O}(\sqrt{N})$. I am not entirely sure why this is the case, but I conjecture what is presented here does not contain an oracle. That is, at no point is there one subroutine which is singularly charged with knowing which element is marked. The existence of a quantum oracle is the crux of the arguments given in Refs. [5, 6, 46]. In my case, the non-marked coin operators are not ignorant of the marked element as is the case with Shenvi et al. [37]. In a sense, the oracle is dispersed amongst all the block parts of coin operator, and so for a single step, the smallest sequential block of gates that could be designated as the oracle is the coin operator itself. I concede that for a computer scientist, this may be a problem, but even if it is, it suggests there are perhaps more creative ways to beat the Grover limit in a way which is useful for implementation.

CHAPTER V

IMPLEMENTATION: STRATEGY FOR A GENERAL QUANTUM WALK

In this chapter, I do not consider a physical system capable of performing a QW. Just as classical logic and logic gates are realized in different systems, quantum computing has the possibility of being realized in different systems. Also similar to classical logic, there exists a finite, relatively small set of unitary operators–quantum gates–such that any unitary operator on a finite but arbitrary-sized quantum system can be realized as some combination of the members of the small set. Such a collection is call a *universal gate set* and its member *primitive gates*. There are a few different universal gate sets, some of which obtain an arbitrary gate exactly and some approximately. What I assume is there exists some physical system containing an arbitrary (finite) number of well-characterized *qubits* which can be initialized to a single fiducial state, manipulated to apply any member of the universal gate set an arbitrary number of times before decoherence (which implies the qubits can be entangled), and each qubit can be reliably measured [45]. I also assume any arbitrary initial state can be obtained by applying some number of gates to the fiducial state. Of course, this is an idealization which omits many of the challenges of a real quantum computer such as finite decoherence time, gate error, error correction, and so on. An example of a practical system which may be able to reliably achieve these conditions is cold ions trapped in an optical lattice. For more on this possibility, see Häffner et al. [24]. Here I present a strategy for implementing an arbitrary DTQW in a system which meets these requirements.

By virtue of Ch. III, this extends to an arbitrary CTQW. To avoid some difficulty, I only consider the QW choice.

V.1 Qubits and the Universal Gate Set

For completeness, I define a qubit here:

Definition V.1. A qubit is any system with a two-dimensional Hilbert space, $\mathcal{H}_2$.

One of the benefits of quantum systems is that if d qubits can be entangled, then the resulting system is of dimension 2^d, which gives an exponentially larger space than the actual size of the system [4]. As for the universal gate set, I consider the collection of all unitary operators in $\mathcal{H}_2$ and the CNOT gate, $\hat{\oplus}$, which acts on a 2-qubit system. The CNOT calculates the XOR operation on the second bit, i.e. $\hat{\oplus} |i\rangle |j\rangle = |i\rangle |i \oplus j\rangle$ and can be represented in lexicographical order ($|00\rangle$, $|01\rangle$, $|10\rangle$, $|11\rangle$) by the matrix

$$
\hat{\oplus}_2 \doteq \begin{pmatrix} 1 & 0 & 0 & 0 \\ 0 & 1 & 0 & 0 \\ 0 & 0 & 0 & 1 \\ 0 & 0 & 1 & 0 \end{pmatrix}. \tag{V.1}
$$

That is, if the first qubit is $|0\rangle$, then it acts as the identity on the second, and if the first qubit is $|1\rangle$ then it acts as $\hat{\sigma}_x$ on the second. The diagram for CNOT is shown in Fig. V.1a. Each horizontal line represents a qubit and features on that line represent the sequence of operations on that qubit going from left to right. The vertical line between the qubits is an operation which entangles the qubits. The solid dot represents a control and the circle-cross represents $\hat{\sigma}_x$. It is shown by Barenco et al. [4] that this set is universal. Barenco

et al. also provide an important result and method for generalizing the CNOT to any $\mathcal{H}_2$ unitary operator controlled by any number of qubits. Using their notation, if $\hat{U}_2$ is the arbitrary unitary operator in $\mathcal{H}_2$, then $\bigwedge_n \left(\hat{U}_2\right)$ is an operator in $n+1$ qubits which uses the first n qubits as a control for $\hat{U}_2$ as depicted in Fig. V.1b. So, $\hat{U}_2$ is activated on the last qubit for the basis state of all ones for the control qubits. For more details on this, see Ref. [4], but it is possible and the method is clearly outline in the reference. Furthermore, this can be generalized to a unitary acting on any number of qubits and controlled by any other number of qubits. One takes the sequence of primitive operations used to generate the desired operation, each under the control of the control qubits. Thus in terms of the diagrams, $\hat{U}_2$ in Fig. V.1b is replaced by the arbitrary unitary operator in any number of qubits.

(a) CNOT   (b) $\bigwedge_n \left(\hat{U}_2\right)$
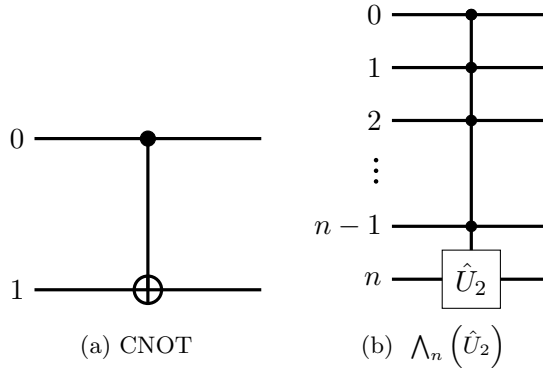
FIGURE V.1: Graphical depiction of quantum gates.

V.2   Method for Simulating the General Discrete-time Quantum Walk

Instead of limiting the DTQW to a Hilbert space, $\mathcal{H}_\mathcal{E}$, it is more general to use the space $\mathcal{H}_\mathcal{V} \times \mathcal{H}_\mathcal{V}$. That is, this method uses two times the number of qubits required to represent

every member of the graph. For example, the d-dimensional hypercube requires $2d$ qubits. Let d generally represent the number of qubits need to represent every member of $\mathcal{V}$. This allows edge basis state to be split, i.e. $|j, i\rangle = |j\rangle |i\rangle$. Thus the qubits are organized into two quantum registers each of size d, and because of this, I refer to the method as the *parallel-register method*. Registers are represented in diagrams by multiple horizontal lines.

For this setup, note that the coin operator only changes states on the first register under the control of the second. So, the last section gives the tools to create the coin operator. However, the control activates the unitary operation for the basis state of all 1's in the register. To be more selective of the basis state, each qubit for which the control number has a component of 0 is modified by the $\hat{\sigma}_x$ gate before the controlled gate. This effectively makes the input control on that bit 0 instead of 1. After the controlled gate is complete, the qubit is flipped back by a second $\hat{\sigma}_x$ gate. This is depicted in Fig. V.2 for the number $2 = (010)_2$. There, I also suggest a diagrammatic shorthand for this selective control.
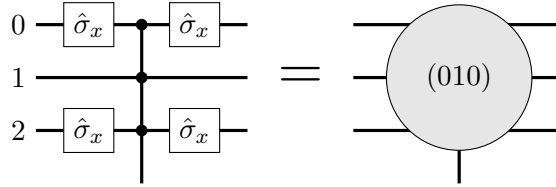

FIGURE V.2: Method for converting control on a register to control targeted to a specific number, here $2 = (010)_2$.

The coin operator is implemented by systematically controlling the first register, what I refer to as the *slave* register, under the control of the second register, the *control*. This can be done for each vertex index with the appropriate coin operation as depicted in Fig. V.3. Once all the individual coin operations have been performed, the same diagram is implemented but with an exchange in the registers' roles. That is, the swap operator is not implemented by a set of gates, but is achieved simply by making the former slave register the control and vice versa. This is also depicted in Fig. V.3, where the point at which the swap

occurs is denoted by the dashed vertical line. This line does not represent any gate action. The process then repeats for the appropriate number of steps according to the algorithm design. Once complete if one wants to measure the incoming state of the system, the sum in Eq. (II.10) is done all at once by measuring the state of the last slave register.
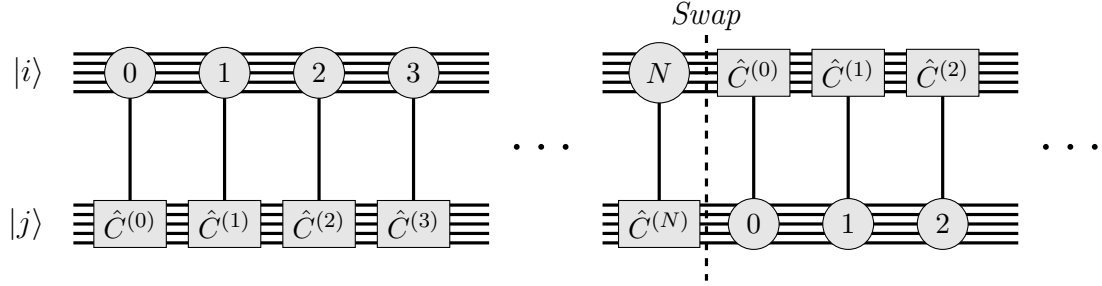

FIGURE V.3: Basic structure of the parallel register method for implementing the general DTQW.

As a trivial but insightful example, consider the simplest possible system of two qubits. Such a system would imitate a DTQW on a graph of two vertices. The coin operator on vertex 1 is given by $\bigwedge_1 \left(\hat{C}^{(1)} \right)$. For vertex 0, the implementation is given by $\left(\hat{\sigma}_x \otimes \hat{I}_2 \right) \left(\bigwedge_1 \left(\hat{C}^{(0)} \right) \right) \left(\hat{\sigma}_x \otimes \hat{I}_2 \right)$, which is represented in block form as

$$
\begin{pmatrix} 0 & \hat{I}_2 \\ \hat{I}_2 & 0 \end{pmatrix} \begin{pmatrix} \hat{I}_2 & 0 \\ 0 & \hat{C}^{(0)} \end{pmatrix} \begin{pmatrix} 0 & \hat{I}_2 \\ \hat{I}_2 & 0 \end{pmatrix} = \begin{pmatrix} \hat{C}^{(0)} & 0 \\ 0 & \hat{I}_2 \end{pmatrix}. \tag{V.2}
$$

This multiplied by $\bigwedge_1 \left(\hat{C}^{(1)} \right)$ gives the block-diagonal form required for the coin operator. Just before the swap in register roles, one might as well look at the matrix representation

the way it is acted upon in the next step:

$$\hat{C} \doteq \begin{pmatrix} \hat{C}^{(0)} & 0 \\ 0 & \hat{C}^{(1)} \end{pmatrix} \rightarrow \begin{pmatrix} c_{00}^{(0)} & 0 & c_{01}^{(0)} & 0 \\ 0 & c_{00}^{(1)} & 0 & c_{01}^{(1)} \\ c_{10}^{(0)} & 0 & c_{11}^{(0)} & 0 \\ 0 & c_{10}^{(1)} & 0 & c_{11}^{(1)} \end{pmatrix}, \tag{V.3}$$

where the new representation order is $|00\rangle$, $|10\rangle$, $|01\rangle$, $|11\rangle$. This could be consider the representation in the outgoing space block diagonal form, for which the subsequent coin operations act just as they did in the incoming space block diagonal form.

V.3 Benefits and Issues with the Parallel-Register Method

There are many appealing factors to consider for the parallel-register method. First, it general enough to implement any DTQW, but the most interesting is the fact that half the unitary time-evolution requires no gates to implement. This avoids gate error that otherwise can compound when gates are not performing exactly as designed. This also increases the efficiency of the computation since any gate will take a finite amount of time to complete. Furthermore, the complexity of the coin operations are directly related to the connectivity of the graph. If the graph has relatively low connectivity, then the coin operators are sparse and thus easier to design in terms of gate structure.

The greatest downside to this method is for a spatial-homogeneous walk, each individual coin operator must still be applied in turn. The more common way to implement a DTQW for a regular graph is to have a coin register and a position register. In that case, a homogeneous coin is performed once for all, and the shift entangles the resulting state with the position. The single implementation of the coin operator likely wipes out any gains from

the gate-less implementation of the shift/swap operator. Furthermore, the parallel-register method almost always requires more qubits. More has to be done to make this comparison quantitative.

It is worth mentioning a method of implementation discussed by Childs et al. in Ref. [9]. The reference presents a method to simulate a CTQW that uses two registers of equal size and an operator very similar the swap operator which is implemented via gates (Ref. [9] refers to it as $\hat{T}$). So, perhaps this enlarging of the space is not such a hindrance. It would be worthwhile in future work to compare the efficiency of this method for implementing the CTQW and the parallel-register method using the connected DTQW as discussed in Ch. III.

One last possible issue is that the parallel-register method almost always contains basis states intended to be empty or null, but for which probability amplitude can leak into if gates are not performed perfectly. However, the additional states could provide the benefit of error detection. For the incoming probability, only the last slave register is measured. If the last control register is also measured, the result could be checked to see that the two measured register values are adjacent in the graph. If they are not, the result would be considered inconclusive.

Ultimately, the parallel register method appears to be an efficient method for implementation, especially when the number of qubits is not an issue and the coin operator is not homogeneous. More work has to be done to quantify the efficiency in terms of the number of gates and compare that to other methods.

CHAPTER VI

CONCLUSIONS AND FINAL DISCUSSION

This thesis started by introducing the QW and some of the relevant background literature in Ch. I. This was followed in Ch. II by a more formal definition and explanation of both the CTQW and the DTQW. I addressed some of the possible variations on the DTQW, how they are equivalent to the formalism I present, and how to use a DTQW to simulate continuous-time dynamics in the edge space. In Ch. III, I discussed a method for connecting any CTQW to some DTQW through the use of the projectors. These projectors were expanded upon in terms of the dynamic subspace and edge space operators they create. This led to continuous-time edge space dynamics related to the CTQW. A few example simulations on the one- and two-dimensional lattices were shown and discussed. Most importantly, they were used to motivate the very-lazy QW choice which showed striking agreement with the exact CTQW. This led to an expansion of the DTQW generated by the projectors from which an analytic expression could be found if the spectral decomposition of the regular graph Hamiltonian was known. This expansion was also used to understand the particular behavior of the QW choice and the very-lazy QW choice. Ch. IV presented a possible application of the ideas in Ch. III which took the form of a search algorithm on the hypercube. According to the presented simulations, this algorithm appeared to have no scaling for the time of completion with the size of the search space. The behavior of this algorithm was reduced to $d+1$ eigenvectors and a rough approximation to those eigenvectors

was found. Though the approximation did not yield good quantitative agreement, it did show reasonable qualitative agreement. Finally, Ch. V discussed a gate implementation scheme for a general DTQW referred to as the parallel-register method. In theory, this method could be realized in an experimental quantum computer of sufficient quality and capable of performing the universal gate set described.

From what was presented, one could see that most if not all time-homogeneous QWs fit into the general formalism presented here. Furthermore, given any time-homogeneous CTQW, a connected DTQW can be formed and used to simulate the CTQW probability dynamics. Although most of the results dealt with the case of a regular graph Hamiltonian, it seems reasonable that the non-regular connected DTQW would maintain many of the features of the CTQW and other variations could be used such as initial conditions composed of various combinations of the A- and B-projectors. Combining these result with the idea of the parallel-register method of implementation, one sees that experiments could be designed to implement any QW for a quantum computing scheme that is sufficiently robust. That includes the algorithm presented in Ch.IV as well as others such as the algorithm presented in Ref. [37].

The formalism can be extended to time-inhomogeneous evolution by performing a new coin operator on each time step. It seems reasonable that one could extend the connected DTQW formalism presented here to include time-dependent graph Hamiltonians. Thus, the task would be to find a series of time-dependent coin operators which would approximate the dynamics generated by the time-dependent graph Hamiltonian. As for the algorithm presented in Ch. IV, analysis must be completed to fully understand the behavior. Furthermore, it would be worth considering other applications and variations for the DTQW presented there. For example, consider that as a search algorithm, it was the ignorance of the marked element that led to the specific choice of initial state. As shown in Sec. IV.5, this caused some of the initial probability amplitude to be projected into the null space of

$\hat{J}'_1$ and it did so to the detriment of maximizing probability on the marked element since $\langle n, n | \hat{\mathscr{P}}_1^{null} | \psi_0^+ \rangle \sim \frac{1}{\sqrt{w_n}}$. There may be other applications where ignorance of the marked element is not necessary. In that case, the initial state could start in the dynamic space of the perturbed hypercube, which does require knowledge of the marked element. Then, one might find a larger maximum probability for the marked element. One such application might be a state-initialization algorithm, in which case, the time for initialization would not scale in the number of steps of the DTQW with the size of the register (although the number of gates would almost certainly scale with the size of the register). Furthermore, if initialization of only one register is required, the parallel-register method gives a test for the success of the initialization by measuring the last control register. Finally, I would like to design a simple DTQW implementation of the algorithm presented in Ch. IV with all the details of the gate structure using the parallel-register method. This would facilitate an experimental realization of all the ideas presented in this thesis.

APPENDICES

APPENDIX A

Solution for the Continuous-time Quantum Walk in One and Two Dimensions

The one-dimensional quantum walk is best understood as a cycle of N vertices. This is also thought of as a finite chain with periodic boundary conditions. The adjacency Hamiltonian is given as

$$\hat{H}_0^{(1D)} = \sum_{n \in \mathbb{Z}_N} \left(|n\rangle\langle n+1| + |n\rangle\langle n-1| \right), \tag{A.1}$$

where the sum, $n \pm 1$, is understood as modulo N. By Bloch's theorem, which is a special case of the VanVleck symmetrization process [43], the eigenvectors of this graph Hamiltonian are

$$|\phi_k^{(1D)}\rangle = \frac{1}{\sqrt{N}} \sum_{n \in \mathbb{Z}_N} \exp\left(ikn\right) |n\rangle, \tag{A.2}$$

and the eigenvalues are

$$E_k^{(1D)} = 2\cos\left(k\right), \tag{A.3}$$

where k takes of the values $k = m\frac{2\pi}{N}$ for some $m \in \mathbb{Z}_N$. This condition is to insure the periodic boundary conditions. Using the spectral decomposition of the CTQW time-translation operator, the propagator is expanded as

$$\langle n| \exp\left(-it\hat{H}_0^{(1D)}\right)|0\rangle = \sum_k \exp\left(-itE_k^{(1D)}\right) \langle n|\phi_k^{(1D)}\rangle\langle\phi_k^{(1D)}|0\rangle$$

$$= \frac{1}{N} \sum_k \exp\left(-i2t\cos k + ikn\right). \tag{A.4}$$

APPENDIX A

If the cycle is long enough, the sum can be approximated by an integral where k becomes a continuous parameter and $\Delta k = \frac{2\pi}{N} \to dk$. Thus the factor of N cancels and one has

$$
\begin{aligned}
\langle n | \exp\left(-it\hat{H}_0^{(1D)}\right) |0\rangle &= \frac{1}{2\pi} \int_{-\pi}^{\pi} dk \exp\left(-i2t\cos(k) - ikn\right) \\
&= i^n \mathcal{J}_n(2t),
\end{aligned}
\tag{A.5}
$$

where the last equality comes from the definition of the Bessel functions [17, 32].

The graph Hamiltonian for the two dimensional lattice with $N \times N$ vertices and periodic boundary conditions can be written as

$$
\hat{H}_0^{(2D)} = \hat{H}_0^{(1D)} \otimes \hat{I}_0 + \hat{I}_0 \otimes \hat{H}_0^{(1D)}.
\tag{A.6}
$$

Thus the 2D eigenvectors are

$$
|\phi_{\vec{k}}^{(2D)}\rangle = |\phi_{k_x}^{(1D)}\rangle |\phi_{k_y}^{(1D)}\rangle,
\tag{A.7}
$$

and eigenvalues are

$$
E_{\vec{k}}^{(2D)} = 2(\cos(k_x) + \cos(k_y)),
\tag{A.8}
$$

where $k_x = m\frac{2\pi}{N}$ and $k_y = n\frac{2\pi}{N}$ for some $m, n \in \mathbb{Z}_N$. From this, it is obvious that the 2D propagator is the product of two 1D propagators:

$$
\langle (m, n) | \exp\left(-it\hat{H}_0^{(1D)}\right) |(0, 0)\rangle = i^{n+m} \mathcal{J}_n(2t) \mathcal{J}_m(2t),
\tag{A.9}
$$

where each vertex is labeled by two indices $(m, n) \in (\mathbb{Z}_N)^2$.

APPENDIX B

Proof of the Expansion of the Quantum Walk in the Dynamic Space

In this appendix, I prove Eq. (III.42), which I restate here:

Proposition B.1. *For the definitions given in the main body of the thesis,*

$$
\begin{pmatrix} \hat{f}_0^{(t)} \\ \hat{g}_0^{(t)} \end{pmatrix} = \exp\left(-i\frac{\omega\epsilon(t+1)}{2}\right) \begin{pmatrix} \not{c}\, p_{t-1}(\hat{\gamma}_0) - \exp\left(i\frac{\epsilon\omega}{2}\right) p_{t-2}(\hat{\gamma}_0) \\ -i\not{s}\, p_{t-1}(\hat{\gamma}_0) \end{pmatrix}. \tag{B.1}
$$

Proof. The method of this proof is induction. Note the recursion equations for the Chebyshev polynomials are [17, 32]

$$
p_0(x) = 1; \tag{B.2a}
$$

$$
p_1(x) = 2x; \tag{B.2b}
$$

$$
p_{n+1}(x) = 2x p_n(x) - p_{n-1}(x). \tag{B.2c}
$$

Even though the polynomials are not defined for $n < 0$, I can use the recursion to infer the cases $n = -1, -2$. This implies $p_{-1}(x) = 0$ and $p_{-2}(x) = -1$. For the sake of brevity, I will suppress the argument of the Chebyshev polynomials, where it is understood that for the remainder of the proof the argument is $\hat{\gamma}_0$.

Consider when t=0,

$$
\exp\left(-i\frac{\omega\epsilon(0+1)}{2}\right) \begin{pmatrix} \not{c}\, p_{0-1} - \exp\left(i\frac{\epsilon\omega}{2}\right) p_{0-2} \\ -i\not{s}\, p_{0-1} \end{pmatrix} = \begin{pmatrix} 1 \\ 0 \end{pmatrix} = \begin{pmatrix} \hat{f}_0^{(0)} \\ \hat{g}_0^{(0)} \end{pmatrix}. \tag{B.3}
$$

93

Now assume for all integer $t' \leq t$, Eq. (B.1) is true and multiply Eq. (B.1) for t on the left by $\underline{U}$:

$$
\exp\left(-i\frac{\omega\epsilon(t+1)}{2}\right)
\begin{pmatrix}
\not{c}\exp\left(-i\epsilon\omega\right) & -i(\not{c}\mathscr{E}\hat{H}_0 + \not{s}) \\
-i\not{s}\exp\left(-i\epsilon\omega\right) & -\not{s}\mathscr{E}\hat{H}_0 + \not{c}
\end{pmatrix}
\begin{pmatrix}
\not{c}\,p_{t-1} - \exp\left(i\frac{\epsilon\omega}{2}\right)p_{t-2} \\
-i\not{s}\,p_{t-1}
\end{pmatrix}
$$

$$
= \exp\left(-i\frac{\omega\epsilon(t+2)}{2}\right)
\begin{pmatrix}
\exp\left(\frac{i\epsilon\omega}{2}\right)(\not{c}^2\exp\left(-i\epsilon\omega\right) + \not{c}^2 - \not{c}^2 - \not{s}^2 - \not{s}\not{c}\mathscr{E}\hat{H}_0)p_{t-1} - \not{c}p_{t-2} \\
-i\not{s}\left(\exp\left(\frac{i\epsilon\omega}{2}\right)(\not{c}\exp\left(-i\epsilon\omega\right) + \not{c} - \not{s}\mathscr{E}\hat{H}_0)p_{t-1} - p_{t-2}\right)
\end{pmatrix},
$$

$$(\text{B.4})$$

where $\exp\left(\frac{i\epsilon\omega}{2}\right)\not{c}^2 p_{t-1}$ was added and subtracted to the top component. Recall that $2\hat{\gamma}_0 = \exp\left(\frac{i\epsilon\omega}{2}\right)\mathrm{Tr}(\underline{U}) = \exp\left(\frac{i\epsilon\omega}{2}\right)(\not{c}\exp\left(-i\epsilon\omega\right) + \not{c} - \not{s}\mathscr{E}\hat{H}_0)$. Thus I can rearrange Eq. (B.4) and use the recursion equation for the Chebyshev polynomials to get

$$
\underline{U}
\begin{pmatrix}
\hat{f}_0^{(t)} \\
\hat{g}_0^{(t)}
\end{pmatrix}
= \exp\left(-i\frac{\omega\epsilon(t+2)}{2}\right)
\begin{pmatrix}
\not{c}(2\hat{\gamma}_0 p_{t-1} - p_{t-2}) - \exp\left(\frac{i\epsilon\omega}{2}\right)p_{t-1} \\
-i\not{s}(2\hat{\gamma}_0 p_{t-1} - p_{t-2})
\end{pmatrix}
$$

$$
= \exp\left(-i\frac{\omega\epsilon(t+2)}{2}\right)
\begin{pmatrix}
\not{c}p_t - \exp\left(\frac{i\epsilon\omega}{2}\right)p_{t-1} \\
-i\not{s}p_t
\end{pmatrix}
=
\begin{pmatrix}
\hat{f}_0^{(t+1)} \\
\hat{g}_0^{(t+1)}
\end{pmatrix}.
$$

$$(\text{B.5})$$

Therefore by induction, Eq. (B.1) is true for all integer $t \geq 0$. $\qquad\square$

APPENDIX C

Combinatorial Proof of Sums over Constant Hamming Weight and their Generating Functions

In this appendix, I prove Eq. (IV.26), which I restate here:

Proposition C.1.

$$\sum_{k}^{\|k\|=const.} (-1)^{k \circ n} = \sum_{m=0}^{d} \binom{\|n\|}{m} \binom{d - \|n\|}{\|k\| - m} (-1)^m. \tag{C.1}$$

First I prove a lemma:

Lemma C.2. *The sum $\sum_{k}^{\|k\|=const.} (-1)^{k \circ n}$ is only dependent on the Hamming weight of n.*

Proof. Consider the group $\mathcal{S}_d$ which permutes the components of the binary expansion of any integer number $0 \le n < 2^d$. Note that $\mathcal{S}_d$ is generated by the set of all two-cycles on d binary components. Since such a two-cycle does not alter the Hamming weight, this implies the Hamming weight is an invariant quantity under the action of all members of $\mathcal{S}_d$. Consider any such two-cycle, $g_{pq} \in \mathcal{S}_d$, which exchanges the pth and q^{th} digit in the binary expansion. So, $g_{pq}(m_i) = m_i$ for any $i \ne p, q$ and $g_{pq}(m_p) = m_q$, $g_{pq}(m_q) = m_p$ for any appropriate m. This implies

$$k \circ g_{pq}(n) = \sum_{i} k_i g_{pq}(n_i) = \sum_{i \ne p,q} k_i n_i + k_p n_q + k_q n_p =$$

$$= \sum_{i \ne p,q} g_{pq}^{-1}(k_i) n_i + g_{pq}^{-1}(k_q) n_q + g(k_p)^{-1} n_p = \sum_{i} g_{pq}^{-1}(k_i) n_i$$

$$= g_{pq}^{-1}(k) \circ n. \tag{C.2}$$

So for any $g \in \mathcal{S}_d$, $k \circ g(n) = g^{-1}(k) \circ n$. Thus one has

$$\sum_{k}^{\|k\|=const.} (-1)^{k \circ g(n)} = \sum_{k}^{\|k\|=const.} (-1)^{g^{-1}(k) \circ n} = \frac{\binom{d}{\|k\|}}{d!} \sum_{g \in \mathcal{S}_d} (-1)^{g^{-1}(k) \circ n}, \qquad \text{(C.3)}$$

where the last sum is for some fixed representative of the $\|k\| = const.$ equivalence class. Thus by the rearrangement theorem of group theory [43],

$$\sum_{k}^{\|k\|=const.} (-1)^{k \circ g(n)} = \sum_{k}^{\|k\|=const.} (-1)^{k \circ n}. \qquad \text{(C.4)}$$

Therefore, the sum is invariant under the action of any member of $\mathcal{S}_d$ on n and must only be dependent on the Hamming weight of n. $\qquad \square$

Intuitively, this comes from the idea that for fixed Hamming weight on n, no matter how one rearranges the digits, every binary dot product with a k of fixed Hamming weight is eventually a term in the sum. With the lemma, I can proceed with a combinatorial proof of Eq. (C.1):

Proof. By the Lemma C.2, I can consider without loss of generality the member of the $\|n\| = const.$ equivalence class which has all $\|n\|$ one binary digits stacked to the left and all $d - \|n\|$ zero digits to the right. For any member k of the $\|k\| = const.$ equivalence class, let m be the number of ones in its binary expansion which are to the left of the $\|n\|^{th}$ digit, inclusively, as depicted in Fig. C.1. So $(-1)^{k \circ n} = (-1)^m$. By combinatorics, the number of cases of $\|k\| = const.$ for which m ones are to the left of the $\|n\|^{th}$ digit, inclusively, is the number of ways to put m things in $\|n\|$ spots which is $\binom{\|n\|}{m}$. However, this makes no reference to the number of combinations for rearranging the remaining $\|k\| - m$ ones amongst the digits to the right of the $\|n\|$ digit. This is given by $\binom{d-\|n\|}{\|k\|-m}$. So the total

number of cases of $\|k\| = const.$ such that $k \circ n = m$ is $\binom{\|n\|}{m}\binom{d-\|n\|}{\|k\|-m}$. Therefore, Eq. (C.1) is true for all integer n such that $0 \le n < 2^d$. $\qquad\square$

$$
\begin{array}{cc}
\overbrace{}^{\|n\|} & \overbrace{}^{d-\|n\|} \\
n: \quad 111\cdots1 & 000\cdots0 \\
k: \quad 111\cdots0 & 111\cdots0 \\
\underbrace{}_{m} & \underbrace{}_{\|k\|-m}
\end{array}
$$

FIGURE C.1: Combinatorics of terms in the sum $\sum_{k}^{\|k\|=const.}(-1)^{k\circ n}$.

Finally, I show that $\tilde{w}_p(x)$ is the generating function for $P_q^p = \sum_{m=0}^{d}\binom{p}{m}\binom{d-p}{q-m}(-1)^m$ on q. To do this, one expands $\tilde{w}_p(x)$:

$$
\begin{aligned}
\tilde{w}_p(x) &= (1-x)^p(1+x)^{d-p} = \sum_{l=0}^{d}\sum_{m=0}^{d}\binom{p}{m}\binom{d-p}{l}(-1)^m x^{l+m} \\
&= \sum_{q=0}^{d}\left(\sum_{m=0}^{d}\binom{p}{m}\binom{d-p}{q-m}(-1)^m\right)x^q = \sum_{q=0}^{d}P_q^p x^q.
\end{aligned}
\qquad\text{(C.5)}
$$

REFERENCES

[1] Y. Aharonov, L. Davidovich, and N. Zagury. Quantum random walks. Physical Review A, 48(2):1687–1690, 1993.

[2] A. Ambainis. Quantum walk algorithm for element distinctness. SIAM Journal on Computing, 37(1):210–239, 2007.

[3] F.M. Andrade and M.G.E. Da Luz. Equivalence between discrete quantum walk models in arbitrary topologies. Physical Review A - Atomic, Molecular, and Optical Physics, 80(5), 2009.

[4] A. Barenco, C.H. Bennett, R. Cleve, D.P. Divincenzo, N. Margolus, P. Shor, T. Sleator, J.A. Smolin, and H. Weinfurter. Elementary gates for quantum computation. Physical Review A, 52(5):3457–3467, 1995.

[5] C.H. Bennett, E. Bernstein, G. Brassard, and U. Vazirani. Strengths and weaknesses of quantum computing. SIAM Journal on Computing, 26(5):1510–1523, 1997.

[6] M. Boyer, G. Brassard, P. Høyer, and A. Tapp. Tight bounds on quantum searching. Fortschritte der Physik, 46(4-5):493–505, 1998.

[7] A.M. Childs. Universal computation by quantum walk. Physical Review Letters, 102(18), 2009.

[8] A.M. Childs. On the relationship between continuous- and discrete-time quantum walk. Communications in Mathematical Physics, 294(2):581–603, 2010.

[9] A.M. Childs, R. Cleve, E. Deotto, E. Farhi, S. Gutmann, and D.A. Spielman. Exponential algorithmic speedup by a quantum walk. Conference Proceedings of the Annual ACM Symposium on Theory of Computing, pages 59–68, 2003.

REFERENCES

[10] A.M. Childs and J. Goldstone. Spatial search by quantum walk. Physical Review A - Atomic, Molecular, and Optical Physics, 70(2):022314–1–022314–11, 2004.

[11] K. Chisaki, N. Konno, E. Segawa, and Y. Sikano. Crossovers induced by discrete-time quantum walks. Quantum Information and Computation, 11(9-10):741–760, 2011.

[12] D. D'Alessandro. Connection between continuous and discrete time quantum walks. from d-dimensional lattices to general graphs. Reports on Mathematical Physics, 66(1):85–102, 2010.

[13] D. Dalessandro and R. Romano. A method for exact simulation of quantum dynamics. Journal of Physics A: Mathematical and Theoretical, 45(2), 2012.

[14] F. Debbasch and G. Di Molfetta. Discrete time quantum walks continuous limit in 1+1 and 1+2 dimension. Journal of Computational and Theoretical Nanoscience, 10(7):1621–1625, 2013.

[15] M.N. Dheeraj and T.A. Brun. Continuous limit of discrete quantum walks. Physical Review A - Atomic, Molecular, and Optical Physics, 91(6), 2015.

[16] G. Di Molfetta and F. Debbasch. Discrete-time quantum walks: Continuous limit symmetries. Journal of Mathematical Physics, 53(12), 2012.

[17] NIST Digital Library of Mathematical Functions. http://dlmf.nist.gov/, Release 1.0.10 of 2015-08-07. Online companion to [32].

[18] J. Du, H. Li, X. Xu, M. Shi, J. Wu, X. Zhou, and R. Han. Experimental implementation of the quantum random-walk algorithm. Physical Review A - Atomic, Molecular, and Optical Physics, 67(4):423161–423165, 2003.

[19] E. Farhi and S. Gutmann. Quantum computation and decision trees. Physical Review A - Atomic, Molecular, and Optical Physics, 58(2):915–928, 1998.

[20] E. Feldman and M. Hillery. Modifying quantum walks: A scattering theory approach. Journal of Physics A: Mathematical and Theoretical, 40(37):11343–11359, 2007.

[21] R.P. Feynman. Simulating physics with computers. International Journal of Theoretical Physics, 21(6-7):467–488, 1982.

[22] R.P. Feynman. Quantum mechanical computers. Foundations of Physics, 16(6):507–531, 1986.

[23] L.K. Grover. Fast quantum mechanical algorithm for database search. Conference Proceedings of the Annual ACM Symposium on Theory of Computing, pages 212–219, 1996.

[24] H. Häffner, C.F. Roos, and R. Blatt. Quantum computing with trapped ions. Physics Reports, 469(4):155–203, 2008.

[25] R.A. Horn and C.R. Johnson. Matrix Analysis. Cambridge University Press, Cambridge, UK, 20th reprinting edition, 2006.

[26] M. Karski, L. Förster, J.-M. Choi, A. Steffen, W. Alt, D. Meschede, and A. Widera. Quantum walk in position space with single optically trapped atoms. Science, 325(5937):174–177, 2009.

[27] N.B. Lovett, S. Cooper, M. Everitt, M. Trevers, and V. Kendon. Universal quantum computation using the discrete-time quantum walk. Physical Review A - Atomic, Molecular, and Optical Physics, 81(4), 2010.

[28] F. Magniez, A. Nayak, J. Roland, and M. Santha. Search via quantum walk. SIAM Journal on Computing, 40(1):142–164, 2011.

[29] F. Magniez, M. Santha, and M. Szegedy. Quantum algorithms for the triangle problem. SIAM Journal on Computing, 37(2):413–424, 2007.

[30] D.A. Meyer. From quantum cellular automata to quantum lattice gases. Journal of Statistical Physics, 85(5-6):551–574, 1996.

[31] D.A. Meyer. On the absence of homogeneous scalar unitary cellular automata. Physics Letters, Section A: General, Atomic and Solid State Physics, 223(5):337–340, 1996.

[32] F.W.J. Olver, D.W. Lozier, R.F. Boisvert, and C.W. Clark, editors. NIST handbook of mathematical functions. Cambridge University Press, New York, NY, 2010. Print companion to [17].

[33] R. Peierls. Zur theorie des diamagnetismus von leitungselektronen. Zeitschrift fr Physik, 80(11-12):763–791, 1933.

[34] A. Peruzzo, M. Lobino, J.C.F. Matthews, N. Matsuda, A. Politi, K. Poulios, X.-Q. Zhou, Y. Lahini, N. Ismail, K. Wörhoff, Y. Bromberg, Y. Silberberg, M.G. Thompson, and J.L. OBrien. Quantum walks of correlated photons. Science, 329(5998):1500–1503, 2010.

[35] J.J. Sakuri and J. Napolitano. Modern Quantum Mechanics. Addison-Wesley, Boston, MA, second edition, 2011.

[36] A.T. Schmitz and W.A. Schwalm. Simulating continuous-time hamiltonian dynamics by way of a discrete-time quantum walk. Physics Letters, Section A: General, Atomic and Solid State Physics, 380(11-12):1125–1134, 2016.

[37] N. Shenvi, J. Kempe, and K.B. Whaley. Quantum random-walk search algorithm. Physical Review A - Atomic, Molecular, and Optical Physics, 67(5):523071–5230711, 2003.

[38] Y. Shikano. From discrete time quantum walk to continuous time quantum walk in limit distribution. Journal of Computational and Theoretical Nanoscience, 10(7):1558–1570, 2013.

REFERENCES

[39] P.W. Shor. Polynomial-time algorithms for prime factorization and discrete logarithms on a quantum computer. SIAM Journal on Computing, 26(5):1484–1509, 1997.

[40] F.W. Strauch. Connecting the discrete- and continuous-time quantum walks. Physical Review A - Atomic, Molecular, and Optical Physics, 74(3), 2006.

[41] F.W. Strauch. Relativistic effects and rigorous limits for discrete- and continuous-time quantum walks. Journal of Mathematical Physics, 48(8), 2007.

[42] M. Szegedy. Quantum speed-up of markov chain based algorithms. Proceedings - Annual IEEE Symposium on Foundations of Computer Science, FOCS, pages 32–41, 2004.

[43] M. Tinkham. Group Theory and Quantum Mechanics. Dover Publications Inc., Mineola, NY, 2003.

[44] S.E. Venegas-Andraca. Quantum walks: A comprehensive review. Quantum Information Processing, 11(5):1015–1106, 2012.

[45] A.M. Zagoskin. Quantum Engineering: Theory and Design of Quantum Coherent Structures. Cambridge University Press, Cambridge UK, 2011.

[46] C. Zalka. Grover's quantum searching algorithm is optimal. Physical Review A - Atomic, Molecular, and Optical Physics, 60(4):2746–2751, 1999.